Department of Neurology
Helsinki University Central Hospital
University of Helsinki
Helsinki, Finland

BLOOD-BRAIN BARRIER LEAKAGE

AFTER TRANSIENT CEREBRAL ISCHEMIA

Aysan Durukan Tolvanen

ACADEMIC DISSERTATION

To be publicly discussed with the permission of the Medical Faculty of the University of Helsinki in Lecture Hall 3, Biomedicum Helsinki 1, Haartmaninkatu 8, on January 31, 2014, at 12 noon.

Helsinki, 2014

SUPERVISORS

Docent Turgut Tatlisumak
Department of Neurology
Helsinki University Central Hospital
and Experimental MRI Laboratory, Biomedicum Helsinki

Docent Daniel Strbian
Department of Neurology
Helsinki University Central Hospital
and Experimental MRI Laboratory, Biomedicum Helsinki

REVIEWERS

Professor Olli Gröhn
Department of Neurobiology
A. I. Virtanen Institute for Molecular Sciences
University of Eastern Finland

Docent Jari Honkaniemi
Department of Neurology
University of Tampere
Tampere, Finland

OPPONENT

Professor Schäebitz Wolf-Rudiger
Department of Neurology
University of Münster
Münster, Germany

Aysan Durukan Tolvanen, M.D.
aysan.durukan@hus.fi

Cover photo: *Brain party* by Geneviève Gauckler,
reproduced with the kind permission of Geneviève Gauckler.

ISBN 978-952-10-9698-3 (paperback)
ISBN 978-952-10-9699-0 (PDF)
http://ethesis.helsinki.fi

Helsinki University Print
Helsinki, Finland 2014

“Imagination is more important than knowledge.”

Albert Einstein

CONTENTS

LIST OF ORIGINAL PUBLICATIONS and AUTHOR'S CONTRIBUTION

This thesis is based on the following publications, referred to in the text by their Roman numerals:

I Strbian D*, Durukan A*, Pitkonen M, Marinkovic I, Tatlisumak E, Pedrono E, Abo-Ramadan U, Tatlisumak T. The blood-brain barrier is continuously open for several weeks following transient focal cerebral ischemia. *Neuroscience* 2008; 153:175-181

II Abo-Ramadan U*, Durukan A*, Pitkonen M, Marinkovic I, Pedrono E, Soinne L, Strbian D, Tatlisumak T. Post-ischemic leakiness of the blood-brain barrier: a quantitative and systematic assessment by Patlak plots. *Exp Neurol* 2009; 219:328-333

III Durukan A*, Marinkovic I*, Pitkonen M, Abo-Ramadan U, Pedrono E, Soinne L, Strbian D, Tatlisumak T. Post-ischemic blood-brain barrier leakage in rats: one-week follow-up by MRI. *Brain Res* 2009; 1280:158-165

IV Durukan Tolvanen A, Westberg JA; Serlachius M, Chang AC-M ; Reddel RR, Andersson LC; Tatlisumak T. Stanniocalcin 1 is important for poststroke functionality, but dispensable for ischemic tolerance. *Neuroscience* 2013; 229: 49-54

*Equal contribution.
In Study **I**, Aysan Durukan Tolvanen performed most of the experiments, contributed to data analysis and interpretation, and provided intellectual content to the manuscript. In Study **II**, the author performed most of the experiments, contributed to data analysis and interpretation, and wrote the manuscript. In Study **III**, Aysan Durukan Tolvanen performed most of the experiments, contributed to data analysis and interpretation, and wrote the manuscript. In Study **IV**, the author performed all experiments, except mRNA analyses, analyzed and interpreted the data, and wrote the manuscript.

ABBREVIATIONS

ADC	Apparent diffusion coefficient
AIS	Acute ischemic stroke
AQP4	Aquaporine-4
BBB	Blood-brain barrier
BBBP	BBB permeability
CBF	Cerebral blood flow
CT	Computed tomography
DCE-MRI	Dynamic contrast-enhanced MRI
DWI	Diffusion-weighted imaging
EB	Evans blue
ET-1	Endothelin-1
FLAIR	Fluid-attenuated inversion-recovery
Gd-DTPA	Gadolinium diethylenetriaminepentaacetic acid
HIF-1	Hypoxia-inducible factor-1
HPC	Hypoxic preconditioning
IL	interleukin
IR-FLASH	inversion recovery snapshot-fast low-angled shot
JAM	Junctional adhesion molecule
K_i	Blood-to-brain transfer rate constant of the contrast agent
MCA	Middle cerebral artery
MCAO	MCA occlusion
MMP	Matrix metalloproteinase
MRI	Magnetic resonance imaging
PWI	Perfusion-weighted imaging
ROI	Region of interest
STC	Stanniocalcin
STC1$^{-/-}$	STC1 knockout
TJ	Tight junctions
TTC	2,3,5-Triphenyltetrazolium chloride
t-PA	Tissue-plasminogen activator
T1-WI	T1-weighted image
WT	Wild type
ZO	Zonula occludens

ABSTRACT

Acute ischemic stroke (AIS) is a devastating disease leaving more than half of its victims disabled and causing nearly 5% of all deaths worldwide. In large ischemic strokes, a major cause of death is **brain edema**, which follows **blood-brain barrier (BBB) leakage**. The BBB ensures brain homeostasis in health and disease by limiting the entry of harmful blood-borne substances into the brain parenchyma. With a leaky BBB, the brain becomes devoid of protection from detrimental components of the circulating blood.

The BBB leakage in animal models of ischemia–reperfusion has long been considered to be **biphasic**; however, a considerable amount of discrepancies exist among the studies. Knowing exact temporal changes of the BBB permeability (BBBP) is important for the management of stroke patients. When the BBB is open, BBBP alleviating therapies would be effective, neuroprotective or neurorestorative drugs would be introduced, and if the BBB is closed these drugs would not enter the brain. Practical and reliable biomarkers of BBBP status are needed.

Stanniocalcins (STCs) are widely expressed in the brain and STC-1 expression is elevated in pathologies, such as hypoxia and focal ischemia. Recent data suggest a **neuroprotective** role for STC-1 especially trough **hypoxic preconditioning (HPC)**. No previous data associate STC-1 and the BBB.

We systematically evaluated disruption of the BBB following ischemia-reperfusion in a rat model of transient focal ischemia via suture occlusion of the middle cerebral artery for 90 min. Firstly (I, II), animals were allocated to 15 groups after reperfusion (25 min to 5 weeks). Secondly (III), a group of animals were evaluated repeatedly from 2 h to 1 week after reperfusion. BBBP to both **small (gadolinium)** (I, II, III), and **large (Evans blue)** (I) molecules were quantified by magnetic resonance imaging and fluorescence, respectively. Lastly, the contribution of STC-1 to HPC and the BBB was explored using STC-1 deficient mice ($STC^{-/-}$).

(I, **II, III)** After transient ischemia, the BBB leakage was **continuous**. Leakage to Evans Blue persisted up to 3 weeks and to gadolinium up to 5 weeks. Evans blue leakage slightly decreased at 36 and 72 h, gadolinium leakage was lesser at 25 min, 3 and 4 weeks. **(IV)** In $STC^{-/-}$ mice, HPC was effective in reducing lesion size, but these mice scored worse than wild type littermates. BBBP to Evans blue was not increased in $STC^{-/-}$ mice; neither under normal conditions, nor after hypoxia.

To conclude, transient focal ischemia in rats triggers a continuous BBB leakage lasting for several weeks. Until the final closure of the BBB, no earlier transient closure occurs. This finding indicates a long therapeutic window opportunity in respect to BBB passage of drugs to treat stroke. BBBP imaging method used in these studies may be easily translated to clinics. STC-1 is not obligatory for hypoxic preconditioning and is not a determining component of the BBB. Yet, STC-1 is important for preservation of neurological function after transient ischemia.

1 REVIEW OF THE LITERATURE

1.1 ISCHEMIC STROKE

Stroke is a devastating disease. At the year 2010, stroke ranked the second leading cause of death, responsible for 8.9% of all deaths worldwide.[1] It is estimated that each year nearly 6 million people die from stroke and another 5 million are left dependant on others.[2] Although the incidence of stroke is declining in many industrial countries due to improved preventive treatment, absolute number of strokes increases because of ageing. The world's 65-and-older population is estimated to triple by midcentury, from 516 million in 2009 to 1.53 billion in 2050.[3] Europeans will likely continue to be the oldest people in the world: by 2050, 29 percent of Europe's population is estimated to be 65 years and older.[3] Stroke burden calculated as disability-adjusted life years (a combination of years of life lost due to death and years of disability) is projected to rise by nearly two-fold from year 1990 to year 2020. In 2001, disability-adjusted life years due to stroke were around 72 millions.[4] In Finland stroke absorbs 7% of the health care budget.[5] In the United States, the total cost of stroke in 2008 was 34.3 billion and doubled in 2010, and the mean lifetime cost of ischemic stroke is estimated at $140,048 per patient.[6]

Ischemic stroke accounts for 80 to 85% of all cases of stroke and results from a thrombotic or embolic occlusion of a cerebral artery. Over half of all ischemic strokes occur in the middle cerebral artery (MCA) territory.[7] Etiologically atherosclerosis, embolism of cardiac origin, and small artery disease explain majority of cases.[8] A minority is caused by dissections and over 100 other causes. Eighty per cent of all ischemic strokes are preventable. Key risk factors for ischemic stroke are arterial hypertension, smoking, and hypercholesterolemia. Other risk factors can be classified as: traits (advanced age, male gender, African-American race, family history), medical conditions (diabetes mellitus, ischemic heart disease, atrial fibrillation, carotid artery disease, heart failure, peripheral arterial disease, thrombotic disorders, chronic kidney disease, sleep apnea), life style choices (obesity, excessive alcohol use, insufficient sleep, physical inactivity), and use of certain drugs (oral contraceptives, hormone replacement therapy, illicit drugs).

Intravenous thrombolysis with tissue plasminogen activator (t-PA) opened a new era in the management of acute ischemic stroke (AIS). Besides thrombolysis, the effect of stroke unit care, aspirin, and hemicraniectomy are evidence-based. Secondary prevention requires control of modifiable risk factors and etiology-oriented treatment (such as anticoagulation in atrial fibrillation, thrombophilia, and dissection, or carotid endarterectomy in significant large-artery atherosclerosis).

1.1.1 Pathophysiology of ischemic stroke

The brain, although a tiny organ in size (2% of body weight), uses nearly one fifth of body's oxygen and blood supply. Stores of energy lack in the brain making it highly dependent on continuous cerebral blood flow (CBF). Therefore, within minutes of cessation of blood supply to a territory of the brain, a complex sequence of pathophysiological spatial and temporal events (ischemic cascade) occurs.

1.1.1.1 Core and penumbra

Conventionally, core represents the irreversibly injured part of the ischemic lesion that destined to infarction and penumbra represents the region that is dysfunctional but salvageable if regional CBF is restored.[9-12] Positron emission tomography techniques revealed: 1) the **core** with a CBF of <12mL/100g per min and 2) the **penumbra** with a CBF of 12 to 22mL/100g per min.[13] A third **benign oligemic area** with CBF >22mL/100g per min also appeared[13] (Figure 1). This oligemic tissue probably maintains its function for a very long time and is unlikely proceed to infarction.[14] Animal studies using autoradiography to measure local CBF defined the core as a ischemic zone where CBF reduced to 0% to 20% of control, and the penumbra showed intermediate reductions of the flow, 20% to 40% of the control.[15] In the core, protein synthesis seizes related to ATP loss and irreversible translation blockade. In the penumbra ATP is preserved, protein synthesis is decreased, heat shock proteins are produced, and probably an unfolded protein response occurs.[16]

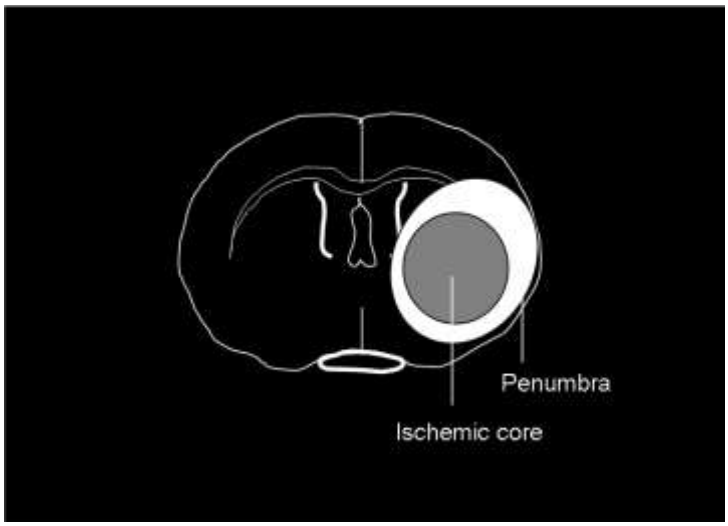

Figure 1 Schematic presentation of ischemic core and penumbra.

Pathologic outcome of focal ischemia is determined by two main factors: the degree of ischemia (rate of CBF decrease) and the duration of ischemia (time from CBF decrease to its recovery).[17, 18] The probability of infarction is greater than 95% if early CBF falls below 25% of control.[19] Early reperfusion preserves penumbra, but if the blood flow is not restored, the core extents to the entire penumbra. In most animal models, transient focal ischemia lasting 4 hours or more induces similar infarct size to that induced by permanent ischemia, that is, penumbra does not exist after 4 hours. But in humans, some penumbra can still be detected up to 48 hours from the beginning of symptoms.[20, 21]

Recent data suggest that not only penumbra, but also ischemic core is heterogeneous and dynamic. It is hypothesized that, in the early minutes and hours of ischemia onset, the core contains islets of injury ("**mini-cores**"), surrounded by salvageable viable tissue pockets ("mini-penumbras").[13] Microvascular heterogeneous responses to ischemia support this hypothesis.[22] Saving the penumbra is the main target of acute stroke therapy, but this new theory implies that with extremely early interventions we may have impact on progression of infarct core as well.

Evidence on cell death mechanisms in the core is scarce, because if not all, most of the agents failed to prevent damage in the core region. An exception is experimental use of antioxidant uric acid,[23] which is as effective as thrombolysis,[24] and suggests that a major

mechanism of cell death in the core is generation of free radicals. In general necrosis dominates in the core and apoptosis in the penumbra, but some ischemic cells may exhibit combined biochemical features of apoptotic and necrotic pathways.[25]

1.1.1.2 Ischemic cascade

Leading pathogenic mechanisms of ischemic cascade include energy failure, elevation of intracellular Ca^{2+} level, excitotoxicity, spreading depression, generation of free radicals, blood-brain barrier (BBB) disruption, inflammation, and apoptosis (Figure 2). These follow each other in a certain pattern, but not strictly in order, because they have overlapping features. Progression of ischemic brain injury may last hours to days, inflammation and apoptosis being the most long-lasting events.

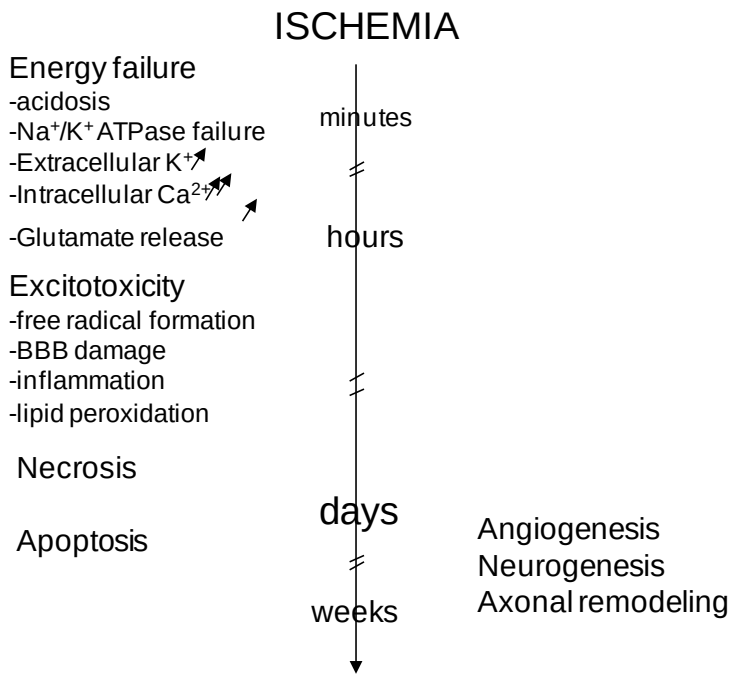

Figure 2 Mainstream events following focal cerebral ischemia.

First consequence of CBF reduction is the depletion of substrates, particularly oxygen and glucose, which causes accumulation of lactate via anaerobic glycolysis. **Acidosis** potentiates oxidative injury.[26] With energy depletion membrane potential is lost and neurons and glia depolarize.[27] Energy failure leads to perturbation of the Na^+/K^+-ATPase and Ca^{2+}/H-ATPase

pumps; in addition Na^+-Ca^{2+} transporter is reversed.[28] **Excitatory amino acids** (mainly glutamate) are released into the extracellular space and **intracellular levels of Na^+, Ca^{2+}, Cl^-** and **extracellular level of K^+ are increased**. In contrast to core cells where anoxic depolarization occur, peri-infarct penumbral cells can repolarize due to partly preserved reperfusion, but depolarize again in response to increasing glutamate and K^+ levels. **Spreading depression** defines depolarization starting within the ischemic core and extending outwards to surrounding tissue. It is an energy consuming process with the duration and number of peri-infarct depolarizations being correlated with the final infarct volume.[29-31]

Excitotoxicity of accumulated glutamate and imbalance of ions lead to **activation of a variety of Ca^{2+} dependent enzymes**, including protein kinase C, phospholipase A2, phospholipase C, cyclooxygenase, calcium-dependent nitric oxide synthase, calpain, various proteases, and endonucleases. As a result, free-radical species and leukotrienes generate, leading to irreversible mitochondrial damage, inflammation, and both necrotic and apoptotic cell death. Due to the formation of mitochondrial permeability transition pore, the mitochondrial membrane becomes leaky. This follows two important events: first, a burst of free radicals[32] and second, the release of cytochrome C.[33] **Free radicals** react irreversibly with several cellular constituents such as proteins, double bonds of phospholipids, and nuclear DNA. Further, in conjunction with a weakened scavenger system, free radicals cause lipid peroxidation, membrane damage, dysregulation of cellular processes, and mutations of the genome. **Cytochrome C** is a central mediator of apoptosis (programmed cell death). Other triggers of **apoptosis** include oxygen free radicals, death receptor ligation, DNA damage, protease activation, and ionic imbalance. Pro-apoptotic signals lead to caspase activation. Activated caspases are protein-cleaving enzymes, which lead to characteristic DNA-laddering and cleavage of structural proteins (such as laminin, actin, gelsolin). Apoptotic cell, differing greatly from necrotic cell, is characterized by: shrinkage of the cytoplasm, marked condensation of chromatin, and fragmentation of the cell.[34] Apoptotic cells are rapidly removed by phagocytosis without eliciting an inflammatory reaction.[35]

An acute and prolonged **inflammation** reaction contributes to ischemic injury. Within minutes of arterial occlusion, residents cells (mainly microglia) are activated and along with other affected brain cells produce a plethora of proinflammatory mediators (tumor necrosis factor-α,[36] interleukin-6,[37] monocyte chemoattractant protein-1,[38] interleukin-1β,[39] and granulocyte-

colony stimulating factor[40]). Especially monocyte chemoattractant protein-1 appears as a key molecule in post-stroke inflammation that leads to transmigration of hematogenous leukocytes.[38, 41] After the expression of adhesion molecules (including intercellular adhesion molecule 1 and selectins) at the vascular endothelium, neutrophils are the first inflammatory cells to arrive to the ischemic tissue, as early as within hours after reperfusion, followed by macrophages and monocytes within few days.[42] Microvascular obstruction by neutrophils (no-reflow phenomenon) can worsen the degree of ischemia, production of toxic mediators by activated inflammatory cells and injured neurons can amplify tissue damage. Pathogenic role of neutrophils and other leukocytes in cerebral ischemia is still a subject of debate.[42] Inflammation seems to exert a dual role, acutely worsens the ischemic injury and in the long-term proves beneficial through tissue remodelling.[43]

Another important component of ischemic pathophysiology is **edema** formation. Edema is initially cellular (cytotoxic edema) and follows cellular metabolic disturbances. Cytotoxic edema is an important indicator of ultimate final infarct size.[44] With the **disruption of the BBB**, intravascular fluid leaks into brain tissue (vasogenic edema), increases tissue volume, and proves number one reason of mortality in stroke. Mechanical or hypoxic damage of vascular endothelium, toxic damage of inflammatory molecules and free radicals, and especially destruction of the basal lamina by matrix metalloproteinases are potential causes of BBB disruption. This issue will be further discussed in a dedicated section.

Late reperfusion can exacerbate the injury initially caused by ischemia. This so-called **reperfusion injury** was first noticed when three hours of focal ischemia followed by three hours of reperfusion in the rat have produced more damage than six hours of permanent ischemia.[45] Reperfusion injury triggers alterations in production of various cytotoxic substances, including free radicals, excitatory amino acids, free fatty acids, proinflammatory cytokines, and adhesion molecules.[46] Involved pathological processes include leukocyte infiltration, platelet and complement activation, postischemic hyperperfusion, and BBB disruption.[47] In some AIS patients, thrombolysis follows fatal edema or intracranial hemorrhage; underlying event of these disastrous outcomes is reperfusion injury.

A late phase in the pathophysiology of infarcted tissue is **tissue remodeling**. Days to weeks after a stroke, an active process of neural progenitor cell proliferation occurs. **Neurogenesis** has been documented in several focal ischemia models.[48] Trophic factors, such as brain-

derived neurotrophic factor and granulocyte-colony stimulating factor (G-CSF), promote neurogenesis.[49, 50] Active angiogenesis is observed both in experimental animals and humans 3 days and further after an ischemic insult.[51] Functional neuroimaging has demonstrated changes in a number of features of brain function related to recovery after stroke, including a period of functional growth characterized by demonstrable structural and functional changes in both the ipsilateral and contralateral hemispheres that last several weeks.[52, 53]

1.1.2 Acute ischemic stroke therapy

The main approach of treating AIS is timely recanalization. Thrombolytics or mechanical devices (not yet evidence-based) are used to open the occluded artery and thus to restore blood flow. In experimental scenario, a lot of of resources were spent on developing an effective neuroprotective agent, which would protect neurons from necrosis, by interacting with the components of ischemic cascade.

1.1.2.1 Recanalization

In 1996, intravenous recombinant **t-PA** became the first US Food and Drug Administration-approved treatment for AIS. Original labeling requires the drug be given in 3 hours after symptom onset based on the National Institute of Neurological Disorders and Stroke t-PA trial.[54] A restricted conditional license for the use of t-PA was granted in Europe in 2002 allowing treatment within 3 hours in AIS patients younger than 80 years who also met other specified criteria. Results from the ECASS-III trial have since expanded time window to **4.5 hours**.[55] Thrombolysis with t-PA significantly improves clinical outcomes at 90 days compared with placebo, for every 1000 patients treated, 97 more are alive and avoid disability.[56] The sooner the t-PA is given, the greater the benefit is, especially within 90 min from symptom onset.[57] A recent systematic review of 12 randomized trials of t-PA indicates the same fact, the greatest benefit is gained with early treatment, although some patients might benefit from t-PA up to 6 hours after stroke.[56] Unfortunately, only a minority of AIS patients receive t-PA: in the U.S. 3% to 8.5%[58] and in the capital area of Finland as much as 15%[59] of all AIS patients. The main reasons for this low rate of utilization of t-PA are economical and educational: Cost of acute stroke care is high (though probably cost-effective[60]) and awareness level on stroke in general public is low. The risk of symptomatic hemorrhage (approximately 6%[56]) is another cause for withholding t-PA therapy.

Several novel thrombolytic agents are under progress. A recent successful example is **tenecteplase**, which was more effective than t-PA in a phase II trial.[61] **Desmatoplase** in Acute Ischemic Stroke-3 (DIAS-3) and DIAS-4 phase III trials test the safety and efficacy of desmatoplase given three- to nine hours after symptom onset in patients with proved vascular occlusion.[62]

Bridging therapy of concomitant use of both iv and intraarterial t-PA aims to combine the fast effect of iv use and higher recanalization rates of intraarterial use. Although yet an investigational technique,[63] a recent meta-analysis found the bridging therapy safe and effective, suggesting that it may be the first choice of therapy in AIS patients with proven arterial occlusion.[64] This hypothesis is tested in an ongoing phase III trial.[65]

Endovascular revascularization is a local therapy of of therapy for AIS patients who have a contraindication for systemic thrombolysis or who do not respond to it. Large vessel occlusions are less prone to recanalization by t-PA.[66] Clot retrieval with FDA-approved **MERCI® Retriever** has been an evolving treatment option due to positive results of MERCI trial.[67] Pooled analysis of MERCI trial and the trial of combination of embolectomy and thrombolysis (Multi MERCI) provides additional evidence that increasing rates of recanalization improves clinical outcomes.[68] Recently, mechanical embolectomy was not found superior to standard care within 8 h of symptom onset in large-vessel, anterior circulation strokes (MR-RESCUE).[69]

The Penumbra system was approved for use in the United States in 2008 for “the revascularization of patients with acute ischemic stroke secondary to intracranial large vessel occlusive disease (in the internal carotid, middle cerebral artery M1 and M2 segments, basilar, and vertebral arteries) within 8 hours of symptom onset”. Penumbra system initiates recanalization by in situ suction of the clot. According to the pivotal study[70] and publication of results from post-market experience[71] the device seemed effective and safe. A phase IV study testing t-PA-Penumbra System combined therapy over standard t-PA therapy in anterior circulation strokes with a large clot is ongoing.[72]

Ultrasound-enhanced thrombolysis increases recanalization compared with t-PA.[73] A phase III trial in the USA (CLOTBUST-ER) is under progress.[74]

1.1.2.2 Neuroprotection

To year 2003 over 1000 agents were tested in animals, out of which 60% exerted neuroprotection from focal ischemia.[75] Nearly 200 clinical trials used candidate neuroprotective agents in humans with no success. Potential reasons of this translation failure have been extensively discussed elsewhere.[76-81] Main reasons are the methodological differences between preclinical and clinical studies, inadequate quality of animal testing and the heterogeneity of stroke in humans compared to homogenous experimental strokes in animals.[82-84] After these many failures to prove a neuroprotective efficacy of drugs tested in AIS patients, recently, the Evaluating Neuroprotection in Aneurysm Coiling Therapy (ENACT) trial showed that neuroprotection worked in reducing ischemic infarcts after the endovascular repair of an intracranial aneurysm.[85] This study perhaps will alleviate the ignorance of neuroprotection to treat AIS.

Besides others,[84] a group of candidates holds hope for neuroprotection: 1) **Hypothermia** combined with t-PA is tested for efficacy in a phase III trial[86] and The European Hypothermia trial, EuroHyp-1, is also a randomized multicenter study to assess efficacy and safety of hypothermia in ischemic stroke patients,[87]) **Free radical scavenging** has become a promising approach with proven efficacy of NXY-059 in the first clinical trial SAINT-I.[88] Unfortunately SAINT-II was neutral,[89] but indicated that treatment window should match the preclinical data and patient selection should be improved.[90] Currently another free radical scavenger, ebselen, is tested in a phase III trial in patients with a cortical infarct.[91] Drug will be started within 24 hours of stroke and given during14 days. Edaravone was introduced as the first free radical scavenger for the treatment of stroke[92] and is widely used to treat acute ischemic stroke in Japan, although evidence from large-scaled clinical trials are lacking, and 3) **Minocycline**, an antiinflammatory and antioxidant agent, was safe and effective in small open-label studies,[93] a phase IV study has been terminated, but yet results are missing.[94]

Animal data suggest that **combining thrombolysis with neuroprotection** may be superior to thrombolysis alone and may extend the time window of thrombolysis.[95] Erythropoietin was harmful for this purpose,[96] and currently uric acid[97] and hypotermia[98] are tested in phase III clinical trials. A novel approach of neuroprotection has proven effective in primates by **selective inhibition of N-Methyl-D-aspartate receptor neurotoxicity**.[99] This high-quality preclinical work is giving hope that neuroprotection may be feasible in AIS patients and should be tested in a narrow population at first.[100]

For protecting neurons from dying, by only focusing on mechanisms of injury, we may have been seeing only half of the picture.[101] Brain's response to stroke is complex and includes multiple processes of endogenous repair and remodeling.[51, 101, 102] It is suggested that candidate drugs for AIS should possess regenerative mechanisms of action in addition to neuroprotective actions, in order to achieve sustained neurological improvement.[103] Thus, another group of drugs are designed to enrich neurorecovery and remodeling of the infarcted tissue. Among potential neurorestorative and neuroregenerative compounds, G-CSF has been extensively studied[104] and appeared effective in reducing infarct size and enhancing functional recovery through its anti-apoptotic and neurogenesis inducing capacities.[105, 104] Despite these encouraging preclinical results, a phase II trial (AXIS-II) of G-CSF in AIS patient resumed negative.[100] However, the drug awaits efficacy testing in chronic stroke patients.[106] Cerebrolysin, a peptide preparation which acts as a neurotrophic factor, promotes neuroplasticity and neurogenesis in experimental models, but a phase III trial of cerebrolysin plus t-PA in AIS patients resumed negative.[107]

1.1.3 Magnetic resonance imaging (MRI) in acute ischemic stroke

Recent developments in AIS imaging have revolutionized our approach to acute stroke. Noncontrast computed tomography (CT), due to its wide accessibility, is most commonly used diagnostic tool for acute stroke diagnostics. Noncontrast CT has been sufficient as an imaging modality in thrombolysis candidates to receive tissue plasminogen activator in 3-hour therapeutic window,[54] but MRI may suit as a brain clock replacing the currently used epidemiological time clock when deciding patient recruitment to thrombolysis.[108] Magnetic resonance is superior to CT to detect early ischemic changes[109-112] and to detect involvement of more than one third of the middle cerebral artery territory.[113, 114] Although CT remains the best method for detection of intracerebral hemorrhage, MRI with T2*can be equally sensitive.[14]

MRI is noninvasive, patient compatible with only few contraindications, has relatively high spatial and temporal resolution with superior signal contrast, and clinical availability is constantly increasing. MRI may serve in AIS for several purposes: to ensure the diagnosis, to give insights on etiology, and to guide the selection of therapeutic approach.

1.1.3.1 Lesion evaluation by MRI

Diffusion-weighted imaging (DWI) has revolutionized stroke research since this technique is extremely sensitive to the hyperacute phase of brain ischemia. Another advantage of DWI in stroke imaging is high sensitivity in detection of multiple acute ischemic lesions.[115-117] Perfusion-weighted imaging (PWI) is a semiquantitative method of evaluating brain perfusion, which provides imaging and measuring blood flow at the capillary level. Combination of DWI to PWI provides further insights on ischemic lesion evaluation. It is generally accepted that the difference between PWI-based hypoperfusion volume and the DWI-based lesion volume (the so-called mismatch) is operationally approximate the ischemic penumbra.[118, 119]

It is thought that AIS patients with DWI-PWI mismatch may respond to thrombolysis beyond the therapeutic window. Unfortunately, first-ever randomized controlled study in this context (EPITHET)[120] failed to prove effectiveness of t-PA in the 3- to 6 h treatment window concerning the primary end point (geometric mean relative infarct growth), probably due to spontaneously recovering subjects among mismatch patients.[121] However, when a modified method for calculating mismatch volume (co-registration method) is used, reanalysis of EPITHET patients indicates attenuation in infarct growth.[122] CT perfusion imaging-based detection of penumbra has driven the patient selection in the positive phase II trial of tenecteplase.[61] A candidate group of patients to whom to apply mismatched-based thrombolysis are wake-up stroke patients (an estimated 25% of AISs occur during sleep[123-125]).

There is a lack of consensus regarding which PWI-derived parameter best defines hypoperfused region or predicts infarct growth.[126-129] Other unsolved issues in MRI-based penumbra imaging are the optimal method of postprocessing,[129] the use of an automated processing software,[130] and method for delineation core and hypoperfusion. Optimization of PWI/DWI mismatch clearly requires further studies.

A controversial issue is the clinical relevance of reversibility of DWI lesion.[131] The definition of PWI/DWI mismatch is questioned after the recognition that the PWI boundary includes a region of benign oligemia and that a portion of the DWI core is potentially salvageable with rapid reperfusion.[132] But, sustained DWI reversal seems infrequent and rarely clinically relevant by altering PWI/DWI mismatch.[133]

1.1.3.2 BBB disruption: contrast-enhanced imaging

A wide spectrum of appearances of contrast enhancement of the ischemic lesion on the CT scans was noticed since late 70's. Different patterns of enhancement (e.g. homogeneous or heterogeneous) were observed at different degrees (e.g. minimal to marked), and in different phases of the stroke,[134-137] with a frequency varying from 26% to 95%.[137] Enhancement was seen as early as first day and as late as 9 months after the onset of symptoms,[136] but most often at two to three weeks after stroke.[137] Even with modern imaging techniques the frequency of increased BBB permeability (BBBP) in AIS patients varies considerably (from 20 to 88%).[138-140] A higher frequency is recognized with dynamic imaging methods using quantitative approaches.

An association of CT contrast enhancement to hemorrhagic transformation of the infarction was noted more than 30 years ago.[141] In agreement with animal studies,[142-145] early BBB disruption detected by parenchymal enhancement in human ischemic stroke was found highly specific for hemorrhagic transformation.[146-148] With the increasing use of multimodal MRI and CT, parameters related to BBB damage are being discovered and recent studies often indicate an important role for BBBP imaging in prediction of hemorrhagic transformation. Dynamic perfusion CT is increasingly used for this purpose,[140, 149-151] though there exists controversy about the optimal method of acquisition of the data (first-pass vs delayed-acquisition). If the permeability of the BBB is not large enough for blood cellular elements to pass, hemorrhage will not occur, but BBB leakage to much smaller molecules such as albumin, may cause edema.[152] Perfusion CT data analyzed with a modified Patlak model was used to estimate BBBP for predicting malignant MCA and the need for hemicraniectomy.[152]

Another imaging marker for BBB disruption was suggested as the so-called hyperintense acute reperfusion marker. This imaging finding was observed only on non-contrast follow-up examinations if gadolinium was administered during initial MRI and was defined as delayed gadolinium enhancement in the cerebrospinal fluid[153, 154] on fluid-attenuated inversion recovery (FLAIR) images, indicating an early BBB disruption, increased risk of hemorrhagic transformation, and poor outcome.[148, 155, 156] However, hyperintense acute reperfusion marker is a common finding in elderly stroke patients and is not necessarily associated with hemorrhagic transformation.[157]

DCE-MRI based quantification of BBBP via a kinetic model is not standardized yet. Kassner et al.[139] applied Patlak model to DCE-MRI data for this purpose and evaluated BBBP in ten AIS patients (who did not undergo thrombolysis). Increased permeability was found in patients who developed hemorrhagic transformation.

T2*-based BBBP MRI,[158-160] despite its semiquantitative nature, is a strong alternative to DCE-MRI from a practical point-of-view, because perfusion MRI with T2*-WI is a part of routine imaging in most stroke units. Among several candidate T2*-based measures, relative recirculation, which identifies abnormalities in the contrast recirculation phase, provided comparable data to DCE-MRI and proved predictive in identifying patients with AIS who will proceed to hemorrhagic transformation.[160]

1.2 EXPERIMENTAL ISCHEMIC STROKE

1.2.1 Why animal modeling

Modeling of ischemic stroke serves for two main purposes: first, to disclose underlying pathological mechanisms of focal cerebral ischemia and then based on these deciphered mechanisms to develop novel therapies for stroke. Secondly, novel imaging techniques are explored and applied in animal models before their introduction into clinical practice. Thrombolysis[161] and DWI[162] are the mainstream examples of translational success from laboratory to clinics.

Ischemic stroke is a very **heterogeneous disease** in human, varying in etiology, lesion location, and size and is complicated by concomitant diseases. Age, sex, and amount of collaterals are among several other variables affecting the outcome of ischemic stroke. Therefore, very large group of patients are required in clinical trials of stroke. On the other hand, in experimental stroke, a more homogenous disease is mimicked by strictly controlling variables, thus, with a small group of animals statistical power can be already reached, saving money and time. **Rodents**, less costly and more ethically acceptable than larger animals, are most often utilized in experimental stroke research, because of several reasons: the resemblance to humans in cerebrovascular anatomy, moderate size allowing easy manipulations, low costs, the relative homogeneity within strains, and last but not least, the accessibility for use by transgenic technology. In contrast to lissencephalic brains of rodents, large animals have gyrencephalic brains and considerable amount of neocortex akin to humans. Application of sophisticated methods such as evoked potential monitoring, electroencephalography, and functional imaging is easier in larger animals. It is recommended that positive rodent studies must be replicated in higher species before proceeding to clinical trials.[163] Even among **primates** there are considerable differences in brain anatomy and vasculature, stroke in macaques may best represent human AIS.[99]

1.2.2 Major rodent models of ischemic stroke

There is a rich diversity of focal ischemia models, among which none is capable to mimic all aspects of human stroke, but most appropriate model can be chosen to address a specific

question. Model selection is especially important in preclinical drug developmental studies. Recommendations from the **STAIR** committee must be followed in designing such studies.[163, 164] Each model grants superiorities and shortcomings (for reviews see related articles[165-169]).

Blocking of blood flow in the **MCA** is often aimed in animal models, because half of all strokes occur in the territory of this artery.[7] Thromboembolic models mimic closely the disease from etiological aspect and they are suitable for testing thrombolytics. However, the most commonly used method of inducing focal cerebral ischemia is intraluminal occlusion of MCA by a surgical monofilament (suture model), which allows strict control on the timing of the reperfusion. Other models include surgical occlusion of the distal or proximal MCA, endothelin-1 induced ischemia, photothrombotic ischemia, and embolic models using artificial materials as embolus. Models requiring craniectomy are complicated by both negative side effects of exposing brain to the atmosphere and protective effect of craniectomy from malignant MCA infarction.

Either **permanent or transient** ischemia is modeled. Permanent ischemic models represent clinical situation of nearly half of the AIS patients. Others experience transient ischemia by either spontaneous[170] or therapeutic recanalization.[171] In transient ischemia models, an ischemia period of 90 to120 min is most often used, because it induces sustained infarcts. Transient ischemia longer than 3 hours allows studying a specific aspect of the stroke, reperfusion injury, but do not contain penumbra.[172] A candidate neuroprotective compound needs to be tested in both permanent and transient ischemia models, because of different underlying mechanisms in each type of ischemia.[163]

1.2.2.1 Thromboembolic models

Thromboembolic models use two main strategies to induce stroke: clot embolism from an extracranial artery and in situ clot formation in distal MCA. Originally autologous thrombi were injected into extracranial arteries to reach the more distal intracranial arteries.[173, 174] In these earlier embolism models, infarcts induced by a shower of emboli were variable in size and early spontaneous recanalization occurred.[174, 175] Important parameters for inducing consistent CBF decline and reproducible lesions are formation, composition, and final localization of the emboli. By mechanically processing a preformed thrombus, autolysis resistant fibrin-rich emboli may be achieved.[176, 177] Others[178] preferred injecting multiple fibrin-rich autologous clots into the external carotid artery one after another leading to consistent

infarcts without spontaneous recanalization. Another method for increasing reproducibility of thromboembolic infarcts is endovascular delivery of an intact fibrin-rich embolus into the segment of the internal carotid artery near the origin of the MCA by intraarterial catheterization.[179, 180] In situ thromboembolic stroke model ensures exact localization of the clot by microinjection of purified thrombin into the lumen of distal MCA.[181] This model induces reproducible cortical infarcts in mice and responds to t-PA treatment when t-PA is introduced 20 min after clot formation. In situ thrombus model avoids potential damaging effects of intraarterial catheterization, but necessitates a craniectomy. Yet efforts are spent to improve reproducibility in the thromboembolic model.[182]

Thromboembolic models responding to thrombolysis[183-185] suit for testing new thrombolytics and combination therapies of thrombolysis and neuroprotection for acute stroke.[186] Preclinical drug testing may use rabbit embolic models of stroke[187] secondary to a rodent model. A large vessel thromboembolic occlusion model in rabbits may allow testing also mechanical devices in combination to thrombolysis.[188]

1.2.2.2 Suture occlusion of the MCA

Originally introduced by Koizumi et al.[189] this model includes insertion of a monofilament suture into the internal carotid artery and advancing until it blocks blood flow to MCA. Suture MCAO model induces MCA territory infarctions involving both frontoparietal cortex and striatum with good reproducibility and reliability even among investigators of varying experience.[190] Reperfusion is easily achieved by retracting the suture. The model is suitable to apply in the MRI scanner.[191] Several modifications have been made to the initial model by using differently coated sutures or external carotid artery insertion of the suture.[192, 193] Suture diameter, type of coating of the suture (with silicone or poly-L-lysine), and insertion length of the suture are among factors affecting the outcome. Size of the filament correlates well with the size of the infarct.[194, 195] Silicone-coated suture causes larger and more consistent infarcts then uncoated suture induces.[196, 197] The deeper the suture insertion is, the greater the achieved lesion is.[198, 199]

Suture occlusion model carries some complications: Subarachnoid hemorrhage due to mechanical vessel rupture and hyperthermia due to hypothalamic injury may occur. Silicone coating of the suture and laser Doppler-flowmetry guidance may reduce the incidence of subarachnoid hemorrhage.[200] Spontaneous hyperthermia can be avoided by limiting

ischemia duration to 90 minutes or less[201] or adjusting suture tip to a size that does not occlude the hypothalamic artery.[166]

Intraluminal suture MCAO model was suggested suitable for neuroprotective drug studies because a substantial penumbra exists within the first 60-90 min of injury.[202] An MRI study showed, however, that the mismatch volume is larger and persists longer in thromboembolic model relative to permanent suture MCAO model in rats.[203] Transient suture MCAO was also compared to embolic model combined with t-PA treatment (thrombolysis model).[204] Even though infarct sizes were equal in these two models, perfusion recovers immediately and completely in the suture model, but slowly and incompletely in the thrombolysis model. The latter is associated with increased BBBP in the periphery of the infarct. Recently, serious concerns raised on the use of transient MCAO occlusion with suture model in preclinical studies.[205] It has been argued that prompt recirculation achieved with this model is uncommon in naturally occurring strokes and the model misleads clinicians in translating an appropriately long time window for the agent under investigation.

1.2.2.3 Other models

Surgical methods aim to expose MCA by one of the several surgical approaches, among which orbital route is less traumatic.[206] While electrocauterization of a portion of MCA results in permanent occlusion, the use of microclips and ligature snares allows reperfusion.[207, 208] Originally induced by frontoparietal approach,[209] distal MCAO at the rhinal fissure spares lenticulostriate branches and leads only a restricted cortical infarction in rats. Tamura's subtemporal approach[210] gained a greater acceptance because with Tamura's method more proximal regions of the MCA are accessible and infarcts are more reproducible. Not only the site, but also the length of the ligated portion of MCAO affects the outcome.[211] To overcome variability in infarcts several modifications to surgical MCO have been proposed: tandem occlusion of the distal MCA and ipsilateral common carotid artery,[212] tandem occlusion of the distal MCA and bilateral common carotid arteries (three vessel occlusion technique),[207] and distal MCAO with temporary clip compression of both common carotid arteries.[213, 214] Orset et al.[181] have utilized temporal approach in their in situ MCA thrombosis model. Main handicap of surgical methods is their invasiveness. Additionally, they require good surgical skills and in transient surgical models recanalization is abrupt as in the intraluminal suture method. On the other hand, the site of occlusion is well-controlled.

In models of **non-clot embolus**, many compounds or materials were used as artificial emboli.[215-219] Embolization with multiple microspheres[187, 220-222] has been proposed to simulate atheromata and fat embolization. It induces permanent ischemia, infarct maturation is slower (i.e. penumbra persists longer[223]) than MCAO models, and infarcts are multifocal and heterogeneous.[224]

In photothrombosis models, after systemic intravenous injection of a photoactive dye (traditionally Rose Bengal), a cortical brain area is irradiated by a light beam at a specific wavelength through the intact skull.[225] Resulting perioxidative damage to the endothelium causes platelet adhesion and aggregation in both pial and intraparenchymal vessels within the irradiated area.[226] Originally, this model induces cortical ischemic lesion with acute severe endothelial cell damage, BBB disruption, and edema formation.[227] Additionally, ischemic lesion involves relatively restricted penumbral area, because of the associated end arterial occlusion. However, a variation of the original phothrombotic model, ring model,[228] successfully induces a penumbra-like lesion.[229] Use of thinner ring irradiation may allow achieving late spontaneous reperfusion and a morphological tissue recovery.[230] Another modification was made to occlude the MCA,[231] simply MCA was exposed surgically and irradiated after the injection of the photoactive dye. In this variant, although penumbral part of the lesion is also minimal,[232] a therapeutic effect of rtPA has been shown.[233] Advantages of the cortical phothrombotic models are control on the location and size of the lesion, and low mortality.

Endothelin-1 (ET-1) is a potent vasoactive peptide, which produces a marked vasoconstriction.[234] Either by subtemporal approach[235] or intracerebral injection technique,[236] ET-1 application onto MCA provides significant decrease of CBF in the MCA territory, resulting in an ischemic lesion pattern similar to that induced by direct surgical MCAO.[236, 237] Direct cortical application of ET-1 induces a semicircular infarct involving all layers of the neocortex.[238] Endothelin-1 induced MCAO model mimics slow recanalization (lasting approximately 4 hours) in a dose dependent manner of applied ET-1.[237, 239] Therefore, less control on the ischemia duration and intensity are disadvantages of the model. Furthermore, it is not suitable for testing thrombolysis.

A number of animal models exist to study posterior circulation strokes;[240] more or less invasive embolic models were described.[241, 242] A main handicap of modeling ischemic stroke originating from posterior circulation is lesser reproducibility compared to MCAO models.[163]

1.2.3 Preconditioning

1.2.3.1 Ischemic tolerance

Introducing the brain a nonlethal insult allows it to be prepared for the next ischemic insult, i.e. preconditions the brain. Preconditioning triggers a defense mechanism as a product of genomic reprogramming, which renders brain tolerant to the final lethal injury. This new defense program may attenuate almost all steps of ischemic cascade; additionally, innate survival mechanisms and endogenous repair mechanisms are enhanced.[243]

Ischemic tolerance occurs in two temporally distinct windows: early tolerance can be achieved within minutes, but wanes also rapidly, within hours; delayed tolerance develops in hours and lasts for days. The main mechanism involved in early tolerance is adaptation of membrane receptors, whereas gene activation with subsequent *de novo* protein synthesis and genetic reprogramming dominates delayed tolerance.[244] Data on early ischemic tolerance in the brain are scarce,[245-249] ischemic tolerance occurs in the brain predominantly with the delayed pattern. Cross tolerance, in which one type of insult promotes protection from a subsequent different type of insult, has been documented in the brain in many variations.[250] Hypoxic preconditioning is a well-known example of cross tolerance.

1.2.3.2 Hypoxic preconditioning

A brief exposure to systemic hypoxia (i.e. hypoxic preconditioning; HPC) prior to transient MCAO reduces infarct volume, blood-brain barrier disruption, and leukocyte migration.[251, 252] Hypoxic treatment was first time used as a preconditioning trigger in a hypoxia-ischemia model in neonatal rats.[253] Later, HPC was proven protective from both transient and permanent focal cerebral ischemia.[254, 255] Sublethal hypoxia (11% oxygen for two hours) applied 48 h prior to transient focal cerebral ischemia protected nearly half of the tissue-at-risk from undergoing infarction in several strains of mice.[254] Compared to permanent ischemia alone, hypoxia applied 24 h prior to ischemia results in 30% smaller infarcts.[255] Single applications of varying hypoxia durations (1, 3, or 6 hours) are similarly efficient, but

protective effect abolishes after 72 hours.[255] Repetitive hypoxic treatment, however, may be protective from focal ischemia up to 4 to 8 weeks.[256, 257]

The mechanisms of hypoxic preconditioning and ischemic tolerance are still being elucidated. Hypoxia-induced tolerance in brain is not blocked by glutamate receptor antagonists, but is blocked by inhibitors of RNA and protein synthesis.[258] A key factor in HPC is the hypoxia-inducible factor-1 (HIF-1). As early as 1 hour after hypoxia and maximally at 6 hours, expressions of many HIF-1-regulated genes are increased.[259] Hypoxia stabilizes alpha subunit of HIF-1, which enters the nucleus in a dimerized form and results in the induction of HIF target genes. Several HIF target genes contribute to protection from ischemia,[255, 258, 259] and their products are involved in a wide range of adaptive and pro-survival events, including cellular metabolism, proliferation, vascularization, iron homeostasis, and glucose metabolism.[243, 260] However, in neuron-specific HIF-1alpha-deficient mice, protective effect of hypoxia from subsequent focal ischemia was significantly attenuated, but not completely abolished, suggesting that alternative mechanisms of neuroprotection are also implicated in HPC.[261] Recently microvascular sphingosine kinase activity was found as an important trigger of hypoxic preconditioning.[262] Blocking sphingosine kinase activity nullifies protective effects of prior hypoxia from transient ischemia. Chemokine signaling seems to be another critical mediator to the induction of hypoxic preconditioning-induced ischemic tolerance. Mice that lacked monocyte chemoattractant protein-1 also lost the capacity to become ischemia tolerant, although they received hypoxic treatment.[251]

1.2.4 Outcome measures

In contrast to human studies, where primary outcome is usually neurological improvement at 3 months, experimental stroke mostly focused on the acute phase of ischemia and the main determinant of the outcome has been infarct volume within few days after the onset of ischemia, mostly ignoring functional outcome.[263] If the model includes mild ischemia, lesion progression is slow, [264] or if a neuroprotective drug[265] or a preconditioning regimen is tested, therapeutic effect may be transient;[266] therefore, long-term outcomes should also be evaluated in such circumstances. Data from preclinical studies suggest a poor correlation between pathologic and functional improvements.[267] Despite the lack of infarct size improvement, behavioral assessment might reveal effectiveness of a neuroprotective drug.[268, 269] Lack of correlation between different outcome measures indicates that behavioral, neurological, and histological endpoints are conjointly necessary.

1.2.4.1 Infarct volume

Infarct volume is traditionally evaluated post mortem with hematoxylin-eosin staining (i.e. the gold standard histological method) or with less costly 2,3,5-triphenyltetrazolium chloride (TTC). Other staining methods (Cresyl violet[270] or silver staining[271]) are also available to delineate the extent of the ischemic lesion. Image analyzing systems allow manual, semiautomated, or fully automated delineation of the lesion area,[272 273] after which lesion volume is calculated by multiplying with slice thickness. The larger the infarct, the more pronounced the edema and enlargement of the injured tissue by edema results in overestimation of the infarct volume. Thus, ischemic volume should be calculated with the correction of edema,[274] especially in models using proximal occlusion of the MCA for periods longer than 60 min. Besides absolute infarct volumes, the percentage of the hemisphere undergone infarction can be reported to facilitate comparison of the data from different laboratories.

In vivo MRI enables monitoring lesion progression by repeated imaging. With DWI sequence ischemic lesion can be identified as early as 3 min after the onset of ischemia[191] and MRI-based lesion volume at 72 h correlates well with the TTC-based infarct volume.[275]

1.2.4.2 Neurological status

Motor deficits are relatively objective end points of a rat stroke model and can be evaluated by a number of easy and quick methods.[192, 211, 276] Tests to examine the effects of focal ischemia on more refined sensorimotor functions include: limb placing, beam walking, grid walking, rotarod, sticky label test, and staircase test.[277] A number of cognitive tests are also available, among which Morris water maze is the prototype.[278] However, in the MCAO model, spatial memory deficits seem minimal and watermaze impairments may be attributable to sensory and motor deficits.[279]

Recently a tendency rose to use composite scores for functional evaluation in rodents. Such an increasingly used evaluation is the modified neurological severity scores, which includes a composite of motor (muscle status and abnormal movement), sensory (visual, tactile, and proprioceptive), reflex, and balance tests.[280] Despite the simplicity of administering the tasks, deficits may be specific to a certain modality or function, and could be masked by the composite score.[281] In addition, the reflexes tested in the modified neurological severity

scores (pinna and startle reflexes) are irrelevant to the damage induced with MCAO.

Following points should be considered to ensure a successful functional evaluation after stroke in a rodent model: 1) The chosen battery of functional assessments should be able to detect even mild impairments, 2) it is important to obtain baseline data before experimental manipulations, 3) for tasks that require pre-training, animals must be properly trained before surgery, 4) experimentalist should be blind to treatment conditions to help eliminate bias.[281]

1.2.5 Sources of variability in experimental ischemic stroke

Age and sex of the animals should be considered. Rodent stroke studies mostly subjected young males.[263] Female rats compared to male rats sustain smaller infarcts after MCAO, even in the presence of an additional pathology, such as diabetes and hypertension.[282-285] This is due to the protective effect of estrogens,[286] which is lost after ovariectomy.[285] Stroke pathophysiology differs between the aged and young rats. Ischemic stroke in aged rats are associated with increased ischemia/reperfusion injury, earlier disruptions of the blood-brain barrier, exacerbated neuronal degeneration, higher mortality, reduced functional outcome, and reduced angiogenesis.[287-290] Response to t-PA[291] or to a neuroprotective agent may also vary depending on the age of the animal.[292, 293] Effectiveness of a neuroprotective agent in aged animals[50] illustrates a larger target population for such candidate drug.

Strain-dependent alterations in ischemia susceptibility are well-recognized.[294-298] Fischer rats are quite unsuitable for suture MCAO.[295] Sprague-Dawley rats are most often used in stroke research, but with very variable results.[166] Strain of the rat may be a factor affecting the outcome in preclinical drug studies.[299-301] Some authors suggest Wistar Kyoto rat the best choice, because it has a sustained vascular anatomy and its genetic relationship to the spontaneously hypertensive stroke-prone strains makes Wistar Kyoto rat an ideal stepping stone for later preclinical evaluations.[166]

The spontaneously hypertensive stroke-prone rats are species susceptible to develop larger and much less variable infarcts following MCAO compared to other rat species.[296, 302] In these rats, cortical infarcts and cerebral hemorrhages occur spontaneously, but predominant lesions are small subcortical lesions, most probably with an initiating event of BBB disruption rather than vasospasm, thrombosis, or ischemia.[303] Therefore, spontaneously hypertensive stroke-prone rats are good candidates for lacunar stroke modeling,[304, 305] but

high mortality rate restricts their use in MCAO models.

Once a candidate stroke drug is proven efficient in otherwise healthy animals, next step is to know whether it retains efficacy in the face of **comorbidities**, such as diabetes and hypertension. Animal experiments of neuroprotection rarely involve testing in these conditions,[75] although, rodent models of both type 1 and type 2 diabetes[306] and hypertension[307] are available. Type I diabetic rats subjected to thromboembolic ischemia exhibited resistance to thrombolytic reperfusion, larger infarction volumes, increased intracerebral hemorrhage,[308] and higher BBB leakage.[309] Type 2 diabetic rats showed a defective angiogenesis after transient ischemia.[310] Using these models one can decipher how these comorbidities can influence the pathophysiology of stroke.

Several **physiological parameters** need to be monitored and regulated if they alternate during an experiment of stroke. High **blood glucose** levels are not allowed because a body of evidence suggest a role for hyperglycemia concerning deterioration in infarct size, functional outcome, and blood-brain barrier damage.[311-315] Body **temperature** is easily monitored with a rectal probe. Animals should be kept normothermic for the reasons that hyperthermia worsens the ischemic damage[316] and hypothermia is neuroprotective.[317] However, a set of animals should be used for testing whether the experimental treatment itself is inducing hypo- or hyperthermia. **Arterial blood pressure and gases** should be closely followed, particularly in deeply anesthetized animals.

Many of the commonly used **anesthetics** provide some degree of neuroprotection[318] and most of the volatile anesthetics trigger ischemic tolerance,[319] for reasons why experimental groups off animals should receive the same anesthetic and the possibility that anesthetic may interfere with the effects of a candidate neuroprotectant should be considered.

1.3 BLOOD-BRAIN BARRIER

1.3.1 Structure and functions, neurovascular unit

The concept of the BBB date back to the late 18th century when Paul Ehrlich noted that an intravenously injected dye leaked into all the organs except into the central nervous system.[320] The nature of the BBB was debated well into the 1960s.[321] Current understanding of the basic structure of the BBB is built on an electron microscopic discovery, that capillary lumen bridged by tight junctions (TJ) form a continuous, impermeable membrane, which forms the primary anatomical substrate of the BBB.[322] The concept of the BBB has continued to be refined over the past few decades. Currently, it is growingly recognized that, not only cerebral microvascular endothelial cells, but multiple cells (such as glial cells, pericytes, and neurons) constitute together with extracellular matrix a functional unit, “neurovascular unit”, of which the integrity is essential to maintain homeostasis (Figure 3).[323, 324] Concerted synergism of the elements of the neurovascular unit gives rise to a BBB, which is simply more than the sum of its parts. The human adult BBB has the same approximate surface area as a tennis court, and a fifth of the cardiac output, that is, 1 to 1.5 L blood, passes over it every minute at rest.[325] Microvessels involve an estimated 95% of the total surface area of the BBB. This barrier makes the brain practically inaccessible for lipid-insoluble compounds, such as polar molecules and small ions, for which transport have to take place via carrier-mediated or vesicular mechanisms. Gases and small lipophilic molecules can diffuse through the BBB.

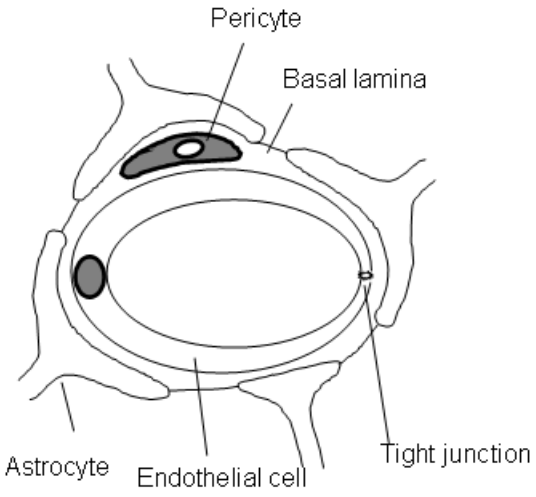

Figure 3 Schematic diagram of neurovascular unit that comprises neurons, endothelial cells, astrocytes, and pericytes. Basal membrane surrounds endothelial cells and pericytes.

1.3.1.1 Endothelial cells and pericytes

Endothelial cells of the BBB are distinguished from other endothelial cells by a number of aspects: the presence of TJs,[322] high number of mitochondria,[326, 327] small number of caveolae (membrane-bound vesicles),[328] lack of fenestrations,[329] minimal pinocytotic activity, and near absence of vesicular transport.[330] The transendothelial electrical resistance, which restricts ion permeability, is in the range of 1000–5000 Ω cm^2 in brain capillaries,[331] more than a hundred times higher than in noncerebral capillaries. Maturation of the BBB necessitates endothelial cell expression of specific molecules (overviews exist[332, 333]). Specific transport systems selectively expressed in the membranes of brain capillary endothelial cells mediate the directed transport of essential nutrients into the central nervous system or of toxic metabolites out of the central nervous system.[332] Transendothelial transport occurs, among many others, for hexoses (glucose, galactose), amino acids, purines, and nucleosides. A receptor-mediated transport system resides in brain endothelial cells for many substrates, including low-density lipoprotein, insulin, immunoglobulin G, and transferrin. Active efflux pumps are also expressed in endothelial cells. Three classes of transporters are implicated in the efflux of drugs from the brain:1) monocarboxylic acid transporters, 2) organic ion transporters, and 3) multidrug resistance transporters (prototype is P-glycoprotein).[334] Enzymatic roles of the endothelial cells comprise another level of barrier between cerebral circulation and brain (“metabolic BBB”). A well-known example of this enzymatic barrier is DOPA-decarboxylase within the endothelial cells, which restricts the transfer of dopamine from blood to brain.

Pericytes are located at the abluminal surface of the microvessels and encircle with their processes 30 to 70% of the capillary wall.[335] They are ensheathed by basal lamina, which separates them from endothelium and astrocyte end-feet (Figure 3). There is approximately one pericyte for every two to four endothelial cells. Pericytes are multifunctional in the brain and they are required for both the stabilization and maturation of the capillary, as well as the BBB.[336] Pericytes-lacking mice develop perinatally brain edema and hemorrhages due to increased BBBP,[337, 338] of which one essential reason is deficient TJ formation. In mouse brain during ischemia, pericytes contract and impair capillary flow.[339] Additional roles are suggested for pericytes in angiogenesis and neurogenesis occurring after stroke.[336]

1.3.1.2 Basal lamina

The basal lamina separates endothelial cells of brain vasculature from its neighboring cells (Figure 3). It is composed of different extracellular matrix proteins, including collagen and laminin. Matrix adhesion receptors, which are essential for the maintenance of the integrity of the BBB, are expressed in the endothelial cells, neurons, and glia. Integrin and dystroglycan receptors appear to bind endothelial cells and astrocyte end-feet to the individual intervening matrix components.[340]

Focal ischemia initiates a rapid loss of integrity of the extracellular matrix within the microvasculature and matrix adhesion receptors.[340] With the disappearance of antigens of the three main constituents of the basal lamina (laminin, fibronection, and collagen type IV), the basal lamina loses its integrity.[22, 341] Loss of the matrix proteins has been associated with the rapid generation of members of four protease families: matrix metalloproteinases (MMPs), serine proteases, cysteine proteinases, and heparinase, sources of which have not entirely been worked out.[342] Several lines of evidence from animal stroke experiments suggest involvement of MMP-2 and MMP-9 in digestion of basal lamina leading to BBB disruption, edema, and hemorrhagic transformation.[341, 343-348] Additionally MMPs contribute to the disruption of TJ proteins.[349, 350] Caveolin-1 was recently discovered as an upstream regulator of MMP activity after ischemia-reperfusion injury.[351] A systematic review of AIS patients indicated that serum MMP-9 levels are significantly correlated with infarct volume, severity of stroke, and functional outcome, and MMP-9 may be a predictor of development of intracerebral hemorrhage in patients treated with thrombolytic therapy.[352]

1.3.1.3 Tight junctions

TJs appear in endothelial and epithelial cells as a system of fusion with two main parameters: the complexity of strands and the association of the particles with the inner (P-face) or outer (E-face) lipidic leaflet of the membrane. Brain endothelial tight junctions are the most complex in the whole body vasculature, with respect to high number of strands (which reflects high transcellular electrical resistance) and high P-face association. TJs, along with adherens junctions, form a circumferential zipper-like structure between endothelial cells, limiting paracellular passage of hydrophilic molecules. The degree of tightness of this zipper varies within the microvasculature, as capillary endothelium proceeds to post-capillary venous endothelium, strand complexity of TJs is reduced. The detailed molecular structure of

the TJs and the impact of ischemia on BBB with respect to TJs are reviewed elsewhere.[353-357] Here, only main components of TJs are briefly summarized.

Junctional proteins can be categorized as **transmembrane proteins** and **peripheral membrane proteins.** Transmembrane components of the TJ include junctional adhesion molecule (JAM)-1, occludin, and claudins. Peripheral membrane proteins associate with TJs in the cytoplasm; these are membrane-associated guanylate kinase –like proteins, including zonula occludens (ZO)-1, ZO-2, and ZO-3.

Occludin, the first transmembrane TJ protein discovered,[358] has four transmembrane domains with two extracellular loops. Occludin is not mandatory for TJs or TJ strands to form,[359] however, presence of occludin is correlated with increased transcellular electrical resistance and decreased paracellular activity.[360] It is a critical regulatory protein for mediating TJ responses in disease states.[357] The carboxy-terminal of the occludin binds to ZO, which in turn binds to the actin cytoskeleton, localizing it to the cellular membrane. Dissociation of occludin from ZO may be related to increased BBBP after ischemia.[361]

The claudins, which share a similar membrane topography with occludin, but no sequence homology, are believed to be the major transmembrane proteins of TJs, because occludin knockout mice are still capable of forming these inter-endothelial connections, while claudin knockout mice are nonviable[362] and claudin-5 gene lacking mice show a loss of BBB integrity.[363] It is believed that claudins are responsible for the regulation of paracellular permeability through the formation of paired strands.[355] Among more than 20 identified members of claudins, at least four (claudin-1, -3, -5, and -12) are expressed by BBB endothelial cells, however, claudin-1 seems to be not targeted to the TJ.[355] Claudins interact directly with all ZO proteins. Claudin-5 and occluding mRNA expression are decreased and these TJ proteins are degraded by MMP-2 and MMP-9 early after focal ischemia.[349]

JAMs are a family of immunoglobulin superfamily proteins that localize within the intercellular cleft of TJs. JAMs participate in the assembly and maintenance of the TJs,[357] overexpression of JAMs in cells that do not normally form TJs increases their resistance to the diffusion of soluble tracers, suggesting a role for permeability control for JAMs.[364]Among several JAMs identified, JAM-A is highly expressed in the cerebrovasculature, but the status of JAMs after stroke has not yet been studied.

ZO-1 was the first peripheral membrane component identified at TJs.[365] Since then, many further cytoplasmic components of TJs have been described, such as ZO-2, ZO-3, cingulin, and afadin among others. Because the vast majority of experiments, addressing the role of these proteins for TJ formation and regulation, were performed with epithelial cells, the BBB related information on peripheral membrane proteins of TJs is still limited. ZO-1 acts as a central organizer of the TJs, linking its carboxy-terminal region to the actin cytoskeleton. Further, ZO-1 translocation from TJ membrane to cytoplasm is associated with an increased barrier permeability.[366] ZO-1 expression is reduced 24 h after focal cerebral ischemia and this correlates with increased MMP-9 activity.[346, 351, 367] MMP inhibition, nitric oxide synthase inhibition, and knocking-out of MMP-9 gene, all prevent focal ischemia-induced ZO-1 degradation and BBB disruption.

1.3.1.4 Adherens junctions

Adherens junctions are primarily composed of **vascular endothelial cadherin**, which is linked to cytoskeleton via catenins. The role of catenins in adherens junctions bears resemblance to that of ZOI proteins in TJs.[362] Disruption of adherens junctions at the BBB can result in increased BBBP.[321] Adherens junctions are functionally and structurally linked to TJs, presumably playing an important role in the localization and the stabilization of the TJs by forming a continuous belt localized near the apical end of the junctional cleft, just below the TJs.[368] The contribution of vascular endothelial cadherin and the catenins in BBB disruption following stroke remains to be investigated.

1.3.1.5 Astrocytes

More than 99% of the surface of the brain capillaries is enveloped by astrocytic foot processes, which allow communication between endothelial cells, neurons, and pericytes. Many of the factors released by astrocytes (e.g. growth factors, cytokines, extracellular matrix proteins) are able to induce specific features of the BBB in brain endothelium, which are required during BBB development.[366] Perivascular glial endfeet contribute to ionic, amino acid, neurotransmitters, and water homeostasis at the BBB level.[369] A close relationship exists between the BBB and astrocyte membrane channel (aquaporin-4, AQP4). AQP4 dysregulation is coupled with BBB dysfunction and edema formation.[370] However, consequences of focal cerebral ischemia in AQP4 knockout mice are conflicting.[371, 372] After

mild ischemia post-stroke brain swelling is not influenced by the lack of AQP4, but mice score worse than their wild-type littermates.[372] In contrast, after permanent ischemia swelling and neurological scores are improved in AQP4 knockout mice.[371]

1.3.2 Methods to evaluate BBB permeability

The history of BBBP quantification stretches back at least 50 years.[373] Currently, BBBP studies utilize two main methods: in vitro analysis or in vivo imaging of an extravasated exogenous tracer. Tracers can be classified into two categories: indicators for solute and ion permeability and indicators for protein permeability.[374] The most common contrast agents, typically gadolinium diethylenetriaminepentaacetic acid (Gd-DTPA, MW 550 Da), are in vivo imaging markers for solute and ion permeability, while Evans blue (EB) dye, which binds to albumin (MW ≈68 kDa), is accepted as the gold standard marker for protein permeability.[375]

1.3.2.1 Qualitative methods

1.3.2.1.1 Visualization of dye extravasation

To monitor vascular protein leakage, in vivo studies most often used EB, which is an azo dye (MW 980 Da) binding irreversibly to plasma albumin in a 10:1 molar ratio.[376] The EB-albumin complex extravasates from blood vessels into the surrounding tissues when the BBB is disrupted. Intravenously injected 2% EB in saline (intraperitoneal administration is also acceptable[377]) should circulate in the vasculature for a minimum of 30 min. Circulation times vary from 20 min to 24 h between experiments, however, accumulation with longer circulations than 30 min barely affects the results.[377] Before terminating the experimental animal, the dye is cleared from the bloodstream by transcardiac saline perfusion. Macroscopically, blue-stained tissues indicate areas of BBB disruption. Red fluorescence of EB (excitation at 620 nm, emission at 680 nm) can be visualized with a fluorescence microscope or scanner.

1.3.2.1.2 Visualization of contrast agent extravasation

Intravenously injected contrast agent, of which bolus administration is preferable in conditions other than tumors,[378] leaks into extravascular space in the presence of BBB disruption. Once in the extravascular space, voxels with higher concentrations of contrast

agent will appear bright on T1-weighted MR images due to T_1 relaxation time shortening caused by the contrast agent. Simple visual analysis of this enhancement has been found to be a valuable tool to depict BBB disruption after many pathological conditions including AIS. Early BBB disruption visualized with MRI predicted subsequent hemorrhagic transformation in both experimental[142, 143] and clinical settings.[147, 379, 380] Although qualitative visual evidence of parenchymal enhancement on postcontrast T1-weighted MRI is a highly specific (specificity approximately 85%) predictor of hemorrhagic transformation, it is infrequent during the crucial hours after symptom onset and insensitive (sensitivity near 35%).[381]

1.3.2.2 Quantitative methods

1.3.2.2.1 Colorimetric and fluorometric methods

The extravasated EB is extracted after the brain tissue is homogenized, centrifuged, and the supernatant is diluted. Homogenization can include the entire brain, ischemic hemisphere, or ischemic area only. Colorimetry at the absorbance of 600 to 620 nm after the subtraction of background (baseline absorbance between 500 and 740 nm) determines EB content within the limitations of the blue color. Fluorescence spectrophotometer at an excitation wavelength of 620 nm and an emission wavelength of 680 nm detects EB 100 times more sensitively than the colorimetric method.[382, 383]

1.3.2.2.2 Autoradiographic method

Although radiolabeled compounds enable highly sensitive measurements, safety concerns and the need to process tissues for scintillation counting preclude immunochemical or histological evaluation in the same experimental animals.[384] Radiolabeled tracer is left in the circulation for some time (typically 10 to 30 min), when a number of arterial blood samples are collected. Brain samples undergo several procedures lasting over 24 h, thereafter Beta counting is performed in a spectrometer. Blood concentration of the radiolabel is measured by liquid scintillation counting. A blood-to-brain transfer ratio for the tracer is then determined according to an analytic method.[385] ^{14}C-sucrose (MW 342 Da), ^{3}H-sucrose (MW 341 Da), ^{3}H-inulin (MW 5 kDa), and ^{3}H-aminoisobutyric acid (MW 103 Da) were often applied in experimental models of stroke studying BBBP.[45, 344, 386, 387]

1.3.2.2.3 Fluorescence methods

Fluorescent-labeled tracers can be introduced intravenously; after obtaining simultaneous blood samples, tissue and blood concentration of fluorescent-labeled tracer can be quantified by a spectrofluorometer. By analyzing these data with an analytic method, as it is done in autoradiography analyses, BBBP to the tracer is estimated. Availability of intravital confocal microscopy to monitor extravasated fluorescent tracer is a substantial advantage of fluorescent-labeling technique.[388, 389] BBBP to both proteins and solutes can be examined via the use of fluorescein isothiocynate-albumin (MW 67 kDa)[390] and sodium fluorescein (MW 376 Da),[384] respectively.

1.3.2.2.4 Other methods

Immunohistochemical staining methods enable the detection and quantification of an extravasated endogenous macromolecule, such as IgG[389] and albumin,[391] or of blood cells, such as polymorphonuclear leukocytes.[389] A recent technique, near-infrared optical imaging, provides intravital evaluation of BBBP with a higher spatial resolution than intravital confocal microscopy.[392, 393]

1.3.2.2.5 Dynamic contrast-enhanced MRI (DCE-MRI)

As mentioned previously, contrast enhancement of the brain tissue indicates BBB leakage. Dynamic method of permeability assessment is more sensitive to subtle T1 enhancements than simple postcontrast SE imaging alone, because DCE-MRI provides about several dozens of sampling times to characterize the enhancement, which increases conspicuity of low “effect-to-noise” ratio.[139]

Determination of contrast agent concentration is a challenge that usually is solved via the measurement of the T_1 of the tissue and the change in T_1, with the assumption that the increase in T_1 relaxation rate is proportional to the concentration of contrast agent.[394] For this purpose, before, during, and after an intravenous bolus contrast agent, T1-weighted gradient-recalled echo imaging of the brain is repeated dozens of times over a course of several minutes. Then, one can analyze the data gathered with this DCE-MRI technique by one of available mathematical models,[394] quantify contrast as a function of time, and estimate BBBP.[381] In stroke animal experiments, a graphical approach to analyze DCE-MRI data, the Patlak plot approach,[395] proved relevant in comparison to gold standard methods.[142, 396, 397]

and is increasingly used.[291, 389] Clinical use of BBBP imaging with DCE-MRI and Patlak method is yet in its infancy, but retains promise for estimating clinical prediction of hemorrhagic transformation after t-PA treatment.[398] A disadvantage of the BBBP MRI is the long acquisition time of the images, however, a recent study reported three and a half minutes as feasible.[399]

1.3.3 BBB disruption in experimental stroke

The profile of BBB disruption following transient focal cerebral ischemia is typically described as biphasic, referring constantly to same studies (more specifically to studies by Kuroiwa et al,[400] Belayev et al,[401] Rosenberg et al,[344] and Huang et al[386]). These deserve a closer look and will be discussed in detail in Discussion. Table 1 resumes characteristic features of all animal studies which reported biphasic BBB disruption after focal ischemia-reperfusion injury. If one attempts to combine results from all these studies (Figure 4), it becomes clear that some agreement exists on the decreased leakage around 24 h and increased leakage around 48 h after reperfusion.

Table 1 Animal studies of transient focal ischemia reporting biphasic BBB leakage

Ischemia model	Animal	BBB evaluation method	Evaluated time-points*	Open	Closed	Less open	More open	References
Proximal MCA ligation for 1 h	cat	EB qualitative	2, 3, 5, 72 h	0-2 h	3 h	NA	5, 72 h	Kuroiwa et al.[400]
Intraluminal MCAO for 2 h	rat	EB quantitative	0-1, 1-2, 1-3, 22-24, 46-48 h	1-3 h	0-1 h	22-24 h	46-48 h	Belayev et al.[401]
Intraluminal MCAO for 2 h	rat	14C-sucrose quantitative	3, 6, 15, 24, 48, 120, 336 h	3 h	336 h	6, 15, 24, 120	48 h	Rosenberg et al.[344]
Distal MCA ligation for 2 h	SHR	3H-sucrose quantitative	1.5-2 min, 1, 4, 22, 46 h	1.5-2 min	NA	1, 4, 22 h	46 h	Huang et al.[386]
Intraluminal MCAO for 2 h	rat	EB qualitative	2, 6, 24, 48 h	6 h	NA	2, 24 h	48 h	Wu et al.[443]
Intraluminal MCAO for 2 h	rat	CE-MRI semiquantitative	15 min, 3, 6, 24, 72 h	15 min-6 h	NA	NA	72 h	Veltkamp et al.[438]
Intraluminal MCAO for 1,5 h	rat	CE-MRI semiquantitative	4, 24, 48 h	4 h	NA	24 h	48 h	Pillai et al.[444]
Intraluminal MCAO for 1 h	mouse	EB qualitative	0-4, 4-8, 8-12, 12-16, 16-20 h	4-8 h	8-12 h	16-20 h	12-16 h	Klohs et al.[392]
Intraluminal MCAO for 1 h	mouse	NIRF imaging qualitative	4-8, 8-12, 12-16 h	4-8 h	8-12 h	12-16 h	NA	Klohs et al.[392]

*time-points after reperfusion
BBB, blood-brain barrier; **EB**, Evans blue; **CE-MRI**, contrast-enhanced magnetic resonance imaging; **MCA**, middle cerebral artery; **MCAO**, MCA occlusion; **NA**, not applicable; **NIRF**, near-infrared fluorescence; **SHR**, spontaneously hypertensive rat

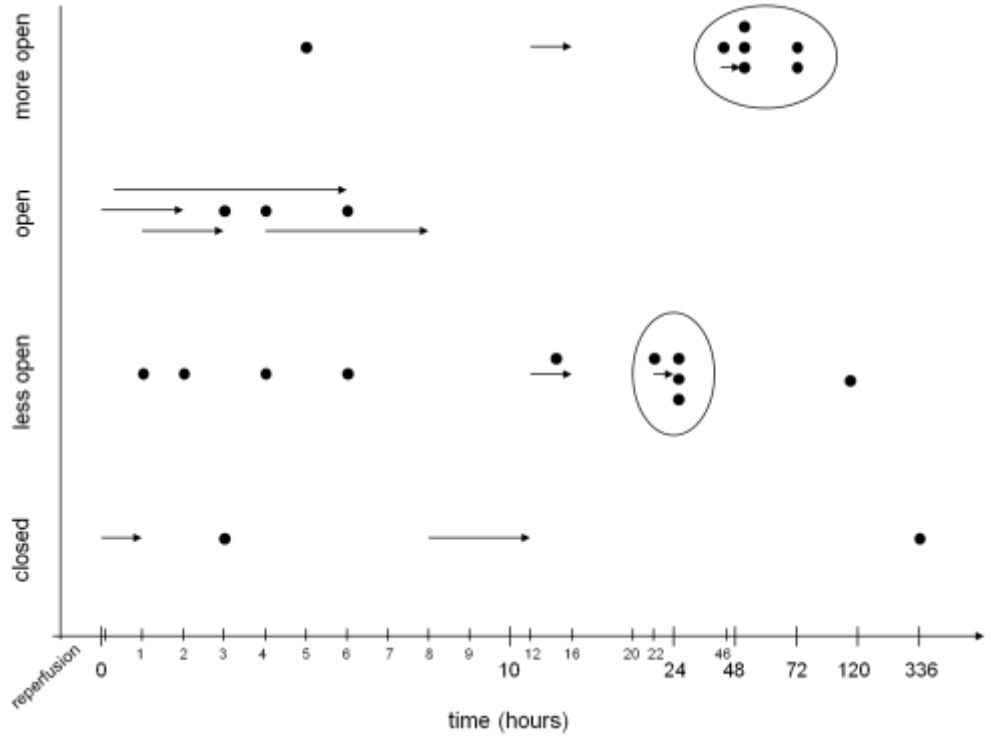

Figure 4 Compiled BBB opening data of the studies resumed in Table 1. The ordinate is the BBB status. Closed circle indicates data collection at a single time-point; arrow indicates data collection during a period. Note accumulation of the data on specific time-points (ovals).

1.3.3.1 Theories of biphasic BBB disruption

The first phase of the biphasic permeability has been attributed to increased inflammatory and oxidative stress on the BBB, in conjunction with enzymatic degradation of the ECM by MMPs.[44, 344] A synthetic MMP inhibitor blocked this initial opening, but had no effect on delayed aggravation of BBB leakage.[344, 349] Associates of **the final phase** of the biphasic BBBP appears as angiogenesis[357] and induction of MMP-3 and MMP-9 by cyclooxygenase-2[402, 403] The period between the two barrier openings, the "**refractory period**", was assumed as a result of normalization of the BBB function due to subsiding hyperemia and re-establishment of autoregulation.[400] Alternatively, post-ischemic inhibition of pinocytotic transport[400] and no-reflow phenomenon were used to explain the transient "closure" of the BBB.

Some authors acknowledge a **triphasic** course for BBB opening, adding a hyperacute

opening, which occurs immediately after reperfusion and prior to above stated phases.[357] Theoretical explanation for this initial phase is opening of the BBB with passive disassembly of TJs due to hyperemia and closing by the following pericyte contraction, which supports the BBB.[357] Actually, hyperemia has coincided with the first phase of opening reported by Kuroiwa et al.[400] and Huang et al. confirmed a hyperacute opening, but found as the first phase of the biphasic opening.

1.3.3.2 Continuous BBB disruption

In recent years, with the increasing use of BBBP imaging in experimental stroke studies, accumulating data suggest that BBB leakage to contrast agents (because most commonly Gd-DTPA is used), thus to solute and ions, occurs in a continuous pattern. In addition, a review of previous studies reporting a biphasic BBB opening (Table 1) disclose that some studies in fact have failed to show any closure between two phases of increased BBB leakage, therefore they are also included in Table 2, which summarizes animal studies showing continuous BBB leakage after focal ischemia-reperfusion injury.

Table 2 Animal studies of focal cerebral ischemia suggesting a continuous BBB disruption.

Ischemia model	Animal	BBB evaluation method	Evaluated time-points*	References
Intraluminal MCAO for 2 h	rat	albumin fluorescence qualitative	6, 12 , 24 h	Albayrak et al.[400]
Proximal MCA ligation for 3 h	rat	CE-MRI qualitative	0.5, 1.5, 2.5, 3.5, 4.5, 6 h	Kastrup et al.[433]
Intraluminal MCAO for 1 and 2.5 h	rat	CE-MRI qualitative	0.5, 1.5, 2.5 h	Neumann-Haefelin et al.[434]
Intraluminal MCAO for 2 h	rat	EB qualitative	2, 6, 24, 48 h	Wu et al.[443]
Intraluminal MCAO for 1.5 h	rat	CE-MRI semiquantitative	0, 1, 4 days	Lennmyr et al.[435]
Intraluminal MCAO for 2 h	rat	CE-MRI semiquantitative	3, 5, 8, 12 h	Nagel et al.[436]
Intraluminal MCAO for 2 h	rat	CE-MRI semiquantitative analysis	15 min, 3, 6, 24, 72 h	Veltkamp et al.[438]
Intraluminal MCAO for 1.5 h	rat	CE-MRI semiquantitative analysis	3.5, 24, 120 h	Nagel et al.[437]
Three-vessel occlusion for 1 h	rat	DCE-MRI quantitative	1, 3, 7, 14, 21 days	Lin et al.[439]
Intraluminal MCAO for 1.5 h	rat	CE-MRI semiquantitative analysis	4, 28, 48 h	Pillai et al.[444]

*time-points after reperfusion
BBB, blood-brain barrier; **CE-MRI**, contrast-enhanced magnetic resonance imaging; **MCA**, middle cerebral artery; **MCAO**, MCA occlusion

1.4 BRAIN ISCHEMIA AND STANNIOCALCIN

Stanniocalcin (STC) is a glycoprotein originally discovered in bony fish, in which it acts as a calcium/phosphate regulating hormone.[404] In human, two members of STC homologs were discovered: STC1, which shares about 72% amino acid sequence and 80% protein similarity to fish[405] and STC2, with approximately 34% identity and 60% homology to amino acid sequences to STC1.[406] STCs are made in virtually all tissues and regulate various biological functions. Based on their ubiquitous expression patterns and generally undetectable levels in blood serum, it is unlikely that the mammalian STCs play important roles in serum Ca2+/Pi homeostasis.[407] Accumulating evidence denote the involvement of STC1 and STC2 in the subcellular functions of mitochondria and endoplasmic reticulum, respectively, particularly responding to oxidative stress and unfolded protein response.[407-411]

STCs are widely expressed in brain neurons, in choroid plexus epithelium, and to some degree in microvascular endothelial cells.[412-415] Considerable data suggest a neuroprotective role for STCs. Pathological events, such as focal ischemia,[416] traumatic injury,[417] focal cryoinjury,[418] and hypoxia[418] increase brain levels of STC1. Overexpression of STC1 was linked to expression of interleukin 6 (IL-6)[418] and increased neuronal resistance to hypoxia and hypercalcemia in vivo.[416] Enhanced brain expression of STC2 followed focal brain ischemia and hypoxia.[411] Intracerebroventricular injection of STC2 protected hippocampal neurons from kainic acid toxicity.[419]

There exist no previous data regarding STCs and the BBB. Some STC1 staining was observed in brain endothelial cells lining the capillaries.[413] In studies of angiogenesis, STC1 upregulation is a striking finding in endothelial cells.[420] A role for STC1 in maintaining permeability in human coronary artery endothelial cells emerged during cardiovascular inflammation.[421] In vivo hypoxia induced, among others, STC genes in vascular endothelial cells.[422] In human brain microvascular endothelial cells, β-amyloid peptide toxicity induces considerable STC-1 gene expression, which possibly exerted some antiinflammatory and antiapoptotic effects.[414]

2 AIMS OF THE STUDY

1. To critically address the presumed biphasic BBB opening following transient focal cerebral ischemia by a systematic, quantitative, and multimodal approach. (I)

2. To compare the gold standard ex vivo method of BBBP evaluation (quantification of extravasated Evans blue dye) to an in vivo method (DCE-MRI), that may be applicable to humans. (I,II)

3. To compare BBBP to a large (Evans blue-albumin, MW ≈68 kDa) and small molecule (contrast agent Gd-DTPA, MW 550 Da). (I,II)

4. To characterize spatial features of BBB leakage within the ischemic area and to find any correlation between the extent or severity of ischemia and the degree of BBB leakage. (I,II)

5. To extend the findings from studies I and II with a more powerful study design, that included repeated evaluations of post-ischemic BBBP in the same animals. (III)

6. Using genetically modified STC-1 deficient mice in the scenario of transient focal ischemia with and without prior HPC, to test the necessity of STC-1 for HPC to occur; additionally, to uncover the effect of STC-1 deficiency on BBBP. (IV)

3 MATERIALS AND METHODS

All experiments were carried out in Biomedicum Helsinki on the premises of Department of Neurology, Helsinki University Central Hospital. The Animal Research Committee approved all studies.

3.1 ANIMALS

Adult male **Wistar rats** (Harlan Nederland, Horst, The Netherlands), weighing 290 to 340 g (I,II, and III) and adult male **STC1 knockout (STC1$^{-/-}$) mice** on a C57BL/6 background (courtesy of Dr. Andy C.-M. Chang, Children's Medical Research Institute, Parkville, Australia) with **NMRI** (Harlan Nederland, Horst, The Netherlands) wild-type controls weighing 25 to 40g (IV) were used. Previous characterization of the STC1$^{-/-}$ mice revealed normal viability and fertility and no gross histological or morphological abnormality.[423] Prior to surgery, rats were housed in groups of five and mice in groups of 10 and after the surgery individually, in a temperature- and humidity-controlled environment and 12/12 h light/dark cycle with free access to food and water. All efforts were made to minimize animal distress and to reduce the number of animals used.

3.2 ANESTHESIA

Rats received an intraperitoneal injection of **ketamine** hydrochloride (50 mg/kg, Ketalar, Parke-Davis, Detroit, MI, USA) and a subcutaneous injection of **medetomidine** hydrochloride (0.5 mg/kg, Domitor, Orion, Espoo, Finland). Mice received same drugs, but subcutaneously.

3.3 MONITORING OF PHYSIOLOGICAL PARAMETERS

In rats, **arterial blood pressure** monitoring (Olli Blood Pressure Meter 533, Kone, Espoo, Finland) required left femoral artery catheterization by a PE-50 polyethylene tube. Left femoral vein catheter served for injections of contrast agent Gd-DTPA (1mL/kg, Magnevist, 0.5 mmol/mL, Schering, Germany) (I, II, and III) and EB dye (3 mL/kg of 2% solution; 20

mg/mL dissolved in 1% albumin, Sigma-Aldrich, Steinheim, Germany) (I). Catheters were removed after reperfusion, except in Study III the femoral vein catheter was kept in place for one week. **Rectal temperature** was monitored and maintained at the physiological ranges with a heating blanket during the surgery and MRI.

3.4 STUDY DESIGNS

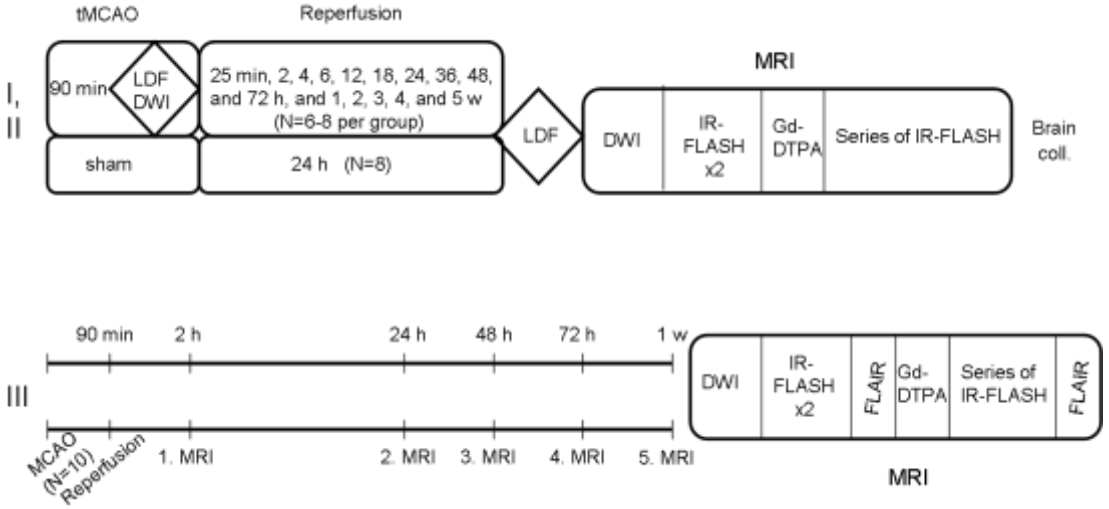

Figure 5 Schematic presentation of study designs of Study I, II, and III. Rats (overall 123) with adequate ischemia/reperfusion were allocated to 15 study groups based on the post-reperfusion interval (I,II). Study III included repeated MRI of the same animals at 5 time-points after reperfusion and MRI protocol was identical to that of Study II, except it included additionally pre- and postcontrast FLAIR images.
DWI, diffusion-weighted imaging; FLAIR, fluid-attenuated inversion-recovery; Gd-DTPA, gadolinium diethylenetriaminepentaacetic acid; IR-FLASH, inversion recovery snapshot-fast low-angled shot; LDF, laser-Doppler flowmetry; tMCAO, transient middle cerebral artery occlusion.

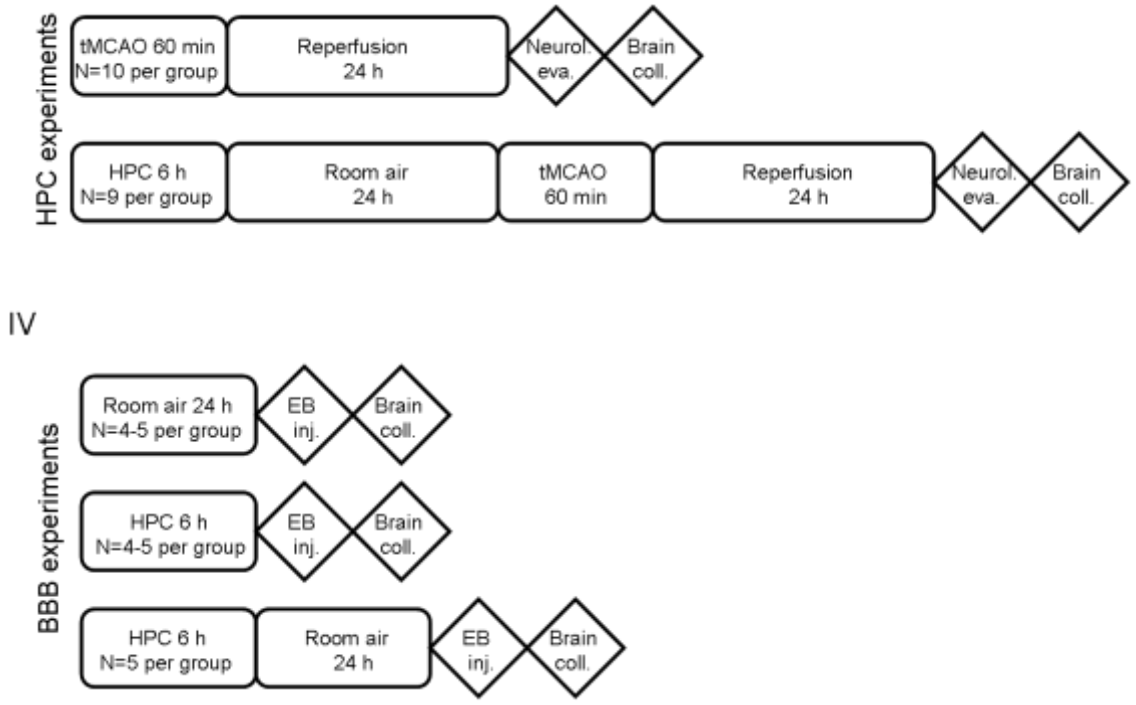

Figure 6 Schematic presentation of study design of Study IV. Each row of the schema resumes a separate experiment, which included two groups of mice: Wild-type and stanniocalcin knockout mice. Coll, collection; EB inj, Evans blue injection; HPC, hypoxic preconditioning; Neurol eva, neurological evaluation; tMCAO, transient middle cerebral artery occlusion.

3.5 FOCAL CEREBRAL ISCHEMIA MODEL

Intraluminal suture occlusion of the right MCA induced focal cerebral ischemia.[274] Rat occluders were prepared from 4-0 nylon monofilament suture (Ethilon Nylon Suture, ETHICON Inc., Somerville, NJ, USA) with its tip rounded by heating near a soldering iron and then coated with low viscous silicone (Provil L, Bayer Dental, Leverkusen, Germany) to a 0.38 to 0.40 mm diameter. Under general anesthesia and the rat lying on its back, the common carotid artery and external carotid artery were exposed through a ventral midline neck incision. The proximal common carotid artery and the origin of the external carotid

artery were ligated. The occluder was inserted into the common carotid artery via an arteriotomy and was advanced into the internal carotid artery approximately 17 mm above the carotid artery bifurcation. At this point, a mild resistance indicated that the tip of the occluder was lodged into the proximal anterior cerebral artery and occluded the origins of the MCA and the posterior communicating artery.

Mouse model was slightly different.[424] Mouse occluders were prepared from 5.0 monofilament nylon suture (Ethilon Nylon Suture, ETHICON Inc., Somerville, NJ, USA) with their tips rounded to 0.15 to 0.20 mm diameter. Occluder was inserted into the internal carotid artery through an arteriotomy made in the external carotid artery. Insertion length from common carotid artery bifurcation was approximately 9 mm. The ligature of the common carotid artery was released after MCAO. Reperfusion was accomplished by withdrawing the suture occluder **90 min** (I, II, and III)
or **60 min** (IV) after MCAO. Sham-operated animals underwent the same surgery, except that the suture occluder was withdrawn before causing MCAO.

3.6 HYPOXIC PRECONDITIONING

Mice (6-8 per procedure) received hypoxia in an airtight transparent low-oxygenation chamber perfused with **8% vol/vol oxygen in nitrogen for six hours**.[418] During hypoxic treatment mice exhibited reduced locomotor activity, which was normalized within minutes after returning to normal environment.

3.7 LASER-DOPPLER FLOWMETRY

CBF was measured in all animals with LDF (OxyFlo, Oxford Optronix Instruments, Oxford, UK) by applying a flexible fiber-optic probe. The scalp was incised in the midline exposing the skull. In rats, the skull area over the ipsilateral MCA region (1.0-2.5 mm caudal and 6.0 mm lateral from the bregma) was thinned by a dental drill to allow measurement via the probe. In mice, without drilling, the probe was located over the territory supplied by the MCA (2 mm caudal and 3-4 mm lateral from the bregma). CBF was repeatedly measured before and during MCAO as well as after reperfusion.

3.8 MRI STUDIES

MRI studies were performed with a **4.7 T scanner** (PharmaScan, Bruker BioSpin, Ettlingen, Germany) using a 90-mm shielded gradient capable of producing a maximum gradient amplitude of 300 mT/m with an 80-μs rise time. The linear birdcage RF coil used had an inner diameter of 38 mm. Following shimming, a pilot imaging sequence (a multi-slice spin-echo pulse sequence with repetition time/echo time: 200/8.9 ms, matrix size: 128X128, field-of-view: 5.0 cm, number of averages: 1, slice thickness: 2 mm) served for reproducible positioning of the animal in the magnet at different MRI sessions. **DWI** scans were acquired using a spin-echo echo-planar imaging sequence (repetition time/ echo time: 4000/80 ms, matrix size: 128x128, field-of-view: 40x40 mm, slice thickness: 2 mm) with three b values (b0: 0.4, b1: 1280, and b2: 2342 s/mm2, diffusion was measured in the read gradient direction). Longitudinal relaxation time (T_1 value) measurements were obtained with an inversion recovery snapshot-fast low-angled shot (**IR-FLASH**) sequence (repetition time/ echo time: 2.2/1.4 ms, 12 inversion delays from 140 to 3230 ms, flip angle: 5°, matrix size: 128×128, field-of-view: 40×40 mm, slice thickness: 2 mm, number of averages: 15). **FLAIR** images were acquired with rapid acquisition with relaxation enhancement sequence (repetition time/echo time: 10,000/38.6 ms, inversion time: 1800 ms, matrix size: 256×128, zerofilled to 256×256, field-of-view: 40×40 mm, echo train length: 16, number of averages: 1, slice thickness: 2 mm).

During imaging, **rectal temperature** was maintained at the physiological ranges by use of a MRI compatible heating pad and pump (Gaymar Industries, Orchard Park, NY, USA).

During DWI, a 7-slice data set was obtained covering the entire brain except the olfactory bulb. The first axial slice was selected posterior to the olfactory bulb, navigating by the rhinal sulcus detected on the pilot image, and the following slices were placed caudally at 2-mm intervals. Images of IR-FLASH and FLAIR were obtained with a single axial slice at the coordinate of the third slice of the DWI, the optic chiasmal slice, which is approximately at 0.5 mm posterior to the bregma. All the analyses, except ischemic volume calculation, were performed on this slice. The IR-FLASH scan with inversion delay −1826 ms was chosen as the T1-weighted image (**T1-WI**). The DWI scan with b0 provided the T2-weighted image (**T2-WI**). T1 maps were constructed from each IR-FLASH sequence and apparent diffusion coefficient (**ADC**) maps from DWI sequences using ParaVision 2.1.1. Software (Bruker BioSpin, Ettlingen, Germany). All image analyses described below used ParaVision 2.1.1.

Software. Regions of interest (ROIs) were placed manually on the ipsilateral hemisphere and control ROIs were placed on the homologous locations in the contralateral hemisphere (Figure 7).

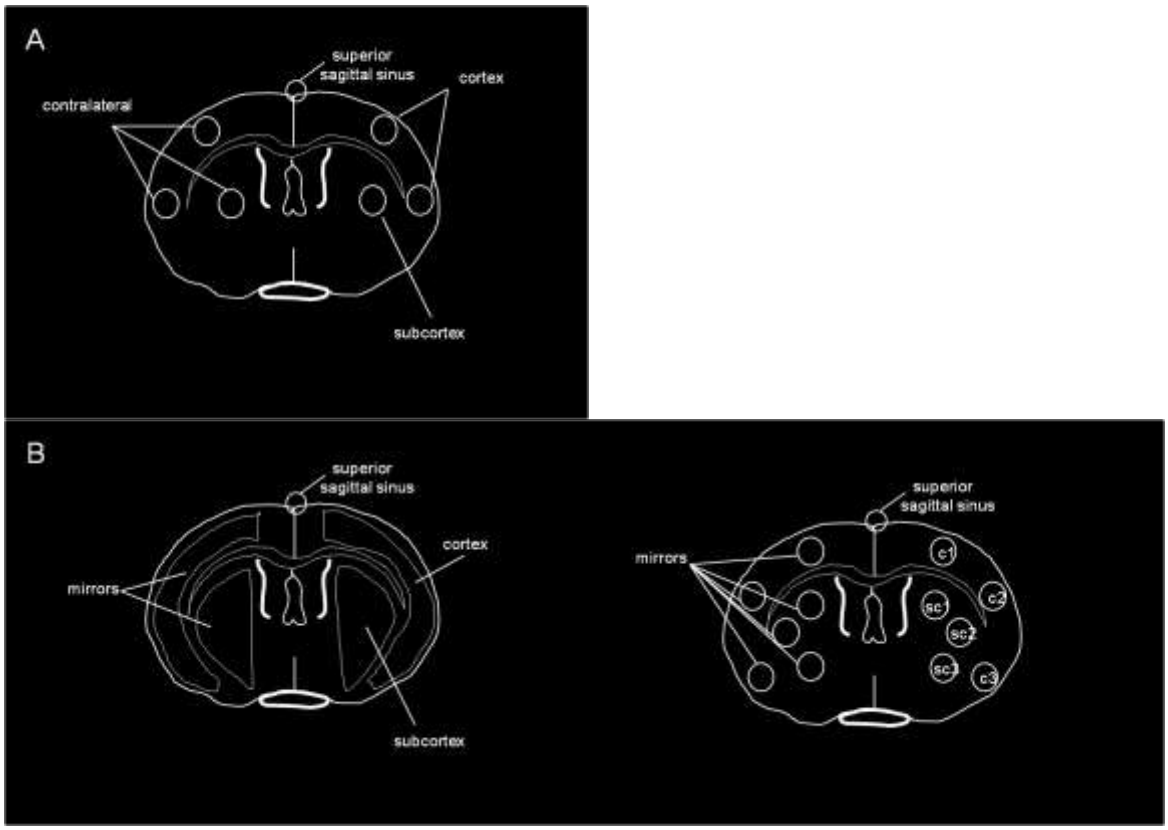

Figure 7 Regions of interest (ROIs). A, from Study II and B, from Study III.

3.8.1 Patlak plotting

Patlak plotting[395] is a graphical analysis method of the plasma and tissue MRI data, to estimate the blood-to-brain transfer rate constant of the contrast agent (K_i) in the permeability-limited circumstances of a two-compartmental model, such as focal brain ischemia. It is assumed that there is a steady phase in the blood-to-brain distribution of the tracer during which the tracer crosses the BBB in one-way direction, towards the brain tissue. If plasma and tissue MRI data, which are collected repeatedly overtime, are plotted, this results in an uptake curve with a linear phase of which the slope approximates Ki.

To make the Patlak plots, arterial plasma and tissue concentration of contrast agent (Gd-

DTPA) are needed. Intravenous administration of Gd-DTPA leads to a change in reverse longitudinal relaxation rates (R1) of protons in its distribution area. With the assumptions that 1) the increase in relaxation rate (ΔR_1) is proportional to the concentration of contrast agent[394] and 2) tissue relaxivity (r_{1t}) and plasma relaxivity (r_{1p}) are the same,[327] following equation is acquired:

$$\Delta R_{1t}(t) = R_{1t}(t)-R_{1t0}(t) = r_{1t}C_t(t) \text{ and } \Delta R_{1p}(t) = R_{1p}(t)-R_{1p0}(t) = r_{1p}C_p(t)\ (1\text{-Hct})$$

where (t) is the duration of the experiment, $R_{1t0}(t)$ is the tissue longitudinal relaxation rate before Gd-DTPA injection and $R_{1t}(t)$ at the end of experiment; $R_{1p0}(t)$ is the plasma longitudinal relaxation rate prior to Gd-DTPA injection, and $R_{1p}(t)$, at the end of the experiment; $C_t(t)$ is the tissue concentration of the Gd- DTPA at the end of the experiment; $C_p(t)$ is the plasma concentration of GD-DTPA at the end of the experiment; Hct is the hematocrit (arbitrarily 43%). C_p of Gd-DTPA was measured from the superior sagittal sinus. This approach of approximating arterial input function of the tracer in arterial blood through measurements from venous system has no significant affect on Ki results.[425]

Accordingly, the relation between tissue and plasma concentrations of Gd-DTPA is described in the following equation:

$$C_t(t) = V_p\, C_p\,(t) \;+\; K_i \int_0^t C_p\,(\tau)\, d\tau$$

where C_p (T) is the plasma concentration at a series of times over the duration of the experiment and is used to calculate the arterial-concentration time integral; K_i is the blood-to-brain transfer rate constant of Gd-DTPA; V_p is the blood plasma volume.

Patlak plots are constructed by plotting $C_t(t) / C_p(t)$ (ordinate) versus $\int_0^t C_p\,(\tau)\, d\tau / C_p\,(t)$ (abscissa). The abscissa has the units of time, which is not the real time but the concentration-adjusted time ($t_{stretch}$). (Figure 8)

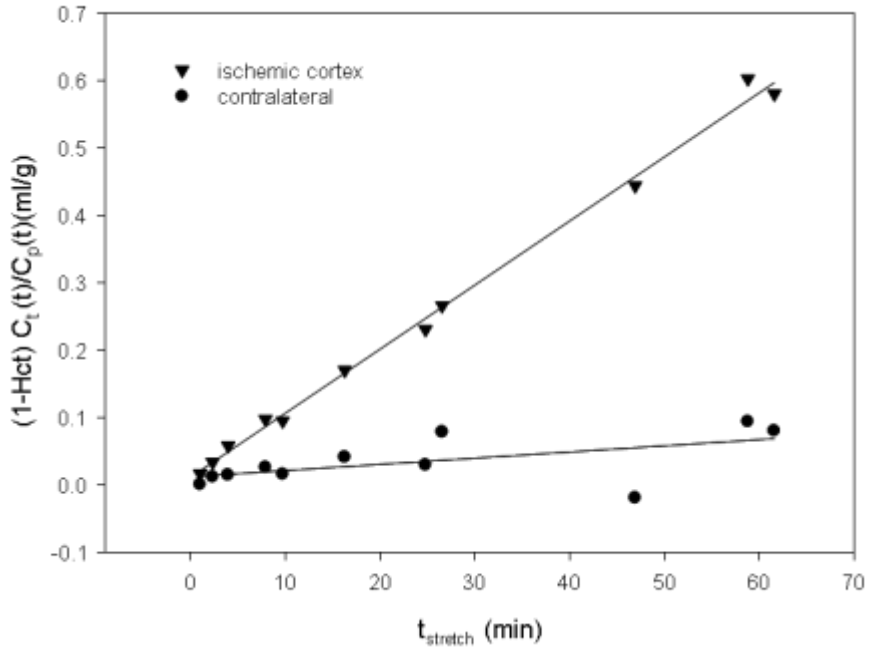

Figure 8 Patlak plots of a representative rat. Imaging was performed at 2 hours after reperfusion that followed 90-min ischemia. The ordinate is the ratio of brain tissue concentration of Gd-DTPA to its plasma concentration. The abscissa represents concentration-adjusted time, stretch time. Plotted data showed linearity during whole imaging time (20 to 30 min).

3.8.2 Imaging protocol

All rats underwent DWI to ensure the presence of stroke immediately after induction of MCAO confirmed by LDF. Sham animals underwent MRI 24 h after sham operation, otherwise MRI was run at the corresponding time-points after reperfusion (see Study design). MRI protocol included: a **pilot** sequence, **DWI**, a pair of **IR-FLASH** sequence, and a post-contrast IR-FLASH sequence 25 min following **a bolus of Gd-DTPA injection** (I) or **repeated IR-FLASH** sequences at approximately 1-min intervals for 20 to 30 min after Gd-DTPA injection (II, III) and pre- and post-contrast **FLAIR** sequences (III). MR imaging took 25 to 35 min.

3.9 NEUROLOGICAL EVALUATION

Sensorimotor performance of mice was scored 24 hours after reperfusion (IV), as follows: 0, normal; 1, contralateral paw paralysis; 2, contralateral paw paralysis plus decreased resistance to lateral push; 3, 2 plus circulating behavior; 4, no spontaneous walking with depressed consciousness; and 5, death.[426]

3.10 TISSUE HANDLING

After various periods of time following reperfusion (see Study design), animals were reanesthetized with a lethal dose of intraperitoneal pentobarbital (1 mL/rat, 0.04 mL/mouse, Mebunat, 60 mg/mL, Orion). For **cardiac perfusion**, after a midline abdominal incision, the chest was opened. A catheter was inserted into the aorta via the left ventricle and ice cold 0.9% saline (200 mL for rats and 30 mL for mice) was infused into the aorta at approximately 100 mmHg pressure. The blood drained out via an incision made to the right atrium. The brains then were quickly collected and dissected into six 2-mm-thick (1-mm-thick in mice) coronal slices for digital imaging (Sony, Tokyo, Japan). Every 3rd slice was cut into two halves coronally (rostral and caudal). The rostral part was embedded in Tissue-Tek (Sakura Finetek Inc., Tokyo, Japan), snapfrozen in liquid nitrogen, and kept thereafter at 80 °C until 15-µm of sections were cut for analysis of EB-albumin extravasation (I) and 150-µm sections were cut for mRNA analysis (IV). All the remaining slices were stained with 0.2% TTC at 37 °C (IV) and immersion-fixed in 10% formaldehyde.

3.11 ISCHEMIC LESION ASSESSMENT

3.11.1 MRI-based infarction

At acute time-points (<72 h) DWI and otherwise T2-WI were used to calculate the area or volume of the ischemic lesion. Regions with increased signal intensity (restricted diffusion in DWI and increased water content in T2-WI) were manually outlined. Area calculation was based on the optic chiasmal slice, where ischemia involved both cortex and subcortex (Figure 9). Lesion areas from all slices were summed up and multiplied by slice thickness, yielding the uncorrected lesion volume. Afterwards, the volumetric difference between the right and left hemisphere (due to swelling) was subtracted from the uncorrected lesion volume, yielding the (edema) corrected lesion volume.

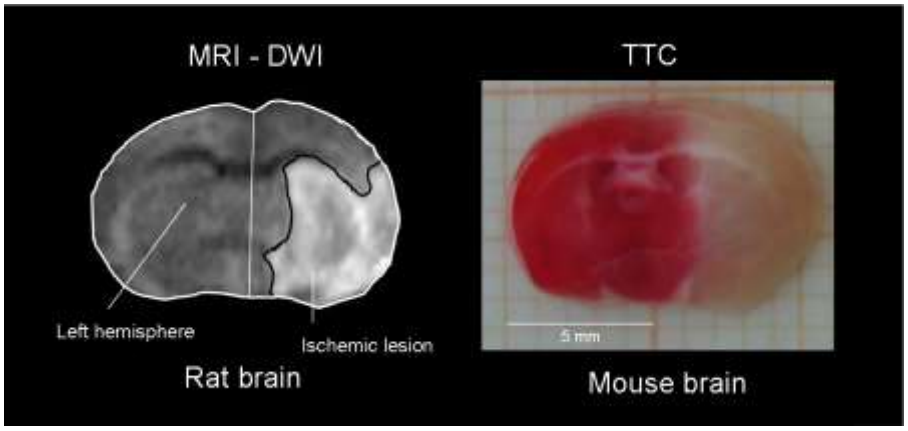

Figure 9 Ischemic lesion delineation. On the left is magnetic resonance imaging (MRI) diffusion weighted image (DWI) taken 2 h after 90-min ischemia. On the right is digital pictures of TTC-stained brain slices of a mouse subjected to 60-min ischemia. TTC, 2,3,5-triphenyltetrazolium chloride.

3.11.2 TTC-based infarction

TTC-stained brain slices were photographed with a digital camera (Figure 9) and images were analyzed using NIH software Image J.[427] In each slice, unstained ischemic tissue, presented as pale areas, was manually outlined. As described above, uncorrected and edema-corrected lesion volumes were calculated.[274] Lesions were reported as the percentage of the intact hemisphere (% hemispheric lesion volume). The percentage of edema was also reported relative to intact hemisphere.

3.12 BLOOD-BRAIN BARRIER PERMEABILITY ASSESSMENTS

3.12.1 Evans blue extravasation

Rats received **intravenously** (I) and mice **retro-orbitally** (IV) a dose of EB (3 mL/kg for rats and 1mL/kg for mice of 2% solution; 20 mg/mL dissolved in 1% albumin, Sigma-Aldrich, Steinheim, Germany) 20 to 25 min before collecting the brains.

Evans blue fluorescence signal intensity (I and IV) and the area of EBA extravasation (I) were measured with a fluorescence scanner (Typhoon 9400, Amersham Biosciences,

Buckinghamshire, UK).[428] In Study I, the area of EB extravasation was manually outlined and the average fluorescence signal intensity within this area and of the intact hemisphere was measured. In Study IV, because, if any, a widespread BBB leakage was expected, EB fluorescence was calculated as the ratio of the average signal intensity of the whole brain specimen to signal intensity of a reference point out of the hemisphere with the image analyzer software ImageQuant (Amersham Biosciences Buckinghamshire, UK).

3.12.2 Contrast-enhanced MRI

3.12.2.1 Percentage of enhancement of the ischemic lesion

The enhancement area on postcontrast T1-weighted image represents the area of BBB leakage. Contrast enhancement area was manually outlined (I, III) and by taking its ratio to the lesion area and multiplying by 100 the percentage of enhanced ischemic lesion (% Gd-DTPA) was calculated.

3.12.2.2 Contrast-to-noise ratio of the enhancement area

Signal intensities (I) were collected from manually outlined enhancement area (S_{inf}), the entire contralateral hemisphere (S_{normal}), and a reference point outside the brain tissue (noise). Thereafter, signal intensity of the nonischemic hemisphere was subtracted from the signal intensity of the enhancement area and the ratio to the noise was calculated yielding contrast-to-noise ratio of the enhancement ((S_{inf}-S_{normal})/noise).

3.12.2.3 Signal intensity change due to enhancement

Signal intensity values were collected (III) from the enhancement area on the postcontrast T1-weighted image (SI_{post}) and from the corresponding area on the precontrast T1-weighted image (SI_{pre}). Signal intensity change due to Gd-DTPA enhancement was calculated by substracting SI_{pre} from SI_{post} and by taking its ratio to SI_{pre} and multiplying by 100 ((SI_{post}−SI_{pre})/SI_{pre}×100).

3.12.2.4 The blood-to-brain transfer constant of Gd-DTPA

ROIs were manually placed (II, III) in the ischemic hemisphere on postcontrast IR-FLASH scans in a standard manner (Figure 7). Arterial concentration of Gd-DTPA was estimated

from the superior sagittal sinus as described by others.[396] Data collected from ROIs of each IR-FLASH sequence were fitted to calculate T_1 values and afterwards inverse T_1 values were calculated (R1). These data were further applied to Patlak plot equations[396, 429] as described above, yielding as slope the blood-to-brain transfer constant of Gd-DTPA (K_i), which is an estimated measure of BBBP to Gd-DTPA.

3.13 QUANTITATIVE ANALYSES OF *Stc1, Stc2,* and *Il-6* mRNA

From pooled brain slices of ischemic mice (IV), total RNA was isolated by use of TRIZOL® Reagent (Invitrogen, Carlsbad, CA, USA). The High Capacity RNA-to-cDNA Kit (Applied Biosystems, Foster City, CA, USA) was used to prepare cDNA and quantitative real-time PCR was performed with the LightCycler® II instrument (Roche Diagnostics, Mannheim, Germany) and the Maxima SYBR Green qPCR Master Mix (2X) (Fermentas, Vilnius, Lithuania). Primers were: *Stc1*; 5'-ATGCTCCAAAACTCAGCAGTGATTC-3' and 5'-CAGGCTTCGGACAAGTCTGT-3', *Stc2*; 5'-GCATGACGTTTCTGCACAAC and 5'-CAGGTTCACAAGGTCCACAT, and *Il-6* 5'-CTTCCCTACTTCACAAGTCC-3' and 5'-GCCACTCCTTCTGTGACTC-3'. *Stc1*, *Stc2*, and *Il-6* mRNA levels were normalized against levels of *beta-2-microglobulin*, of which primers were: 5'-GCTATCCAGAAAACCCCTCA-3' and 5'-ATGTCTCGATCCCAGTAGAC-3'. All primers were from Proligo LLC, Paris, France.

3.14 STATISTICAL ANALYSES

All parametric data are presented as mean ± SD. Normally distributed parametric data sets were analyzed with Student's *t*-test (two groups) or one-way ANOVA followed by Holm-Sidak post hoc test (multiple groups). When normality failed, Kruskal–Wallis test followed by Dunn's method assessed differences between multiple groups. Nonparametric data (neurological scores) from two groups were analyzed by the Mann-Whitney *U* test. Repeated measures of ANOVA followed by Holm-Sidak post hoc test examined the temporal differences of an individual parameter. Paired t-test was used to study differences between data sets from the same animal. MRI data of the superior sagittal sinus were fitted to an exponential curve. Linear regression analysis of each MRI data set, which was obtained from the ROIs of T1 maps, yielded as slope the blood to brain transfer rate constant of Gd-DTPA, Ki. Spearman correlation coefficient analysis served to identify correlations. A two-tailed value of $P < 0.05$ was considered significant.

4 RESULTS

Study I and II

These studies included a comprehensive evaluation of the BBBP following transient occlusion of the MCA in rats. Encompassing all the hyperacute, acute, subacute, and chronic phases of the post-reperfusion period with 15 different groups of rats (2, 4, 6, 12, 18, 24, 36, 48, and 72 h and 1, 2, 3, 4, and 5 weeks), BBBP to both large and small molecules were quantitatively characterized, the former via the gold standard method (Evans blue fluorescence) and the latter with gadolinium-enhanced MRI.

Animals

After the exclusions due to premature death and subarachnoid hemorrhage, 123 rats (N=6-8 per group) completed the experimental period. Control animals included eight sham-operated rats. No significant differences arose in the physiologic parameters (mean arterial blood pressure and temperature) between study groups.

Ischemic lesions

In all animals successful MCAO and reperfusion were ascertained with LDF, which showed a mean CBF value 14% (±3) of the baseline during occlusion and after reperfusion 65% (±4) of the baseline. Ischemic lesions were visualized immediately after occlusion with DWI sequence of MRI, revealing substantial-sized cortico-subcortical lesions. Final infarct volumes at the corresponding time-points were similar among groups (in average 0.22±0.10 cm^3, P=0.42). Volumes were in good correlation with lesion areas (r=0.710, P=0.003) calculated from the optic-chiasmal slice, which was used for BBBP quantifications. Control animals were free of ischemic lesions.

BBB leakage to Evans blue

EB fluorescence quantification indicated that at all time-points, except for 3 and 5 weeks after reperfusion, EB extravasated into ischemic area (P<0.001), with a slight decrease at 36 and 72 h.

BBB leakage to Gd-DTPA

Gd-DTPA presence in the ischemic parenchyma led to increased contrast-to-noise ratio in the post-contrast T1-weighted images at all time-points, except for 5 weeks. This increase was slightly lesser at the earliest time-point (25 min) of the study and at the two latest time-points (3 and 4 weeks) of Gd-DTPA leakage.

GD-DTPA leakage estimated as blood-to-brain transfer constant (K_i) via Patlak plotting of DCE-MRI data, indicated a sustained leakage up to 5 weeks after reperfusion (P<0.001).

Spatial pattern of BBB leakage

BBB leakage to both tracers were limited to ischemic area, but the extent of the leakage varied depending on the time-point and the tracer, though always being smaller than the extent of the ischemic lesion (49-90% of the ischemic lesion)(Figure 10). Starting from 72 h, EB leaking area was smaller than Gd-DTPA leaking area (P<0.01).

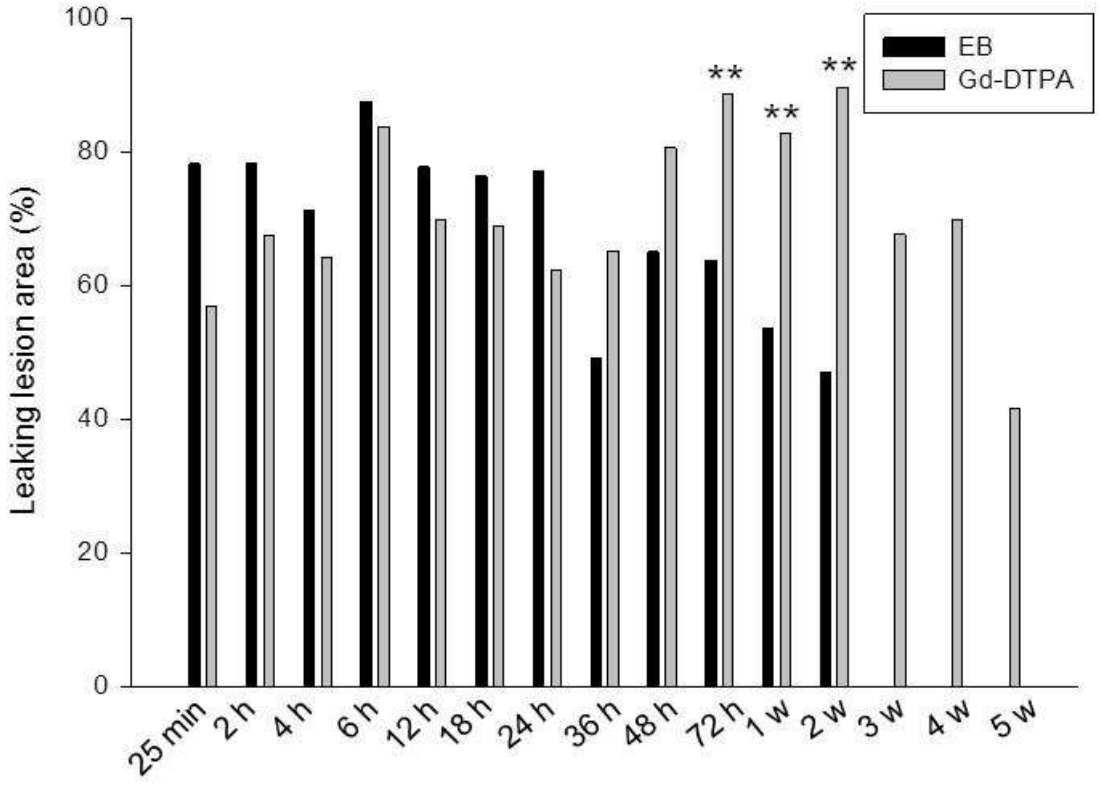

Figure 10 Leaking lesion areas. The size of Evans blue (EB) and contrast agent (Gd-DTPA) leaking areas are compared (**, P<0.01).

Parameters affecting BBB leakage

The severity of the ischemia extrapolated from ADC values correlated with the degree of ischemia (r=-0.58, P=0.02), the lower the ADC value, the higher the blood-to-brain transfer constant of Gd-DTPA. The extent of the ischemic lesion was another factor associated with increased BBB leakage to Gd-DTPA (r=0.75, P=0.0015), larger lesions depicted a more leaky BBB with higher K_i values. K_i values showed a trend of decrease overtime (r=-0.61, P=0.01).

Study III

Appreciating the large standard deviations in BBBP related parameters obtained in previous studies, this study was designed to diminish inter-animal variability and to test more vigorously the hypothesis of continuous BBB leakage following transient ischemia. Study included the same animal model as in the previous studies, and DCE-MRI was repeated at 5 time-points after reperfusion (2, 24, 48, and 72 h and 1 week). Signal intensity analysis and Patlak plotting of MRI data allowed estimating BBBP to Gd-DTPA.

Ten rats with **successful MCAO and reperfusion** as documented by laser-Doppler flowmetry and six sham-operated control animals were included in the study. No significant differences emerged in **physiological parameters** (mean arterial blood pressure, temperature) among animals or time-points. Baseline **ischemic lesions** calculated from DW images were similar among animals (P=0.971). Uncorrected ischemic lesion volumes increased between 2 h and 24 h and decreased thereafter, reflecting formation and resolution of edema, respectively. A good correlation appeared between lesion volumes and areas (r=0.767, P<0.001) calculated from the optic-chiasmal slice, which was used for BBBP quantifications. Sham animals showed no brain pathology.

The Gd-DTPA leakage, analyzed as **signal intensity change** from post-contrast T1-weighted images relative to precontrast images, was higher than that of shams at all time-points (P<0.001, ANOVA), indicating a continuous leakage. Among time-points, 1 week was associated with higher signal intensity change (P<0.001, RM-ANOVA) (Figure 11).

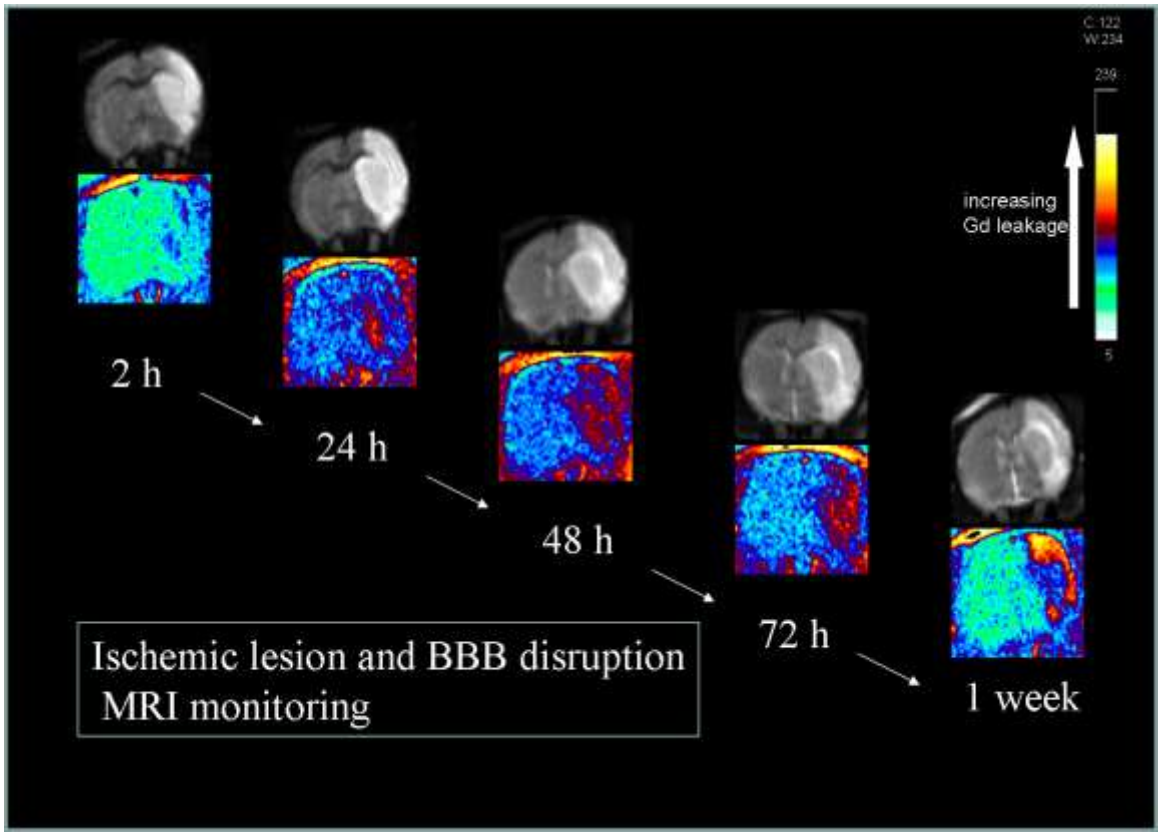

Figure 11 Monitoring of ischemic lesion and blood-brain barrier (BBB) disruption by magnetic resonance imaging (MRI) in a representative rat. Gray scale MRI images are diffusion images (starting from 48 h with b0, which provides T2-weighted image), colored images are color-coded post-contrast fluid attenuated inversion recovery images. There is continuous leakage into ischemic area, which is most pronounced at 1 week. See color scale bar for increasing gadolinium (Gd) leakage.

A second method for estimating BBBP to Gd-DTPA used **Patlak plotting** of the DCE-MRI data, which provided blood-to-brain transfer constant of Gd-DTPA, K_i. With the knowledge of heterogeneity within the ischemic lesion, data collection applied two methods. Firstly, cortical and subcortical parts of the ischemic lesion were analyzed as entireties, and secondly small circular ROIs (3 per cortex and subcortex) provided the data (Figure 7B). With the first approach, neither cortical, nor subcortical K_i values differed among time-points ($P>0.05$, RM-ANOVA), being different than those of sham animals and of contralateral values during the whole experiment ($P<0.005$, ANOVA). With the second approach, a difference in K_i values among time-points appeared only in the comparison of values from a cortical ROI (ROI-c2, Figure 7B).

Study IV

This study explored the role of STC-1 in HPC and in the BBB integrity via the use of genetically modified STC-1 deficient (STC-$1^{-/-}$) mice. Transient (60 min) occlusion of the MCA was introduced to STC-$1^{-/-}$ mice and wild type (WT) littermates, with or without HPC (6 h of 8% oxygenation), 24 h prior to ischemia. BBB experiments assessed EB fluorescence in STC-$1^{-/-}$ mice and WT mice under normal conditions, and immediately and 24 h after hypoxia. Real time polymerase chain reaction quantified *Stc-1*, *Stc-2*, and *Il-6* mRNA with DNA extracted from ischemic brains.

After the exclusions due to subarachnoid hemorrhage, inadequate occlusion or reperfusion, and premature death, HPC experiments included nine to ten mice per group. 28 mice were subjected to BBB experiments (N=4-5 per group). No differences existed in body weights or rectal temperatures of the animals. In HPC experiments, LDF measurements ensured similar rates of CBF reduction during MCAO (P=0.105) and of CBF recovery after reperfusion (P=0.118).

In STC-$1^{-/-}$ mice and WT mice, HPC prior to ischemia resumed in equally smaller infarctions than did ischemia only (22±10% vs. 26±8%, P=0.336). In both scenarios, STC-$1^{-/-}$ mice exhibited worse neurological scores than of WT mice, although HPC improved neurological outcome of ischemia in STC-$1^{-/-}$ mice (P=0.024, Figure 12).

When HPC was introduced prior to ischemia, brain mRNA expressions of *Stc1* (P=0.005) and *Stc2* (P=0.035) in WT mice and of *Stc2* in STC-$1^{-/-}$ mice (P=0.002) were increased compared to ischemia only. After ischemia only, brain *Il-6 mRNA* levels differed between STC-$1^{-/-}$ and WT mice (P=0.033), with 9-time lower levels in STC-$1^{-/-}$ mice.

EB fluorescence results were comparable between STC-$1^{-/-}$ and WT mice under normal conditions (P>0.05) and the application of hypoxia did not result in increased leakage in STC-$^{-/-}$ mice neither immediately (P>0.05), nor 24 h after hypoxia (P>0.05).

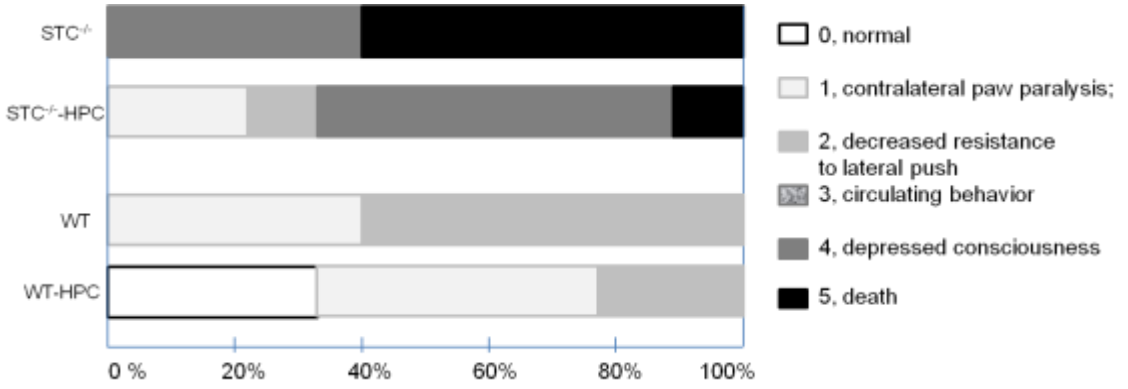

Figure 12 Distribution of neurological scores. STC knockout mice ($STC^{-/-}$) and wild type (WT) mice were subjected to 60-min ischemia; $STC^{-/-}$-HPC and WT-HPC mice received hypoxic preconditioning (HPC) 24 h before ischemia. N=9 to 10 per group.

5 DISCUSSION

Stroke, the second leading cause of death worldwide,[430] will affect approximately one of every six persons,[431] leaving each year 5 million people dependent on others.[2] Ischemic stroke is responsible nearly 80% of all strokes and occurs due to occlusion of a cerebral artery. Consequently, brain region supplied by the occluded artery is left without blood flow and undergoes complex pathophysiological events that cause irreversible damage, unless timely reperfusion occurs. Early reperfusion (spontaneously or therapeutically) is beneficial and limits the injury, but late reperfusion exacerbates the injury through further harmful events. Among these, BBB disruption is the most critical.

The BBB protects central nervous system against harmful ingredients of the circulating blood, first as a physical barrier through its structural components, second as a functional and selective mechanical barrier through its transport mechanisms, and finally as an enzymatic barrier. Accordingly, large molecules, including most proteins, drugs, and cellular elements of the blood, are blocked from the central nervous system under normal conditions. In disease conditions, such as ischemic stroke, the brain is left without this crucial guard at varying degrees; at the extreme, massive edema and symptomatic hemorrhagic transformation occurs.

In animal models of transient focal cerebral ischemia (ischemic stroke with reperfusion), BBB disruption is long believed occurring in a biphasic pattern. This assumption however is based on few studies performed more than two decades ago and are still repeatedly cited.[344, 386, 400, 401] A critical analysis of these works discloses several methodological issues, which complicates the interpretation of their data in order to achieve a common conclusion and raises doubts on the so-called biphasic nature of the BBB leakage following ischemia-reperfusion.

Knowing the time course and the degree of BBB leakage following ischemia-reperfusion is crucially important in AIS patients for several reasons. First, patients at higher risk of experiencing the devastating consequences of severely leaking BBB (massive edema and

symptomatic hemorrhagic transformation) could be detected early; second, candidate regimens to prevent or alleviate these harmful effects could be introduced within a correct therapeutic window, presumably early in the acute phase; third, in the later phases, when repair mechanims take place, it enables offering the brain drugs for enhancing these beneficial mechanisms (i.e. neurorestoration). If the BBB ceases to leak, potential drugs of neuroprotection or neurorestoration would not reach the brain.

Biphasic BBB leakage was originally defined by Kuroiwa et al.[400] as an earlier leakage followed by a non-leaking state and a second leakage. Authors[400] have applied transorbital occlusion of the MCA to cats and they have provided detailed data on CBF values. However, infarct sizes are missing. It is known that this ischemia model is associated with variable outcomes.[432] Only four groups of animals (for EB evaluations at 2, 3, 5 and 72 h after reperfusion) were studied, with 6 to 11 cats per group. First group received EB injection immediately after reperfusion and EB stayed in the circulation for two hours. In other groups, EB was left to circulate for 30 min. BBB leakage was visually analyzed, which is the weakest feature of the study. In all groups, except in 3 h group, EB was observed in ischemic areas. These cats (N=11) without EB leakage however showed serum protein leakage, and this was interpreted as the result of the first barrier opening, which occurred during zero to two hours after reperfusion. They explained the lack of EB leakage ("refractory period") with two contradictory theories: Either BBB functions were fully recovered or were severely disturbed, that EB transport through the BBB into central nervous system was inhibited.

Two following studies reporting biphasic BBB leakage, one by Belayev et al.[401] and the other by Rosenberg et al.,[344] fortunately used the same stroke model (2 h ischemia with suture MCAO) and quantitative evaluations of BBBP, but with tracers of different sizes: EB (large tracer) and radiolabeled sucrose (small tracer), respectively. EB was left in the circulation for one or two hours and radiolabeled sucrose for 10 minutes. Although study of Belayev et al. did not utilize LDF-control on the ischemia, reported lesion volumes indicate that they have induced considerable sizes of infarctions. Rosenberg et al., on the other hand, did not provide any data on the CBF changes or infarctions induced. Time-points included in the study of Belayev et al. generally overlap with the time-points of the study by Kuroiwa et al.[400] However, at earlier time-points (0-2 h after reperfusion) when Kuroiwa et al. found the BBB open, Belayev et al. detected no EB leakage. Starting from one to three hours after reperfusion EB was leaking in the striatum at all the time-points evaluated, with maximum

leakage at 46 to 48 h after reperfusion. Rosenberg et al. studied a high number of time-points, involving several time-points before 24 h (thus covered the long gap in the other studies[386, 400, 401]) and further time-points than 72 h (which were not previously studied). Unfortunately, the first 3 h of reperfusion, at which others were found the first BBB opening,[386, 400] was ignored. Rosenberg et al. reported two BBB openings occurring firstly at 3 h and secondly at 48 h after reperfusion. Although they did not comment on time-points between these two extremes, they reported that BBBP was returned to normal by 14 days; thus, one can suggest that some degree of leakage existed between 3 and 48 h post-reperfusion.

Huang et al.[386] induced small cortical infarcts in spontaneously hypertensive rats using surgical distal MCAO for two hours. BBBP was evaluated with radiolabeled sucrose at time-points mostly similar to those in the studies of Kuroiwa et al. and Belayev et al. The particular difference was in the earliest time-point, which covered the first very minutes of reperfusion. Huang et al. noted an increased BBBP in the neocortex at this earliest time-point that conflicts with the study of Belayev et al. This early BBB leakage was followed by a partial recovery at 1 and 4 h post-reperfusion, which was interpreted resulting from the closure of the BBB. Further increases in the BBBP occurred at 22 h and at 46 h (maximal increase) post-reperfusion.

To summarize, these four most referred studies, which suggest biphasic BBB opening after ischemia-reperfusion, disagree on the course of biphasicity from several aspects and raise serious concerns. Timing of the first opening is uncertain, does it occur very early (within minutes) after reperfusion[386] or within hours? [344, 401] Is there really any closure of the BBB within leaky periods,[400] does it mean a complete functional recovery in the middle of ongoing pathologic events of ischemic cascade? Timing of presumed second opening is ambiguous too, does it occur as early as 5 h[400] or as late as 48h after reperfusion?[344, 401] Does the tracer size affect the results of post-ischemic BBBP? This last issue was not tested in above mentioned studies.

Stimulated by these questions, the first three studies included in this thesis were performed. A well-known transient ischemia model (suture occlusion of the MCA in rats) was assisted with LDF and MRI to ascertain the occlusion and reperfusion, therefore to reduce outcome variability. BBBP changes were monitored, first with a comprehensive study protocol, which

included 15 groups of animals, covering all the phases of post-reperfusion and avoiding long gaps between time-points (I, II). Second, to confirm the findings of the first two studies with a more powerful study design, BBBP changes were monitored longitudinally, in a single group of animals (III). We quantified BBB protein permeability (via large molecule EB-albumin extravasation) (I) and ion permeability (via small molecule, Gd-DTPA extravasation) (I; II, and III), using the gold standard ex vivo technique (EB fluorescence) and a novel in vivo technique (contrast-enhanced MRI), respectively.

The consistent finding in the results (I, II, and III) is that, BBB leakage following ischemia-reperfusion is continuous and long-lasting, without any closure up to several weeks. Acknowledging the complex pathophysiological changes triggered by ischemia-reperfusion, where many mediators and mechanisms take place in a temporal manner, variations in the degree of the BBB leakage is expected. However, the biphasic BBB leakage concept is an oversimplification and is misleading, because it involves not only perturbations (first and second openings) of the leakage, but also cessation of the leakage in between perturbations (so-called closure of the BBB). Such closure was found to happen at a wide range of 0 to 12 h (Table 1), which however falls into acute phase of stroke, when ischemic injury is yet evolving and repair mechanisms are inactive. In the studies included in this thesis (I, II, and III) continuity of the BBB leakage was proven for both large and small molecules and with both transversal and longitudinal study designs. Until the stage of an absolute lack of the leakage at several weeks after reperfusion, no transient closure of the BBB (in other terms, refractory period[400]) occurred. Recent MRI-based evaluations of BBBP discredit the assumption of biphasic BBB leakage and point towards gradually increasing leakage up to 24 h (Table 2).[433-439] Experimental data on long-term behaviors of the BBB following ischemia-reperfusion are scarce and inconsistent. In rats subjected to 90-min MCAO via suture occlusion method[344] sucrose leakage (small molecule) ceased at 2 weeks. In a tree-vessel occlusion model in rats, after 60 min ischemia, Gd-DTPA leakage continued up to 3 weeks. Our studies (I,II) are the most comprehensive off all studies investigating BBBP after focal brain ischemia as we covered a wide range time-points and used both a small (Gd-DTPA) and large molecule (EB).

In vivo BBBP imaging with CT or MRI techniques detects varying rates of increased permeability in ischemic stroke patients (from 20 to 88%),[138-140] more often in the subacute phase. After 3 weeks parenchymal contrast enhancement tends to decrease.[440] Our

quantitative MRI results are in agreement with human findings, that a continuous but slowly decreasing permeability to contrast agent was detectable during 4 weeks after stroke. We should note that our MRI experiments differ from clinical MRI practice from many aspects: First, a high field strength MRI was used (4.7 T). Second, Gd-DTPA dose was 0.5 mmol/kg (a considerably high dose, 5 times higher than in usual clinical practice, that even rarely applied in experimental stroke[437]); and last, contrast-enhanced images were collected as late as 30 min after Gd-DTPA bolus injection (a feature that may not be feasible in AIS patients). All these factors improve the chance to detect even minute amounts of contrast enhancement.

In concert with previous findings (Table 1, Figure 3), a nonsignificant decrease in BBB leakage occurred to both large and small tracers around 24 to 36 h (I, III). Potential explanation for this drop in the leakage is no-reflow phenomenon.[441, 442] According to this concept, plugs of neutrophils can interrupt microvascular circulation early after reperfusion, consequently the delivery of the tracer from blood to the brain may be limited despite a disturbed BBB. An interesting point is that at 24h post-reperfusion while the degree of leakage decreases,[443] the extent of leaky area increases.[444] Another alteration observed was at 1 week, as an increased leakage (III). However, this increase was nonsignificant, when BBBP was evaluated encompassing the entire lesion. Only a limited cortical area was responsible for this trend (Figure 7B, ROI-c2). Recent data concerning post-stroke angiogenesis[439, 445] suggest this finding of increased BBB leakage at 1 week post-reperfusion a proof for regeneration, rather than being related to clinical deterioration.

Previous works disclosed that increasing the duration (therefore the severity) of the transient ischemia results in deterioration of the BBB damage.[142, 433, 434, 446] In agreement with this, our results indicate that brain areas with lower ADC values show higher permeability and the larger the ischemia area is, the higher the BBBP.

A growing body of data suggests increased BBBP as a predictor of hemorrhagic transformation.[140, 141, 149-151] BBBP quantification with imaging methods in stroke is yet a developing area and awaits standardization based on large clinical trials. One unsolved issue is the consequences of varying degrees of BBBP. In theory, if the permeability of the BBB is not large enough for blood cellular elements to pass, hemorrhage will not occur, but BBB leakage to much smaller molecules such as albumin, may cause edema.[152] At this context,

BBBP evaluations with different size of tracers are of importance. In the studies included in this thesis, post-ischemic BBB leakage to large and small tracers showed different temporal and spatial profiles. Leakage to both tracers started early after reperfusion (at 25 min), leakage to large molecule ceased at 3 weeks, and to small tracer at 4 weeks. When leaking areas were compared, at 25 min post-reperfusion, surprisingly large molecule's leakage tended to be larger compared to small molecule's leakage (P=0.063). Afterwards, up to 48 h, both tracers leaked to similar extents. However, from 72 h to 2 weeks EB leaking area was significantly smaller than contrast leaking area. Taken together, these data may suggest that very early BBB disturbance occurring after ischemia-reperfusion is more pronounced for larger molecules, but at the chronic phase BBB function recovers earlier for larger molecules. Tracer size depending behavior of post-ischemic BBB was also previously noted. At 3 h after 3-hour-long transient ischemia in rats, EB extravasated into ischemic area, but red blood cells or dextran did not.[447] At 21 h, all tree elements have leaked through the BBB. In the same animal model, at 21 h after reperfusion, small molecule leaking areas were two times larger than large molecule leaking areas, and leakage of large molecule was associated with higher BBBP.[448] When BBB leakage to a very large molecule at 3 and 21 h post-reperfusion was compared spatially, same authors noticed that from 3 to 21 h leaky areas were increased by nearly 50%.[449] Unfortunately, these authors focused on only 3 and 21 h post-reperfusional periods. Our results on very early or late BBB behavior to different size of tracers require confirmation with further studies.

In the studies where STC1-knockout mice were used (IV), STC1-deficiency was not associated with increased infarct volumes, but resulted in worse neurological scores compared to wild-type mice. Moderate-sized lesions (approximately 23% of the ipsilateral hemisphere) caused mild neurological disability in wild-type mice, but STC1-deficient mice with similar-sized infarcts were severely disabled or died. It is unlikely that the hemorrhagic transformation observed in STC1-deficient mice (3 out of 10) was alone responsible for this deterioration, because although hypoxic preconditioning was effective in reducing lesion size in these mice, they still scored worse than wild-type mice without having hemorrhagic transformation. We suggest that reduced expression of IL-6 (a multipotent neuroprotective cytokine) in ischemic brains of STC1-deficient mice may have led to increased inflammation. Elucidating the role of STC1 in preserving neurological functions after ischemia requires further studies.

BBB permeability in STC1-knockout mice was disturbed neither in health, nor after hypoxia. Although we did not examine BBBP in STC-knockout mice subjected to ischemia, we found no increased edema formation in these mice compared to wild-type littermates. This implies that STC1 has no major contribution in preserving BBB functions in health or disease.

6 SUMMARY AND CONCLUSIONS

This thesis provides strong evidence that, following transient focal ischemia, BBB leakage is continuous (monophasic) and long-lasting. There is a transient reduction in the BBBP around 24 h post-ischemia, but it is not closed. Hence, biphasic BBB leakage for this scenario is an over- and misused term and should be abandoned.

Findings of this thesis are clinically important from several reasons. Firstly, neurotoxicity of thrombolysis with t-PA is increasingly appreciated and BBB protecting drugs are being sought. BBBP imaging may be useful in detecting AIS patients that are under risk of developing massive edema or hemorrhagic transformation. Furthermore, when testing BBB protective strategies, quantitative BBBP evaluations are needed to monitor therapeutical effects. Up to date, no neuroprotective or neurorestorative strategy is proven effective in AIS patients. However, experiences from past clinical trials revealed that there is much to improve in both preclinical studies and clinical trial designs. With these improvements implemented, new drugs with potential long-term application may be offered to AIS patients. From this aspect, it is crucial to elucidate when the BBB is in ischemic stroke patients and for how long it remains so. MRI-based BBBP evaluation method used in this thesis may easily serve for this purpose.

Stanniocalcin is yet a little-known molecule. Our findings emphasize the neuroprotective effect of STC1, through a cross-talk with inflammatory cytokine IL-6. However, STC1 does not appear to have a role in BBB integrity.

ACKNOWLEDGMENTS

This work was carried out at the Department of Neurology, Helsinki University Central Hospital. I am sincerely thankful to all those people who have helped, guided, and supported me during these studies.

Especially, I wish to express my gratitude to my supervisor **Turgut Tatlisumak**, who gave me chance to discover the scientist and writer in me. I am deeply grateful to Turgut for his constant help, optimism, humor, and support. He often believed in me more than I did, he made me feel at home in a foreign country, and despite his busy schedule, he was always available when I needed his help. I truly admire his expertise and the sharpness of his red ink pen is outstanding! I am sincerely thankful to my other supervisor, **Daniel Strbian**, who always astonished me with his limitless talents. I am deeply indebted to Daniel for not only sharing with me his knowledge, but also for his kind friendship. Without his supportive discussions in my miserable times, this work would not have realized.

I express my sincere gratitude to **Markku Kaste** and **Markus Färkkilä**, the former and the present heads of the Department of Neurology and to **Timo Erkinjuntti**, for the opportunity to conduct my research. I would like to thank **Jari Honkaniemi** and **Olli Gröhn** for kindly reviewing and commenting on this thesis to improve it. **Carrol Norris** earns my thanks for author editing the language for articles II and III.

I truly thank **Wolf-Rudiger Schäebitz** for accepting the role of being my opponent. I believe the defense day will be memorable due to his visionary views.

I wish to express my warmest gratitude to my coworkers from Biomedicum, **Usama Abo-Ramadan**, **Ivan Marinkovic**, **Eric Pedrono**, and **Miia Pitkonen**. It has been pleasure to work with you and especially thanks for your friendship. Stimulating discussions during lunch-times had impact on me! I also wish to thank coworkers, **Lauri Soinne** from the Department of Neurology, **Leif C. Andersson**, **Johan A. Westberg**, and **Martina Serlachius** from the Department of Pathology. **Taru Puhakka** earns my thanks for her skilful technical assistance, **Ertugrul Tatlisumak** for co-writing, and **Roger R. Reddel** and **Andy C.-M. Chang** for co-writing and providing knockout mice. I also deeply thank to workers of animal facility unit of Biomedicum, especially to **Anu Ahlroos**. During the journey of this work **Shashank Shekhar** and **Pekka Hassinen** have been temporary members of our lab, to both

I am thankful too. I warmly thank to another visiting colleague, **Ufuk Emre**, we all miss you in Finland.

I owe my sincere gratitude to **Sara Z. Bahar**, who mentored me during my neurology residence in Turkey and who has seen in me a potential for a scientist and introduced me to Turgut. She and other colleagues from my former clinic, **Neurology Department of the Istanbul University**, stimulated in me the enthusiasm for stroke. I also wish to thank to the stuff of **Pitäjänmäki Helthcare Centre**, especially to **Kristian Siekkinen** and **Marjo Parkkila-Harju**, the former and the present chiefs of the centre, for encouragements and for providing me the time I needed for this work.

My deepest thanks go to my beloved family. **Jarno**, thanks for being always there for me, your love and rational thinking has been the most-valuable support to me during this work. I owe my most sincere thanks to my lovely daughter **Aino**, you are the joy of my life, giving reason not to give up! Last, but not least, I thank to my parents, my brother and my grandfather for their trust and encouragements.

This work was supported by grants from the **Centre for International Mobility**, the **Finnish Medical Foundation**, the **Oskar Öflund's Foundation**, the **Orion-Farmos Research Foundation**, the **Biomedicum Helsinki Foundation**, and the **University of Helsinki**.

REFERENCES

1. Murray CJ, Vos T, Lozano R, Naghavi M, Flaxman AD, Michaud C, Ezzati M, Shibuya K, Salomon JA, Abdalla S, et al. Disability-adjusted life years (DALYs) for 291 diseases and injuries in 21 regions, 1990-2010: a systematic analysis for the Global Burden of Disease Study 2010. *Lancet*. 2012;380:2197-2223.
2. World Health Organization. Atlas of heart disease and stroke. 2004. In: www.whi.int [Internet]. [cited 2013 Jan 27]. Available from: http://www.who.int/cardiovascular_diseases/resources/atlas/en/.
3. Kinsella K, He W. An aging world: 2008. 2009. In: U.S. Census Bureau www.census.gov [Internet]. [cited 2013 Jan 27]. Available from: http://www.census.gov/prod/2009pubs/p95-09-1.pdf.
4. Lopez AD, Mathers CD, Ezzati M, Jamison DT, Murray CJ. Global and regional burden of disease and risk factors, 2001: systematic analysis of population health data. *Lancet*. 2006;367:1747-1757.
5. Meretoja A, Kaste M, Roine RO, Juntunen M, Linna M, Hillbom M, Marttila R, Erila T, Rissanen A, Sivenius J, et al. Direct costs of patients with stroke can be continuously monitored on a national level: performance, effectiveness, and Costs of Treatment episodes in Stroke (PERFECT Stroke) Database in Finland. *Stroke*. 2011;42:2007-2012.
6. Roger VL, Go AS, Lloyd-Jones DM, Benjamin EJ, Berry JD, Borden WB, Bravata DM, Dai S, Ford ES, Fox CS, et al. Heart disease and stroke statistics--2012 update: a report from the American Heart Association. *Circulation*. 2012;125:e2-e220.
7. Bamford J, Sandercock P, Dennis M, Burn J, Warlow C. Classification and natural history of clinically identifiable subtypes of cerebral infarction. *Lancet*. 1991;337:1521-1526.
8. Adams HP, Jr., Bendixen BH, Kappelle LJ, Biller J, Love BB, Gordon DL, Marsh EE, 3rd. Classification of subtype of acute ischemic stroke. Definitions for use in a multicenter clinical trial. TOAST. Trial of Org 10172 in Acute Stroke Treatment. *Stroke*. 1993;24:35-41.
9. Astrup J, Siesjo BK, Symon L. Thresholds in cerebral ischemia - the ischemic penumbra. *Stroke*. 1981;12:723-725.
10. Astrup J, Symon L, Branston NM, Lassen NA. Cortical evoked potential and extracellular K+ and H+ at critical levels of brain ischemia. *Stroke*. 1977;8:51-57.
11. Heiss WD, Huber M, Fink GR, Herholz K, Pietrzyk U, Wagner R, Wienhard K. Progressive derangement of periinfarct viable tissue in ischemic stroke. *J Cereb Blood Flow Metab*. 1992;12:193-203.
12. Hossmann KA. Viability thresholds and the penumbra of focal ischemia. *Ann Neurol*. 1994;36:557-565.
13. del Zoppo GJ, Sharp FR, Heiss WD, Albers GW. Heterogeneity in the penumbra. *J Cereb Blood Flow Metab*. 2011;31:1836-1851.
14. Muir KW, Buchan A, von Kummer R, Rother J, Baron JC. Imaging of acute stroke. *Lancet Neurol*. 2006;5:755-768.
15. Ginsberg MD. Adventures in the pathophysiology of brain ischemia: penumbra, gene expression, neuroprotection: the 2002 Thomas Willis Lecture. *Stroke*. 2003;34:214-223.
16. Sharp FR, Lu A, Tang Y, Millhorn DE. Multiple molecular penumbras after focal cerebral ischemia. *J Cereb Blood Flow Metab*. 2000;20:1011-1032.
17. Heiss WD, Rosner G. Functional recovery of cortical neurons as related to degree and duration of ischemia. *Ann Neurol*. 1983;14:294-301.
18. Huang J, Kim LJ, Poisik A, Pinsky DJ, Connolly ES, Jr. Titration of postischemic cerebral hypoperfusion by variation of ischemic severity in a murine model of stroke. *Neurosurgery*. 1999;45:328-333.
19. Heiss WD, Kracht LW, Thiel A, Grond M, Pawlik G. Penumbral probability thresholds of cortical flumazenil binding and blood flow predicting tissue outcome in patients with cerebral ischaemia. *Brain*. 2001;124:20-29.
20. Read SJ, Hirano T, Abbott DF, Markus R, Sachinidis JI, Tochon-Danguy HJ, Chan JG, Egan GF, Scott AM, Bladin CF, et al. The fate of hypoxic tissue on 18F-fluoromisonidazole positron emission tomography after ischemic stroke. *Ann Neurol*. 2000;48:228-235.
21. Read SJ, Hirano T, Abbott DF, Sachinidis JI, Tochon-Danguy HJ, Chan JG, Egan GF, Scott AM, Bladin CF, McKay WJ, et al. Identifying hypoxic tissue after acute ischemic stroke using PET and 18F-fluoromisonidazole. *Neurology*. 1998;51:1617-1621.
22. Tagaya M, Haring HP, Stuiver I, Wagner S, Abumiya T, Lucero J, Lee P, Copeland BR, Seiffert D, del Zoppo GJ. Rapid loss of microvascular integrin expression during focal brain ischemia reflects neuron injury. *J Cereb Blood Flow Metab*. 2001;21:835-846.
23. Yu ZF, Bruce-Keller AJ, Goodman Y, Mattson MP. Uric acid protects neurons against excitotoxic and

metabolic insults in cell culture, and against focal ischemic brain injury in vivo. *J Neurosci Res*. 1998;53:613-625.
24. Romanos E, Planas AM, Amaro S, Chamorro A. Uric acid reduces brain damage and improves the benefits of rt-PA in a rat model of thromboembolic stroke. *J Cereb Blood Flow Metab*. 2007;27:14-20.
25. Unal-Cevik I, Kilinc M, Can A, Gursoy-Ozdemir Y, Dalkara T. Apoptotic and necrotic death mechanisms are concomitantly activated in the same cell after cerebral ischemia. *Stroke*. 2004;35:2189-2194.
26. Ying W, Han SK, Miller JW, Swanson RA. Acidosis potentiates oxidative neuronal death by multiple mechanisms. *J Neurochem*. 1999;73:1549-1556.
27. Katsura K, Kristian T, Siesjo BK. Energy metabolism, ion homeostasis, and cell damage in the brain. *Biochem Soc Trans*. 1994;22:991-996.
28. Phan TG, Wright PM, Markus R, Howells DW, Davis SM, Donnan GA. Salvaging the ischaemic penumbra: more than just reperfusion? *Clin Exp Pharmacol Physiol*. 2002;29:1-10.
29. Dijkhuizen RM, Beekwilder JP, van der Worp HB, Berkelbach van der Sprenkel JW, Tulleken KA, Nicolay K. Correlation between tissue depolarizations and damage in focal ischemic rat brain. *Brain Res*. 1999;840:194-205.
30. Hartings JA, Rolli ML, Lu XC, Tortella FC. Delayed secondary phase of peri-infarct depolarizations after focal cerebral ischemia: relation to infarct growth and neuroprotection. *J Neurosci*. 2003;23:11602-11610.
31. Takano K, Latour LL, Formato JE, Carano RA, Helmer KG, Hasegawa Y, Sotak CH, Fisher M. The role of spreading depression in focal ischemia evaluated by diffusion mapping. *Ann Neurol*. 1996;39:308-318.
32. Kristian T, Siesjo BK. Calcium in ischemic cell death. *Stroke*. 1998;29:705-718.
33. Fujimura M, Morita-Fujimura Y, Murakami K, Kawase M, Chan PH. Cytosolic redistribution of cytochrome c after transient focal cerebral ischemia in rats. *J Cereb Blood Flow Metab*. 1998;18:1239-1247.
34. Mergenthaler P, Dirnagl U, Meisel A. Pathophysiology of stroke: lessons from animal models. *Metab Brain Dis*. 2004;19:151-167.
35. Love S. Apoptosis and brain ischaemia. *Prog Neuropsychopharmacol Biol Psychiatry*. 2003;27:267-282.
36. Liu T, Clark RK, McDonnell PC, Young PR, White RF, Barone FC, Feuerstein GZ. Tumor necrosis factor-alpha expression in ischemic neurons. *Stroke*. 1994;25:1481-1488.
37. Suzuki S, Tanaka K, Nogawa S, Nagata E, Ito D, Dembo T, Fukuuchi Y. Temporal profile and cellular localization of interleukin-6 protein after focal cerebral ischemia in rats. *J Cereb Blood Flow Metab*. 1999;19:1256-1262.
38. Schilling M, Strecker JK, Schabitz WR, Ringelstein EB, Kiefer R. Effects of monocyte chemoattractant protein 1 on blood-borne cell recruitment after transient focal cerebral ischemia in mice. *Neuroscience*. 2009;161:806-812.
39. Touzani O, Boutin H, LeFeuvre R, Parker L, Miller A, Luheshi G, Rothwell N. Interleukin-1 influences ischemic brain damage in the mouse independently of the interleukin-1 type I receptor. *J Neurosci*. 2002;22:38-43.
40. Schneider A, Kruger C, Steigleder T, Weber D, Pitzer C, Laage R, Aronowski J, Maurer MH, Gassler N, Mier W, et al. The hematopoietic factor G-CSF is a neuronal ligand that counteracts programmed cell death and drives neurogenesis. *J Clin Invest*. 2005;115:2083-2098.
41. Strecker JK, Minnerup J, Gess B, Ringelstein EB, Schabitz WR, Schilling M. Monocyte chemoattractant protein-1-deficiency impairs the expression of IL-6, IL-1beta and G-CSF after transient focal ischemia in mice. *PLoS One*. 2011;6:e25863.
42. Emerich DF, Dean RL, 3rd, Bartus RT. The role of leukocytes following cerebral ischemia: pathogenic variable or bystander reaction to emerging infarct? *Exp Neurol*. 2002;173:168-181.
43. Danton GH, Dietrich WD. Inflammatory mechanisms after ischemia and stroke. *J Neuropathol Exp Neurol*. 2003;62:127-136.
44. Heo JH, Han SW, Lee SK. Free radicals as triggers of brain edema formation after stroke. *Free Radic Biol Med*. 2005;39:51-70.
45. Yang GY, Betz AL. Reperfusion-induced injury to the blood-brain barrier after middle cerebral artery occlusion in rats. *Stroke*. 1994;25:1658-1664.
46. Aronowski J, Labiche LA. Perspectives on reperfusion-induced damage in rodent models of experimental focal ischemia and role of gamma-protein kinase C. *Ilar J*. 2003;44:105-109.
47. Pan J, Konstas AA, Bateman B, Ortolano GA, Pile-Spellman J. Reperfusion injury following cerebral ischemia: pathophysiology, MR imaging, and potential therapies. *Neuroradiology*. 2007;49:93-102.
48. Hossmann KA. Pathophysiology and therapy of experimental stroke. *Cell Mol Neurobiol*. 2006;26:1057-1083.
49. Schabitz WR, Steigleder T, Cooper-Kuhn CM, Schwab S, Sommer C, Schneider A, Kuhn HG. Intravenous brain-derived neurotrophic factor enhances poststroke sensorimotor recovery and stimulates neurogenesis. *Stroke*. 2007;38:2165-2172.
50. Popa-Wagner A, Stocker K, Balseanu AT, Rogalewski A, Diederich K, Minnerup J, Margaritescu C, Schabitz WR. Effects of granulocyte-colony stimulating factor after stroke in aged rats. *Stroke*.

2010;41:1027-1031.
51. Beck H, Plate KH. Angiogenesis after cerebral ischemia. *Acta Neuropathol*. 2009;117:481-496.
52. Sahota P, Savitz SI. Investigational therapies for ischemic stroke: neuroprotection and neurorecovery. *Neurotherapeutics*. 2011;8:434-451.
53. Cramer SC. Functional imaging in stroke recovery. *Stroke*. 2004;35:2695-2698.
54. The National Institute of Neurological Disorders and Stroke rt-PA Stroke Study Group. Tissue plasminogen activator for acute ischemic stroke. *N Engl J Med*. 1995;333:1581-1587.
55. Hacke W, Kaste M, Bluhmki E, Brozman M, Davalos A, Guidetti D, Larrue V, Lees KR, Medeghri Z, Machnig T, et al. Thrombolysis with alteplase 3 to 4.5 hours after acute ischemic stroke. *N Engl J Med*. 2008;359:1317-1329.
56. Wardlaw JM, Murray V, Berge E, del Zoppo G, Sandercock P, Lindley RL, Cohen G. Recombinant tissue plasminogen activator for acute ischaemic stroke: an updated systematic review and meta-analysis. *Lancet*. 2012;379:2364-2372.
57. Hacke W, Donnan G, Fieschi C, Kaste M, von Kummer R, Broderick JP, Brott T, Frankel M, Grotta JC, Haley EC, Jr., et al. Association of outcome with early stroke treatment: pooled analysis of ATLANTIS, ECASS, and NINDS rt-PA stroke trials. *Lancet*. 2004;363:768-774.
58. Reeves MJ, Arora S, Broderick JP, Frankel M, Heinrich JP, Hickenbottom S, Karp H, LaBresh KA, Malarcher A, Mensah G, et al. Acute stroke care in the US: results from 4 pilot prototypes of the Paul Coverdell National Acute Stroke Registry. *Stroke*. 2005;36:1232-1240.
59. Kaste M. Do not wait, act now. *Stroke*. 2007;38:3119-3120.
60. Demaerschalk BM, Hwang HM, Leung G. US cost burden of ischemic stroke: a systematic literature review. *Am J Manag Care*. 2010;16:525-533.
61. Parsons M, Spratt N, Bivard A, Campbell B, Chung K, Miteff F, O'Brien B, Bladin C, McElduff P, Allen C, et al. A randomized trial of tenecteplase versus alteplase for acute ischemic stroke. *N Engl J Med*. 2012;366:1099-1107.
62. von Kummer R, Albers GW, Mori E. The Desmoteplase in Acute Ischemic Stroke (DIAS) clinical trial program. *Int J Stroke*. 2012;7:589-596.
63. Mauldin PD, Simpson KN, Palesch YY, Spilker JS, Hill MD, Khatri P, Broderick JP. Design of the economic evaluation for the Interventional Management of Stroke (III) trial. *Int J Stroke*. 2008;3:138-144.
64. Mazighi M, Meseguer E, Labreuche J, Amarenco P. Bridging therapy in acute ischemic stroke: a systematic review and meta-analysis. *Stroke*. 2012;43:1302-1308.
65. Khatri P, Hill MD, Palesch YY, Spilker J, Jauch EC, Carrozzella JA, Demchuk AM, Martin R, Mauldin P, Dillon C, et al. Methodology of the Interventional Management of Stroke III Trial. *Int J Stroke*. 2008;3:130-137.
66. Del Zoppo GJ, Poeck K, Pessin MS, Wolpert SM, Furlan AJ, Ferbert A, Alberts MJ, Zivin JA, Wechsler L, Busse O, et al. Recombinant tissue plasminogen activator in acute thrombotic and embolic stroke. *Ann Neurol*. 1992;32:78-86.
67. Smith WS, Sung G, Starkman S, Saver JL, Kidwell CS, Gobin YP, Lutsep HL, Nesbit GM, Grobelny T, Rymer MM, et al. Safety and efficacy of mechanical embolectomy in acute ischemic stroke: results of the MERCI trial. *Stroke*. 2005;36:1432-1438.
68. Fields JD, Lutsep HL, Smith WS. Higher degrees of recanalization after mechanical thrombectomy for acute stroke are associated with improved outcome and decreased mortality: pooled analysis of the MERCI and Multi MERCI trials. *AJNR Am J Neuroradiol*. 2011;32:2170-2174.
69. Kidwell CS, Jahan R, Gornbein J, Alger JR, Nenov V, Ajani Z, Feng L, Meyer BC, Olson S, Schwamm LH, et al. A Trial of Imaging Selection and Endovascular Treatment for Ischemic Stroke. *N Engl J Med*. 2013:[Epub ahead of print].
70. Penumbra Pivotal Stroke Trial Investigators. The penumbra pivotal stroke trial: safety and effectiveness of a new generation of mechanical devices for clot removal in intracranial large vessel occlusive disease. *Stroke*. 2009;40:2761-2768.
71. Tarr R, Hsu D, Kulcsar Z, Bonvin C, Rufenacht D, Alfke K, Stingele R, Jansen O, Frei D, Bellon R, et al. The POST trial: initial post-market experience of the Penumbra system: revascularization of large vessel occlusion in acute ischemic stroke in the United States and Europe. *J Neurointerv Surg*. 2010;2:341-344.
72. Penumbra Inc. Assess the Penumbra System in the Treatment of Acute Stroke (THERAPY). In:ClinicalTrials.gov [Internet]. Bethesda (MD): National Library of Medicine (US). 2000-. [cited 2013 Jan 18]. Available from: http://clinicaltrials.gov/show/NCT01429350 NLM Identifier:NCT01429350.
73. Ricci S, Dinia L, Del Sette M, Anzola P, Mazzoli T, Cenciarelli S, Gandolfo C. Sonothrombolysis for acute ischaemic stroke. *Cochrane Database Syst Rev*. 2012;6:CD008348.
74. Cerevast Therapeutics Inc. Phase 3, Randomized, Placebo-Controlled, Double-Blinded Trial of the Combined Lysis of Thrombus With Ultrasound and Systemic Tissue Plasminogen Activator (tPA) for Emergent Revascularization in Acute Ischemic Stroke (CLOTBUST-ER). In:ClinicalTrials.gov [Internet]. Bethesda (MD): National Library of Medicine (US). 2000-. [cited 2013 Jan 18]. Available from: http://www.clinicaltrials.gov/show/NCT01098981 NLM Identifier: NCT01098981.
75. O'Collins VE, Macleod MR, Donnan GA, Horky LL, van der Worp BH, Howells DW. 1,026 experimental

treatments in acute stroke. *Ann Neurol*. 2006;59:467-477.
76. Del Zoppo GJ. Why do all drugs work in animals but none in stroke patients? 1. Drugs promoting cerebral blood flow. *J Intern Med*. 1995;237:79-88.
77. Grotta J. Why do all drugs work in animals but none in stroke patients? 2. Neuroprotective therapy. *J Intern Med*. 1995;237:89-94.
78. Ginsberg MD. The validity of rodent brain-ischemia models is self-evident. *Arch Neurol*. 1996;53:1065-1067.
79. Green RA, Odergren T, Ashwood T. Animal models of stroke: do they have value for discovering neuroprotective agents? *Trends Pharmacol Sci*. 2003;24:402-408.
80. Fisher M, Tatlisumak T. Use of animal models has not contributed to development of acute stroke therapies: con. *Stroke*. 2005;36:2324-2325.
81. Sutherland BA, Minnerup J, Balami JS, Arba F, Buchan AM, Kleinschnitz C. Neuroprotection for ischaemic stroke: translation from the bench to the bedside. *Int J Stroke*. 2012;7:407-418.
82. Minnerup J, Wersching H, Diederich K, Schilling M, Ringelstein EB, Wellmann J, Schabitz WR. Methodological quality of preclinical stroke studies is not required for publication in high-impact journals. *J Cereb Blood Flow Metab*. 2010;30:1619-1624.
83. Philip M, Benatar M, Fisher M, Savitz SI. Methodological quality of animal studies of neuroprotective agents currently in phase II/III acute ischemic stroke trials. *Stroke*. 2009;40:577-581.
84. Minnerup J, Sutherland BA, Buchan AM, Kleinschnitz C. Neuroprotection for stroke: current status and future perspectives. *Int J Mol Sci*. 2012;13:11753-11772.
85. Hill MD, Martin RH, Mikulis D, Wong JH, Silver FL, Terbrugge KG, Milot G, Clark WM, Macdonald RL, Kelly ME, et al. Safety and efficacy of NA-1 in patients with iatrogenic stroke after endovascular aneurysm repair (ENACT): a phase 2, randomised, double-blind, placebo-controlled trial. *Lancet Neurol*. 2012;11:942-950.
86. University of California San Diego. The Intravascular Cooling in the Treatment of Stroke 2/3 Trial (ICTuS2/3). In:ClinicalTrials.gov [Internet]. Bethesda (MD): National Library of Medicine (US). 2000-. [cited 2013 Jan 18]. Available from: http://clinicaltrials.gov/show/NCT01123161 NLM Identifier: NCT01123161.
87. EuroHYP-1. 2012
88. Lees KR, Zivin JA, Ashwood T, Davalos A, Davis SM, Diener HC, Grotta J, Lyden P, Shuaib A, Hardemark HG, et al. NXY-059 for acute ischemic stroke. *N Engl J Med*. 2006;354:588-600.
89. Shuaib A, Lees KR, Lyden P, Grotta J, Davalos A, Davis SM, Diener HC, Ashwood T, Wasiewski WW, Emeribe U. NXY-059 for the treatment of acute ischemic stroke. *N Engl J Med*. 2007;357:562-571.
90. Savitz SI. A critical appraisal of the NXY-059 neuroprotection studies for acute stroke: A need for more rigorous testing of neuroprotective agents in animal models of stroke. *Exp Neurol*. 2007;205:20-25.
91. Daiichi Pharmaceutical Co. LTD. Ebselen Trial - Pase III. In:Stroke Trials Registry. [Internet]. Dallas (TX): The Internet Stroke Center web site. 1997-. [cited 2013 Jan 18]. Available from: http://www.strokecenter.org/trials/clinicalstudies/ebselen-trial-phase-iii
92. Kikuchi K, Kawahara KI, Uchikado H, Miyagi N, Kuramoto T, Miyagi T, Morimoto Y, Ito T, Tancharoen S, Miura N, et al. Potential of edaravone for neuroprotection in neurologic diseases that do not involve cerebral infarction. *Exp Ther Med*. 2011;2:771-775.
93. Lampl Y, Boaz M, Gilad R, Lorberboym M, Dabby R, Rapoport A, Anca-Hershkowitz M, Sadeh M. Minocycline treatment in acute stroke: an open-label, evaluator-blinded study. *Neurology*. 2007;69:1404-1410.
94. Singhealth Foundation. Neuroprotection With Minocycline Therapy for Acute Stroke Recovery Trial (NeuMAST). In:ClinicalTrials.gov [Internet]. Bethesda (MD): National Library of Medicine (US). 2000-. Available from: http://clinicaltrials.gov/show/NCT00930020 NLM Identifier: NCT00930020.
95. O'Collins VE, Macleod MR, Donnan GA, Howells DW. Evaluation of combination therapy in animal models of cerebral ischemia. *J Cereb Blood Flow Metab*. 2012;32:585-597.
96. Ehrenreich H, Weissenborn K, Prange H, Schneider D, Weimar C, Wartenberg K, Schellinger PD, Bohn M, Becker H, Wegrzyn M, et al. Recombinant human erythropoietin in the treatment of acute ischemic stroke. *Stroke*. 2009;40:e647-656.
97. Amaro S, Canovas D, Castellanos M, Gallego J, Marti-Febregas J, Segura T, Chamorro A. The URICO-ICTUS study, a phase 3 study of combined treatment with uric acid and rtPA administered intravenously in acute ischaemic stroke patients within the first 4.5 h of onset of symptoms. *Int J Stroke*. 2010;5:325-328.
98. The Intravascular Cooling in the treatment of stroke 2/3 trial (ictus2/3). 2010
99. Cook DJ, Teves L, Tymianski M. Treatment of stroke with a PSD-95 inhibitor in the gyrencephalic primate brain. *Nature*. 2012;483:213-217.
100. Savitz SI, Schabitz WR. Reviving neuroprotection using a new approach: targeting postsynaptic density-95 to arrest glutamate excitotoxicity. *Stroke*. 2012;43:3411-3412.
101. Lo EH. A new penumbra: transitioning from injury into repair after stroke. *Nat Med*. 2008;14:497-500.
102. Zhao BQ, Tejima E, Lo EH. Neurovascular proteases in brain injury, hemorrhage and remodeling after

stroke. *Stroke*. 2007;38:748-752.
103. Savitz SI, Schabitz WR. A Critique of SAINT II: wishful thinking, dashed hopes, and the future of neuroprotection for acute stroke. *Stroke*. 2008;39:1389-1391.
104. Minnerup J, Sevimli S, Schabitz WR. Granulocyte-colony stimulating factor for stroke treatment: mechanisms of action and efficacy in preclinical studies. *Exp Transl Stroke Med*. 2009;1:2.
105. Minnerup J, Heidrich J, Wellmann J, Rogalewski A, Schneider A, Schabitz WR. Meta-analysis of the efficacy of granulocyte-colony stimulating factor in animal models of focal cerebral ischemia. *Stroke*. 2008;39:1855-1861.
106. Floel A, Warnecke T, Duning T, Lating Y, Uhlenbrock J, Schneider A, Vogt G, Laage R, Koch W, Knecht S, et al. Granulocyte-colony stimulating factor (G-CSF) in stroke patients with concomitant vascular disease--a randomized controlled trial. *PLoS One*. 2011;6:e19767.
107. Lang W, Stadler CH, Poljakovic Z, Fleet D. A prospective, randomized, placebo-controlled, double-blind trial about safety and efficacy of combined treatment with alteplase (rt-PA) and Cerebrolysin in acute ischaemic hemispheric stroke. *Int J Stroke*. 2012
108. Hjort N, Butcher K, Davis SM, Kidwell CS, Koroshetz WJ, Rother J, Schellinger PD, Warach S, Ostergaard L. Magnetic resonance imaging criteria for thrombolysis in acute cerebral infarct. *Stroke*. 2005;36:388-397.
109. Urbach H, Flacke S, Keller E, Textor J, Berlis A, Hartmann A, Reul J, Solymosi L, Schild HH. Detectability and detection rate of acute cerebral hemisphere infarcts on CT and diffusion-weighted MRI. *Neuroradiology*. 2000;42:722-727.
110. Mullins ME, Schaefer PW, Sorensen AG, Halpern EF, Ay H, He J, Koroshetz WJ, Gonzalez RG. CT and conventional and diffusion-weighted MR imaging in acute stroke: study in 691 patients at presentation to the emergency department. *Radiology*. 2002;224:353-360.
111. Fiebach J, Jansen O, Schellinger P, Knauth M, Hartmann M, Heiland S, Ryssel H, Pohlers O, Hacke W, Sartor K. Comparison of CT with diffusion-weighted MRI in patients with hyperacute stroke. *Neuroradiology*. 2001;43:628-632.
112. Fiebach JB, Schellinger PD, Jansen O, Meyer M, Wilde P, Bender J, Schramm P, Juttler E, Oehler J, Hartmann M, et al. CT and diffusion-weighted MR imaging in randomized order: diffusion-weighted imaging results in higher accuracy and lower interrater variability in the diagnosis of hyperacute ischemic stroke. *Stroke*. 2002;33:2206-2210.
113. Barber PA, Darby DG, Desmond PM, Gerraty RP, Yang Q, Li T, Jolley D, Donnan GA, Tress BM, Davis SM. Identification of major ischemic change. Diffusion-weighted imaging versus computed tomography. *Stroke*. 1999;30:2059-2065.
114. Lansberg MG, Albers GW, Beaulieu C, Marks MP. Comparison of diffusion-weighted MRI and CT in acute stroke. *Neurology*. 2000;54:1557-1561.
115. Ay H, Oliveira-Filho J, Buonanno FS, Ezzeddine M, Schaefer PW, Rordorf G, Schwamm LH, Gonzalez RG, Koroshetz WJ. Diffusion-weighted imaging identifies a subset of lacunar infarction associated with embolic source. *Stroke*. 1999;30:2644-2650.
116. Wessels T, Rottger C, Jauss M, Kaps M, Traupe H, Stolz E. Identification of embolic stroke patterns by diffusion-weighted MRI in clinically defined lacunar stroke syndromes. *Stroke*. 2005;36:757-761.
117. Baird AE, Lovblad KO, Schlaug G, Edelman RR, Warach S. Multiple acute stroke syndrome: marker of embolic disease? *Neurology*. 2000;54:674-678.
118. Warach S, Gaa J, Siewert B, Wielopolski P, Edelman RR. Acute human stroke studied by whole brain echo planar diffusion-weighted magnetic resonance imaging. *Ann Neurol*. 1995;37:231-241.
119. Schlaug G, Benfield A, Baird AE, Siewert B, Lovblad KO, Parker RA, Edelman RR, Warach S. The ischemic penumbra: operationally defined by diffusion and perfusion MRI. *Neurology*. 1999;53:1528-1537.
120. Davis SM, Donnan GA, Parsons MW, Levi C, Butcher KS, Peeters A, Barber PA, Bladin C, De Silva DA, Byrnes G, et al. Effects of alteplase beyond 3 h after stroke in the Echoplanar Imaging Thrombolytic Evaluation Trial (EPITHET): a placebo-controlled randomised trial. *Lancet Neurol*. 2008;7:299-309.
121. Schabitz WR. MR mismatch is useful for patient selection for thrombolysis: no. *Stroke*. 2009;40:2908-2909.
122. Nagakane Y, Christensen S, Brekenfeld C, Ma H, Churilov L, Parsons MW, Levi CR, Butcher KS, Peeters A, Barber PA, et al. EPITHET: Positive Result After Reanalysis Using Baseline Diffusion-Weighted Imaging/Perfusion-Weighted Imaging Co-Registration. *Stroke*. 2011;42:59-64.
123. Fink JN, Kumar S, Horkan C, Linfante I, Selim MH, Caplan LR, Schlaug G. The stroke patient who woke up: clinical and radiological features, including diffusion and perfusion MRI. *Stroke*. 2002;33:988-993.
124. Lago A, Geffner D, Tembl J, Landete L, Valero C, Baquero M. Circadian variation in acute ischemic stroke: a hospital-based study. *Stroke*. 1998;29:1873-1875.
125. Thomalla G, Cheng B, Ebinger M, Hao Q, Tourdias T, Wu O, Kim JS, Breuer L, Singer OC, Warach S, et al. DWI-FLAIR mismatch for the identification of patients with acute ischaemic stroke within 4.5 h of symptom onset (PRE-FLAIR): a multicentre observational study. *Lancet Neurol*. 2011;10:978-986.
126. Sorensen AG, Copen WA, Ostergaard L, Buonanno FS, Gonzalez RG, Rordorf G, Rosen BR, Schwamm

LH, Weisskoff RM, Koroshetz WJ. Hyperacute stroke: simultaneous measurement of relative cerebral blood volume, relative cerebral blood flow, and mean tissue transit time. *Radiology*. 1999;210:519-527.
127. Neumann-Haefelin T, Wittsack HJ, Wenserski F, Siebler M, Seitz RJ, Modder U, Freund HJ. Diffusion- and perfusion-weighted MRI. The DWI/PWI mismatch region in acute stroke. *Stroke*. 1999;30:1591-1597.
128. Grandin CB, Duprez TP, Smith AM, Oppenheim C, Peeters A, Robert AR, Cosnard G. Which MR-derived perfusion parameters are the best predictors of infarct growth in hyperacute stroke? Comparative study between relative and quantitative measurements. *Radiology*. 2002;223:361-370.
129. Kane I, Carpenter T, Chappell F, Rivers C, Armitage P, Sandercock P, Wardlaw J. Comparison of 10 different magnetic resonance perfusion imaging processing methods in acute ischemic stroke: effect on lesion size, proportion of patients with diffusion/perfusion mismatch, clinical scores, and radiologic outcomes. *Stroke*. 2007;38:3158-3164.
130. Galinovic I, Brunecker P, Ostwaldt AC, Soemmer C, Hotter B, Fiebach JB. Fully automated postprocessing carries a risk of substantial overestimation of perfusion deficits in acute stroke magnetic resonance imaging. *Cerebrovasc Dis*. 2011;31:408-413.
131. Kranz PG, Eastwood JD. Does diffusion-weighted imaging represent the ischemic core? An evidence-based systematic review. *AJNR Am J Neuroradiol*. 2009;30:1206-1212.
132. Maulaz A, Piechowski-Jozwiak B, Michel P, Bogousslavsky J. Selecting patients for early stroke treatment with penumbra images. *Cerebrovasc Dis*. 2005;20 Suppl 2:19-24.
133. Campbell BC, Purushotham A, Christensen S, Desmond PM, Nagakane Y, Parsons MW, Lansberg MG, Mlynash M, Straka M, De Silva DA, et al. The infarct core is well represented by the acute diffusion lesion: sustained reversal is infrequent. *J Cereb Blood Flow Metab*. 2012;32:50-56.
134. Wing SD, Norman D, Pollock JA, Newton TH. Contrast enhancement of cerebral infarcts in computed tomography. *Radiology*. 1976;121:89-92.
135. Lee KF, Chambers RA, Diamond C, Park CH, Thompson NL, Jr., Schnapf D, Pripstein S. Evaluation of cerebral infarction by computed tomography with special emphasis on microinfarction. *Neuroradiology*. 1978;16:156-158.
136. Norton GA, Kishore PR, Lin J. CT contrast enhancement in cerebral infarction. *AJR Am J Roentgenol*. 1978;131:881-885.
137. Hornig CR, Busse O, Buettner T, Dorndorf W, Agnoli A, Akengin Z. CT contrast enhancement on brain scans and blood-CSF barrier disturbances in cerebral ischemic infarction. *Stroke*. 1985;16:268-273.
138. Bang OY, Saver JL, Alger JR, Shah SH, Buck BH, Starkman S, Ovbiagele B, Liebeskind DS. Patterns and predictors of blood-brain barrier permeability derangements in acute ischemic stroke. *Stroke*. 2009;40:454-461.
139. Kassner A, Roberts T, Taylor K, Silver F, Mikulis D. Prediction of hemorrhage in acute ischemic stroke using permeability MR imaging. *AJNR Am J Neuroradiol*. 2005;26:2213-2217.
140. Lin K, Kazmi KS, Law M, Babb J, Peccerelli N, Pramanik BK. Measuring elevated microvascular permeability and predicting hemorrhagic transformation in acute ischemic stroke using first-pass dynamic perfusion CT imaging. *AJNR Am J Neuroradiol*. 2007;28:1292-1298.
141. Hayman LA, Evans RA, Bastion FO, Hinck VC. Delayed high dose contrast CT: identifying patients at risk of massive hemorrhagic infarction. *AJR Am J Roentgenol*. 1981;136:1151-1159.
142. Knight RA, Barker PB, Fagan SC, Li Y, Jacobs MA, Welch KM. Prediction of impending hemorrhagic transformation in ischemic stroke using magnetic resonance imaging in rats. *Stroke*. 1998;29:144-151.
143. Dijkhuizen RM, Asahi M, Wu O, Rosen BR, Lo EH. Delayed rt-PA treatment in a rat embolic stroke model: diagnosis and prognosis of ischemic injury and hemorrhagic transformation with magnetic resonance imaging. *J Cereb Blood Flow Metab*. 2001;21:964-971.
144. Neumann-Haefelin C, Brinker G, Uhlenkuken U, Pillekamp F, Hossmann KA, Hoehn M. Prediction of hemorrhagic transformation after thrombolytic therapy of clot embolism: an MRI investigation in rat brain. *Stroke*. 2002;33:1392-1398.
145. Jiang Q, Zhang RL, Zhang ZG, Knight RA, Ewing JR, Ding G, Lu M, Arniego P, Zhang L, Hu J, et al. Magnetic resonance imaging characterization of hemorrhagic transformation of embolic stroke in the rat. *J Cereb Blood Flow Metab*. 2002;22:559-568.
146. Vo KD, Santiago F, Lin W, Hsu CY, Lee Y, Lee JM. MR imaging enhancement patterns as predictors of hemorrhagic transformation in acute ischemic stroke. *AJNR Am J Neuroradiol*. 2003;24:674-679.
147. Kim EY, Na DG, Kim SS, Lee KH, Ryoo JW, Kim HK. Prediction of hemorrhagic transformation in acute ischemic stroke: role of diffusion-weighted imaging and early parenchymal enhancement. *AJNR Am J Neuroradiol*. 2005;26:1050-1055.
148. Latour LL, Kang DW, Ezzeddine MA, Chalela JA, Warach S. Early blood-brain barrier disruption in human focal brain ischemia. *Ann Neurol*. 2004;56:468-477.
149. Aviv RI, d'Esterre CD, Murphy BD, Hopyan JJ, Buck B, Mallia G, Li V, Zhang L, Symons SP, Lee TY. Hemorrhagic transformation of ischemic stroke: prediction with CT perfusion. *Radiology*. 2009;250:867-877.
150. Hom J, Dankbaar JW, Soares BP, Schneider T, Cheng SC, Bredno J, Lau BC, Smith W, Dillon WP,

Wintermark M. Blood-brain barrier permeability assessed by perfusion CT predicts symptomatic hemorrhagic transformation and malignant edema in acute ischemic stroke. *AJNR Am J Neuroradiol*. 2011;32:41-48.
151. Hom J, Dankbaar JW, Schneider T, Cheng SC, Bredno J, Wintermark M. Optimal duration of acquisition for dynamic perfusion CT assessment of blood-brain barrier permeability using the Patlak model. *AJNR Am J Neuroradiol*. 2009;30:1366-1370.
152. Bektas H, Wu TC, Kasam M, Harun N, Sitton CW, Grotta JC, Savitz SI. Increased blood-brain barrier permeability on perfusion CT might predict malignant middle cerebral artery infarction. *Stroke*. 2010;41:2539-2544.
153. Henning EC, Latour LL, Warach S. Verification of enhancement of the CSF space, not parenchyma, in acute stroke patients with early blood-brain barrier disruption. *J Cereb Blood Flow Metab*. 2008;28:882-886.
154. Kohrmann M, Struffert T, Frenzel T, Schwab S, Doerfler A. The hyperintense acute reperfusion marker on fluid-attenuated inversion recovery magnetic resonance imaging is caused by gadolinium in the cerebrospinal fluid. *Stroke*. 2012;43:259-261.
155. Warach S, Latour LL. Evidence of reperfusion injury, exacerbated by thrombolytic therapy, in human focal brain ischemia using a novel imaging marker of early blood-brain barrier disruption. *Stroke*. 2004;35:2659-2661.
156. Kidwell CS, Latour L, Saver JL, Alger JR, Starkman S, Duckwiler G, Jahan R, Vinuela F, Kang DW, Warach S. Thrombolytic toxicity: blood brain barrier disruption in human ischemic stroke. *Cerebrovasc Dis*. 2008;25:338-343.
157. Rozanski M, Ebinger M, Schmidt WU, Hotter B, Pittl S, Heuschmann PU, Jungehuelsing JG, Fiebach JB. Hyperintense acute reperfusion marker on FLAIR is not associated with early haemorrhagic transformation in the elderly. *Eur Radiol*. 2010;20:2990-2996.
158. Bang OY, Buck BH, Saver JL, Alger JR, Yoon SR, Starkman S, Ovbiagele B, Kim D, Ali LK, Sanossian N, et al. Prediction of hemorrhagic transformation after recanalization therapy using T2*-permeability magnetic resonance imaging. *Ann Neurol*. 2007;62:170-176.
159. Wu S, Thornhill RE, Chen S, Rammo W, Mikulis DJ, Kassner A. Relative recirculation: a fast, model-free surrogate for the measurement of blood-brain barrier permeability and the prediction of hemorrhagic transformation in acute ischemic stroke. *Invest Radiol*. 2009;44:662-668.
160. Thornhill RE, Chen S, Rammo W, Mikulis DJ, Kassner A. Contrast-enhanced MR imaging in acute ischemic stroke: T2* measures of blood-brain barrier permeability and their relationship to T1 estimates and hemorrhagic transformation. *AJNR Am J Neuroradiol*. 2010;31:1015-1022.
161. Hossmann KA. Animal models of cerebral ischemia. 1. Review of literature. *Cerebrovasc Dis*. 1991;1 (suppl 1):2-15.
162. Sevick RJ, Kucharczyk J, Mintorovitch J, Moseley ME, Derugin N, Norman D. Diffusion-weighted MR imaging and T2-weighted MR imaging in acute cerebral ischaemia: comparison and correlation with histopathology. *Acta Neurochir Suppl (Wien)*. 1990;51:210-212.
163. Fisher M, Feuerstein G, Howells DW, Hurn PD, Kent TA, Savitz SI, Lo EH. Update of the stroke therapy academic industry roundtable preclinical recommendations. *Stroke*. 2009;40:2244-2250.
164. Stroke Therapy Academic Industry Roundtable. Recommendations for standards regarding preclinical neuroprotective and restorative drug development. *Stroke*. 1999;30:2752-2758.
165. Macrae IM. Preclinical stroke research--advantages and disadvantages of the most common rodent models of focal ischaemia. *Br J Pharmacol*. 2011;164:1062-1078.
166. Howells DW, Porritt MJ, Rewell SS, O'Collins V, Sena ES, van der Worp HB, Traystman RJ, Macleod MR. Different strokes for different folks: the rich diversity of animal models of focal cerebral ischemia. *J Cereb Blood Flow Metab*. 2010;30:1412-1431.
167. Sicard KM, Fisher M. Animal models of focal brain ischemia. *Exp Transl Stroke Med*. 2009;1:7.
168. Durukan A, Tatlisumak T. Acute ischemic stroke: overview of major experimental rodent models, pathophysiology, and therapy of focal cerebral ischemia. *Pharmacol Biochem Behav*. 2007;87:179-197.
169. Tatlisumak T, Li F, Fisher M. Animal models of ischemic stroke. In: Bhardwaj A, Alkayed NJ, Kirsch JR, Traystman RJ, eds. *Acute stroke, bench to bedside*. New York: Informa Healthcare; 2006:171-186.
170. Kassem-Moussa H, Graffagnino C. Nonocclusion and spontaneous recanalization rates in acute ischemic stroke: a review of cerebral angiography studies. *Arch Neurol*. 2002;59:1870-1873.
171. Rha JH, Saver JL. The impact of recanalization on ischemic stroke outcome: a meta-analysis. *Stroke*. 2007;38:967-973.
172. Grotta J. Stroke treatment in the human versus animal models. In: Ginsberg MD, Bogousslavsky J, eds. *Cerebrovascular disease: pathophysiology, diagnosis, and management*. Blackwell Scientific Publications; 1998.
173. Hill NC, Millikan CH, Wakim KG, Sayre GP. Studies in cerebrovascular disease. VII. Experimental production of cerebral infarction by intracarotid injection of homologous blood clot; preliminary report. *Mayo Clin Proc*. 1955;30:625-633.
174. Kudo M, Aoyama A, Ichimori S, Fukunaga N. An animal model of cerebral infarction. Homologous blood

clot emboli in rats. *Stroke*. 1982;13:505-508.
175. Kaneko D, Nakamura N, Ogawa T. Cerebral infarction in rats using homologous blood emboli: development of a new experimental model. *Stroke*. 1985;16:76-84.
176. Overgaard K, Sereghy T, Boysen G, Pedersen H, Hoyer S, Diemer NH. A rat model of reproducible cerebral infarction using thrombotic blood clot emboli. *J Cereb Blood Flow Metab*. 1992;12:484-490.
177. Takano K, Carano RA, Tatlisumak T, Meiler M, Sotak CH, Kleinert HD, Fisher M. Efficacy of intra-arterial and intravenous prourokinase in an embolic stroke model evaluated by diffusion-perfusion magnetic resonance imaging. *Neurology*. 1998;50:870-875.
178. Busch E, Kruger K, Hossmann KA. Improved model of thromboembolic stroke and rt-PA induced reperfusion in the rat. *Brain Res*. 1997;778:16-24.
179. Zhang Z, Chopp M, Zhang RL, Goussev A. A mouse model of embolic focal cerebral ischemia. *J Cereb Blood Flow Metab*. 1997;17:1081-1088.
180. Wang CX, Yang Y, Yang T, Shuaib A. A focal embolic model of cerebral ischemia in rats: introduction and evaluation. *Brain Res Brain Res Protoc*. 2001;7:115-120.
181. Orset C, Macrez R, Young AR, Panthou D, Angles-Cano E, Maubert E, Agin V, Vivien D. Mouse model of in situ thromboembolic stroke and reperfusion. *Stroke*. 2007;38:2771-2778.
182. Ren M, Lin ZJ, Qian H, Choudhury GR, Liu R, Liu H, Yang SH. Embolic middle cerebral artery occlusion model using thrombin and fibrinogen composed clots in rat. *J Neurosci Methods*. 2012;211:296-304.
183. Overgaard K. Thrombolytic therapy in experimental embolic stroke. *Cerebrovasc Brain Metab Rev*. 1994;6:257-286.
184. Brinker G, Franke C, Hoehn M, Uhlenkuken U, Hossmann KA. Thrombolysis of cerebral clot embolism in rat: effect of treatment delay. *Neuroreport*. 1999;10:3269-3272.
185. Zhang L, Zhang ZG, Zhang C, Zhang RL, Chopp M. Intravenous administration of a GPIIb/IIIa receptor antagonist extends the therapeutic window of intra-arterial tenecteplase-tissue plasminogen activator in a rat stroke model. *Stroke*. 2004;35:2890-2895.
186. Amaro S, Chamorro A. Translational stroke research of the combination of thrombolysis and antioxidant therapy. *Stroke*. 2011;42:1495-1499.
187. Culp WC, Woods SD, Brown AT, Lowery JD, Hennings LJ, Skinner RD, Borrelli MJ, Roberson PK. Three variations in rabbit angiographic stroke models. *J Neurosci Methods*. 2012;212:322-328.
188. Gounis MJ, Nogueira RG, Mehra M, Chueh J, Wakhloo AK. A thromboembolic model for the efficacy and safety evaluation of combined mechanical and pharmacologic revascularization strategies. *J Neurointerv Surg*. 2012
189. Koizumi J, Yoshida Y, Nakazawa T, Ooneda G. Experimental studies of ischemic brain edema: 1. A new experimental model of cerebral embolism in rats in which recirculation can be introduced in the ischemic area. *Jpn J Stroke*. 1986;8:1-8.
190. Takano K, Tatlisumak T, Bergmann AG, Gibson D. G. 3rd, Fisher M. Reproducibility and reliability of middle cerebral artery occlusion using a silicone-coated suture (Koizumi) in rats. *J Neurol Sci*. 1997;153:8-11.
191. Li F, Han S, Tatlisumak T, Carano RA, Irie K, Sotak CH, Fisher M. A new method to improve in-bore middle cerebral artery occlusion in rats: demonstration with diffusion- and perfusion-weighted imaging. *Stroke*. 1998;29:1715-1719.
192. Longa EZ, Weinstein PR, Carlson S, Cummins R. Reversible middle cerebral artery occlusion without craniectomy in rats. *Stroke*. 1989;20:84-91.
193. Belayev L, Alonso OF, Busto R, Zhao W, Ginsberg MD. Middle cerebral artery occlusion in the rat by intraluminal suture. Neurological and pathological evaluation of an improved model. *Stroke*. 1996;27:1616-1622.
194. Abraham H, Somogyvari-Vigh A, Maderdrut JL, Vigh S, Arimura A. Filament size influences temperature changes and brain damage following middle cerebral artery occlusion in rats. *Exp Brain Res*. 2002;142:131-138.
195. Hata R, Mies G, Wiessner C, Fritze K, Hesselbarth D, Brinker G, Hossmann KA. A reproducible model of middle cerebral artery occlusion in mice: hemodynamic, biochemical, and magnetic resonance imaging. *J Cereb Blood Flow Metab*. 1998;18:367-375.
196. Laing RJ, Jakubowski J, Laing RW. Middle cerebral artery occlusion without craniectomy in rats. Which method works best? *Stroke*. 1993;24:294-297.
197. Shimamura N, Matchett G, Tsubokawa T, Ohkuma H, Zhang J. Comparison of silicon-coated nylon suture to plain nylon suture in the rat middle cerebral artery occlusion model. *J Neurosci Methods*. 2006;156:161-165.
198. Zarow GJ, Karibe H, States BA, Graham SH, Weinstein PR. Endovascular suture occlusion of the middle cerebral artery in rats: effect of suture insertion distance on cerebral blood flow, infarct distribution and infarct volume. *Neurol Res*. 1997;19:409-416.
199. He Z, Yamawaki T, Yang S, Day AL, Simpkins JW, Naritomi H. Experimental model of small deep infarcts involving the hypothalamus in rats: changes in body temperature and postural reflex. *Stroke*. 1999;30:2743-2751.

200. Schmid-Elsaesser R, Zausinger S, Hungerhuber E, Baethmann A, Reulen HJ. A critical reevaluation of the intraluminal thread model of focal cerebral ischemia: evidence of inadvertent premature reperfusion and subarachnoid hemorrhage in rats by laser-Doppler flowmetry. *Stroke*. 1998;29:2162-2170.
201. Li F, Omae T, Fisher M. Spontaneous hyperthermia and its mechanism in the intraluminal suture middle cerebral artery occlusion model of rats. *Stroke*. 1999;30:2464-2470.
202. Meng X, Fisher M, Shen Q, Sotak CH, Duong TQ. Characterizing the diffusion/perfusion mismatch in experimental focal cerebral ischemia. *Ann Neurol*. 2004;55:207-212.
203. Henninger N, Sicard KM, Schmidt KF, Bardutzky J, Fisher M. Comparison of ischemic lesion evolution in embolic versus mechanical middle cerebral artery occlusion in Sprague Dawley rats using diffusion and perfusion imaging. *Stroke*. 2006;37:1283-1287.
204. Aoki T, Sumii T, Mori T, Wang X, Lo EH. Blood-brain barrier disruption and matrix metalloproteinase-9 expression during reperfusion injury: mechanical versus embolic focal ischemia in spontaneously hypertensive rats. *Stroke*. 2002;33:2711-2717.
205. Hossmann KA. The two pathophysiologies of focal brain ischemia: implications for translational stroke research. *J Cereb Blood Flow Metab*. 2012;32:1310-1316.
206. Pulsinelli W, Jacewicz M. Animal models of brain ischemia. In: Barnett HJ, Mohr JP, Stein BM, Yatsu FM, eds. *Stroke: Pathophysiology, diagnosis, and management*. New York, NY, USA: Churchill Livingstone; 1992:49-67.
207. Buchan AM, Xue D, Slivka A. A new model of temporary focal neocortical ischemia in the rat. *Stroke*. 1992;23:273-279.
208. Shigeno T, Teasdale GM, McCulloch J, Graham DI. Recirculation model following MCA occlusion in rats. Cerebral blood flow, cerebrovascular permeability, and brain edema. *J Neurosurg*. 1985;63:272-277.
209. Robinson RG, Shoemaker WJ, Schlumpf M, Valk T, Bloom FE. Effect of experimental cerebral infarction in rat brain on catecholamines and behaviour. *Nature*. 1975;255:332-334.
210. Tamura A, Graham DI, McCulloch J, Teasdale GM. Focal cerebral ischaemia in the rat: 1. Description of technique and early neuropathological consequences following middle cerebral artery occlusion. *J Cereb Blood Flow Metab*. 1981;1:53-60.
211. Bederson JB, Pitts LH, Tsuji M, Nishimura MC, Davis RL, Bartkowski H. Rat middle cerebral artery occlusion: evaluation of the model and development of a neurologic examination. *Stroke*. 1986;17:472-476.
212. Brint S, Jacewicz M, Kiessling M, Tanabe J, Pulsinelli W. Focal brain ischemia in the rat: methods for reproducible neocortical infarction using tandem occlusion of the distal middle cerebral and ipsilateral common carotid arteries. *J Cereb Blood Flow Metab*. 1988;8:474-485.
213. Liu TH, Beckman JS, Freeman BA, Hogan EL, Hsu CY. Polyethylene glycol-conjugated superoxide dismutase and catalase reduce ischemic brain injury. *Am J Physiol*. 1989;256:H589-593.
214. Yanamoto H, Nagata I, Niitsu Y, Xue JH, Zhang Z, Kikuchi H. Evaluation of MCAO stroke models in normotensive rats: standardized neocortical infarction by the 3VO technique. *Exp Neurol*. 2003;182:261-274.
215. Lauer KK, Shen H, Stein EA, Ho KC, Kampine JP, Hudetz AG. Focal cerebral ischemia in rats produced by intracarotid embolization with viscous silicone. *Neurol Res*. 2002;24:181-190.
216. Purdy PD, Devous MD, Sr., Batjer HH, White CL, 3rd, Meyer Y, Samson DS. Microfibrillar collagen model of canine cerebral infarction. *Stroke*. 1989;20:1361-1367.
217. Yang Y, Yang T, Li Q, Wang CX, Shuaib A. A new reproducible focal cerebral ischemia model by introduction of polyvinylsiloxane into the middle cerebral artery: a comparison study. *J Neurosci Methods*. 2002;118:199-206.
218. Molnar L, Hegedus K, Fekete I. A new model for inducing transient cerebral ischemia and subsequent reperfusion in rabbits without craniectomy. *Stroke*. 1988;19:1262-1266.
219. Rapp JH, Pan XM, Yu B, Swanson RA, Higashida RT, Simpson P, Saloner D. Cerebral ischemia and infarction from atheroemboli <100 microm in size. *Stroke*. 2003;34:1976-1980.
220. Roos MW, Ericsson A, Berg M, Sperber GO, Sjoquist M, Meyerson BJ. Functional evaluation of cerebral microembolization in the rat. *Brain Res*. 2003;961:15-21.
221. Zivin JA, DeGirolami U, Kochhar A, Lyden PD, Mazzarella V, Hemenway CC, Henry ME. A model for quantitative evaluation of embolic stroke therapy. *Brain Res*. 1987;435:305-309.
222. Fukuchi K, Kusuoka H, Watanabe Y, Nishimura T. Correlation of sequential MR images of microsphere-induced cerebral ischemia with histologic changes in rats. *Invest Radiol*. 1999;34:698-703.
223. Hennings LJ, Flores R, Roberson PK, Brown A, Lowery J, Borrelli M, Culp WC. Persistent penumbra in a rabbit stroke model: incidence and histologic characteristics. *Stroke Res Treat*. 2011;2011:764830.
224. Mayzel-Oreg O, Omae T, Kazemi M, Li F, Fisher M, Cohen Y, Sotak CH. Microsphere-induced embolic stroke: an MRI study. *Magn Reson Med*. 2004;51:1232-1238.
225. Watson BD, Dietrich WD, Busto R, Wachtel MS, Ginsberg MD. Induction of reproducible brain infarction by photochemically initiated thrombosis. *Ann Neurol*. 1985;17:497-504.
226. Dietrich WD, Watson BD, Busto R, Ginsberg MD, Bethea JR. Photochemically induced cerebral infarction. I. Early microvascular alterations. *Acta Neuropathol (Berl)*. 1987;72:315-325.

227. Dietrich WD, Busto R, Watson BD, Scheinberg P, Ginsberg MD. Photochemically induced cerebral infarction. II. Edema and blood-brain barrier disruption. *Acta Neuropathol (Berl)*. 1987;72:326-334.
228. Wester P, Watson BD, Prado R, Dietrich WD. A photothrombotic 'ring' model of rat stroke-in-evolution displaying putative penumbral inversion. *Stroke*. 1995;26:444-450.
229. Hilger T, Blunk JA, Hoehn M, Mies G, Wester P. Characterization of a novel chronic photothrombotic ring stroke model in rats by magnetic resonance imaging, biochemical imaging, and histology. *J Cereb Blood Flow Metab*. 2004;24:789-797.
230. Hu X, Wester P, Brannstrom T, Watson BD, Gu W. Progressive and reproducible focal cortical ischemia with or without late spontaneous reperfusion generated by a ring-shaped, laser-driven photothrombotic lesion in rats. *Brain Res Brain Res Protoc*. 2001;7:76-85.
231. Matsuno H, Uematsu T, Umemura K, Takiguchi Y, Asai Y, Muranaka Y, Nakashima M. A simple and reproducible cerebral thrombosis model in rats induced by a photochemical reaction and the effect of a plasminogen-plasminogen activator chimera in this model. *J Pharmacol Toxicol Methods*. 1993;29:165-173.
232. Chen F, Suzuki Y, Nagai N, Peeters R, Sun X, Coudyzer W, Marchal G, Ni Y. Rat cerebral ischemia induced with photochemical occlusion of proximal middle cerebral artery: a stroke model for MR imaging research. *Magma*. 2004;17:103-108.
233. Chen F, Suzuki Y, Nagai N, Sun X, Wang H, Yu J, Marchal G, Ni Y. Microplasmin and tissue plasminogen activator: comparison of therapeutic effects in rat stroke model at multiparametric MR imaging. *Radiology*. 2007;244:429-438.
234. Yanagisawa M, Kurihara H, Kimura S, Tomobe Y, Kobayashi M, Mitsui Y, Yazaki Y, Goto K, Masaki T. A novel potent vasoconstrictor peptide produced by vascular endothelial cells. *Nature*. 1988;332:411-415.
235. Robinson MJ, Macrae IM, Todd M, Reid JL, McCulloch J. Reduction of local cerebral blood flow to pathological levels by endothelin-1 applied to the middle cerebral artery in the rat. *Neurosci Lett*. 1990;118:269-272.
236. Sharkey J, Ritchie IM, Kelly PA. Perivascular microapplication of endothelin-1: a new model of focal cerebral ischaemia in the rat. *J Cereb Blood Flow Metab*. 1993;13:865-871.
237. Macrae IM, Robinson MJ, Graham DI, Reid JL, McCulloch J. Endothelin-1-induced reductions in cerebral blood flow: dose dependency, time course, and neuropathological consequences. *J Cereb Blood Flow Metab*. 1993;13:276-284.
238. Fuxe K, Bjelke B, Andbjer B, Grahn H, Rimondini R, Agnati LF. Endothelin-1 induced lesions of the frontoparietal cortex of the rat. A possible model of focal cortical ischemia. *Neuroreport*. 1997;8:2623-2629.
239. Nikolova S, Moyanova S, Hughes S, Bellyou-Camilleri M, Lee TY, Bartha R. Endothelin-1 induced MCAO: dose dependency of cerebral blood flow. *J Neurosci Methods*. 2009;179:22-28.
240. Lekic T, Zhang JH. Posterior circulation stroke and animal models. *Front Biosci*. 2008;13:1827-1844.
241. Henninger N, Eberius KH, Sicard KM, Kollmar R, Sommer C, Schwab S, Schabitz WR. A new model of thromboembolic stroke in the posterior circulation of the rat. *J Neurosci Methods*. 2006;156:1-9.
242. Pan G, Wright KC. Clot embolic stroke in the vertebrobasilar system of rabbits: a transfemoral angiographic technique. *Cardiovasc Intervent Radiol*. 1987;10:285-290.
243. Gidday JM. Cerebral preconditioning and ischaemic tolerance. *Nat Rev Neurosci*. 2006;7:437-448.
244. Koerner IP, Alkayed NJ. Ischemic preconditioning. In: Bhardwaj A, Alkayed NJ, Kirsch JR, Traystman RJ, eds. *Acute stroke, bench to bedside*. New York: Informa Helthcare; 2006:345-353.
245. Perez-Pinzon MA, Xu GP, Dietrich WD, Rosenthal M, Sick TJ. Rapid preconditioning protects rats against ischemic neuronal damage after 3 but not 7 days of reperfusion following global cerebral ischemia. *J Cereb Blood Flow Metab*. 1997;17:175-182.
246. Nakamura M, Nakakimura K, Matsumoto M, Sakabe T. Rapid tolerance to focal cerebral ischemia in rats is attenuated by adenosine A1 receptor antagonist. *J Cereb Blood Flow Metab*. 2002;22:161-170.
247. Stagliano NE, Perez-Pinzon MA, Moskowitz MA, Huang PL. Focal ischemic preconditioning induces rapid tolerance to middle cerebral artery occlusion in mice. *J Cereb Blood Flow Metab*. 1999;19:757-761.
248. Atochin DN, Clark J, Demchenko IT, Moskowitz MA, Huang PL. Rapid cerebral ischemic preconditioning in mice deficient in endothelial and neuronal nitric oxide synthases. *Stroke*. 2003;34:1299-1303.
249. Kapinya KJ, Lowl D, Futterer C, Maurer M, Waschke KF, Isaev NK, Dirnagl U. Tolerance against ischemic neuronal injury can be induced by volatile anesthetics and is inducible NO synthase dependent. *Stroke*. 2002;33:1889-1898.
250. Durukan A, Tatlisumak T. Preconditioning-induced ischemic tolerance: a window into endogenous gearing for cerebroprotection. *Exp Transl Stroke Med*. 2010;2:2.
251. Stowe AM, Wacker BK, Cravens PD, Perfater JL, Li MK, Hu R, Freie AB, Stuve O, Gidday JM. CCL2 upregulation triggers hypoxic preconditioning-induced protection from stroke. *J Neuroinflammation*. 2012;9:33.
252. Wacker BK, Freie AB, Perfater JL, Gidday JM. Junctional protein regulation by sphingosine kinase 2 contributes to blood-brain barrier protection in hypoxic preconditioning-induced cerebral ischemic tolerance. *J Cereb Blood Flow Metab*. 2012;32:1014-1023.

253. Gidday JM, Fitzgibbons JC, Shah AR, Park TS. Neuroprotection from ischemic brain injury by hypoxic preconditioning in the neonatal rat. *Neurosci Lett*. 1994;168:221-224.
254. Miller BA, Perez RS, Shah AR, Gonzales ER, Park TS, Gidday JM. Cerebral protection by hypoxic preconditioning in a murine model of focal ischemia-reperfusion. *Neuroreport*. 2001;12:1663-1669.
255. Bernaudin M, Nedelec AS, Divoux D, MacKenzie ET, Petit E, Schumann-Bard P. Normobaric hypoxia induces tolerance to focal permanent cerebral ischemia in association with an increased expression of hypoxia-inducible factor-1 and its target genes, erythropoietin and VEGF, in the adult mouse brain. *J Cereb Blood Flow Metab*. 2002;22:393-403.
256. Lin AM, Dung SW, Chen CF, Chen WH, Ho LT. Hypoxic preconditioning prevents cortical infarction by transient focal ischemia-reperfusion. *Ann N Y Acad Sci*. 2003;993:168-178.
257. Stowe AM, Altay T, Freie AB, Gidday JM. Repetitive hypoxia extends endogenous neurovascular protection for stroke. *Ann Neurol*. 2011;69:975-985.
258. Sharp FR, Ran R, Lu A, Tang Y, Strauss KI, Glass T, Ardizzone T, Bernaudin M. Hypoxic preconditioning protects against ischemic brain injury. *NeuroRx*. 2004;1:26-35.
259. Tang Y, Pacary E, Freret T, Divoux D, Petit E, Schumann-Bard P, Bernaudin M. Effect of hypoxic preconditioning on brain genomic response before and following ischemia in the adult mouse: identification of potential neuroprotective candidates for stroke. *Neurobiol Dis*. 2006;21:18-28.
260. Kapinya KJ. Ischemic tolerance in the brain. *Acta Physiol Hung*. 2005;92:67-92.
261. Baranova O, Miranda LF, Pichiule P, Dragatsis I, Johnson RS, Chavez JC. Neuron-specific inactivation of the hypoxia inducible factor 1 alpha increases brain injury in a mouse model of transient focal cerebral ischemia. *J Neurosci*. 2007;27:6320-6332.
262. Wacker BK, Park TS, Gidday JM. Hypoxic preconditioning-induced cerebral ischemic tolerance: role of microvascular sphingosine kinase 2. *Stroke*. 2009;40:3342-3348.
263. DeBow SB, Clark DL, MacLellan CL, Colbourne F. Incomplete assessment of experimental cytoprotectants in rodent ischemia studies. *Can J Neurol Sci*. 2003;30:368-374.
264. Du C, Hu R, Csernansky CA, Hsu CY, Choi DW. Very delayed infarction after mild focal cerebral ischemia: a role for apoptosis? *J Cereb Blood Flow Metab*. 1996;16:195-201.
265. Valtysson J, Hillered L, Andine P, Hagberg H, Persson L. Neuropathological endpoints in experimental stroke pharmacotherapy: the importance of both early and late evaluation. *Acta Neurochir (Wien)*. 1994;129:58-63.
266. Corbett D, Crooks P. Ischemic preconditioning: a long term survival study using behavioural and histological endpoints. *Brain Res*. 1997;760:129-136.
267. Green AR. Why do neuroprotective drugs that are so promising in animals fail in the clinic? An industry perspective. *Clin Exp Pharmacol Physiol*. 2002;29:1030-1034.
268. Yamaguchi T, Suzuki M, Yamamoto M. YM796, a novel muscarinic agonist, improves the impairment of learning behavior in a rat model of chronic focal cerebral ischemia. *Brain Res*. 1995;669:107-114.
269. Kawamata T, Alexis NE, Dietrich WD, Finklestein SP. Intracisternal basic fibroblast growth factor (bFGF) enhances behavioral recovery following focal cerebral infarction in the rat. *J Cereb Blood Flow Metab*. 1996;16:542-547.
270. Rousselet E, Kriz J, Seidah NG. Mouse model of intraluminal MCAO: cerebral infarct evaluation by cresyl violet staining. *J Vis Exp*. 2012
271. Kloss CU, Thomassen N, Fesl G, Martens KH, Yousri TA, Hamann GF. Tissue-saving infarct volumetry using histochemistry validated by MRI in rat focal ischemia. *Neurol Res*. 2002;24:713-718.
272. Swanson RA, Morton MT, Tsao-Wu G, Savalos RA, Davidson C, Sharp FR. A semiautomated method for measuring brain infarct volume. *J Cereb Blood Flow Metab*. 1990;10:290-293.
273. Goldlust EJ, Paczynski RP, He YY, Hsu CY, Goldberg MP. Automated measurement of infarct size with scanned images of triphenyltetrazolium chloride-stained rat brains. *Stroke*. 1996;27:1657-1662.
274. Tatlisumak T, Takano K, Carano RA, Miller LP, Foster AC, Fisher M. Delayed treatment with an adenosine kinase inhibitor, GP683, attenuates infarct size in rats with temporary middle cerebral artery occlusion. *Stroke*. 1998;29:1952-1958.
275. Mack WJ, Komotar RJ, Mocco J, Coon AL, Hoh DJ, King RG, Ducruet AF, Ransom ER, Oppermann M, DeLaPaz R, et al. Serial magnetic resonance imaging in experimental primate stroke: validation of MRI for pre-clinical cerebroprotective trials. *Neurol Res*. 2003;25:846-852.
276. Menzies SA, Hoff JT, Betz AL. Middle cerebral artery occlusion in rats: a neurological and pathological evaluation of a reproducible model. *Neurosurgery*. 1992;31:100-106.
277. Hunter AJ, Hatcher J, Virley D, Nelson P, Irving E, Hadingham SJ, Parsons AA. Functional assessments in mice and rats after focal stroke. *Neuropharmacology*. 2000;39:806-816.
278. D'Hooge R, De Deyn PP. Applications of the Morris water maze in the study of learning and memory. *Brain Res Brain Res Rev*. 2001;36:60-90.
279. Bingham D, Martin SJ, Macrae IM, Carswell HV. Watermaze performance after middle cerebral artery occlusion in the rat: the role of sensorimotor versus memory impairments. *J Cereb Blood Flow Metab*. 2012;32:989-999.
280. Li Y, Chopp M, Chen J, Wang L, Gautam SC, Xu YX, Zhang Z. Intrastriatal transplantation of bone

marrow nonhematopoietic cells improves functional recovery after stroke in adult mice. *J Cereb Blood Flow Metab*. 2000;20:1311-1319.
281. Schaar KL, Brenneman MM, Savitz SI. Functional assessments in the rodent stroke model. *Exp Transl Stroke Med*. 2010;2:13.
282. Vannucci SJ, Willing LB, Goto S, Alkayed NJ, Brucklacher RM, Wood TL, Towfighi J, Hurn PD, Simpson IA. Experimental stroke in the female diabetic, db/db, mouse. *J Cereb Blood Flow Metab*. 2001;21:52-60.
283. Sieber FE, Hurn P, Alkayed NJ, Traystman RJ. Gender-based differences in Na+ -K+ adenosine triphosphatase activity occur in the microcirculation of the diabetic rat brain. *Anesthesiology*. 2001;94:372-375.
284. Toung TK, Hurn PD, Traystman RJ, Sieber FE. Estrogen decreases infarct size after temporary focal ischemia in a genetic model of type 1 diabetes mellitus. *Stroke*. 2000;31:2701-2706.
285. Alkayed NJ, Harukuni I, Kimes AS, London ED, Traystman RJ, Hurn PD. Gender-linked brain injury in experimental stroke. *Stroke*. 1998;29:159-165.
286. Shi J, Bui JD, Yang SH, He Z, Lucas TH, Buckley DL, Blackband SJ, King MA, Day AL, Simpkins JW. Estrogens decrease reperfusion-associated cortical ischemic damage: an MRI analysis in a transient focal ischemia model. *Stroke*. 2001;32:987-992.
287. Leon RL, Li X, Huber JD, Rosen CL. Worsened outcome from middle cerebral artery occlusion in aged rats receiving 17beta-estradiol. *Endocrinology*. 2012;153:3386-3393.
288. Rosen CL, Dinapoli VA, Nagamine T, Crocco T. Influence of age on stroke outcome following transient focal ischemia. *J Neurosurg*. 2005;103:687-694.
289. DiNapoli VA, Huber JD, Houser K, Li X, Rosen CL. Early disruptions of the blood-brain barrier may contribute to exacerbated neuronal damage and prolonged functional recovery following stroke in aged rats. *Neurobiol Aging*. 2008;29:753-764.
290. Zhang L, Zhang RL, Wang Y, Zhang C, Zhang ZG, Meng H, Chopp M. Functional recovery in aged and young rats after embolic stroke: treatment with a phosphodiesterase type 5 inhibitor. *Stroke*. 2005;36:847-852.
291. Kaur J, Tuor UI, Zhao Z, Barber PA. Quantitative MRI reveals the elderly ischemic brain is susceptible to increased early blood-brain barrier permeability following tissue plasminogen activator related to claudin 5 and occludin disassembly. *J Cereb Blood Flow Metab*. 2011;31:1874-1885.
292. Won SJ, Xie L, Kim SH, Tang H, Wang Y, Mao X, Banwait S, Jin K. Influence of age on the response to fibroblast growth factor-2 treatment in a rat model of stroke. *Brain Res*. 2006;1123:237-244.
293. Kelly KA, Li X, Tan Z, VanGilder RL, Rosen CL, Huber JD. NOX2 inhibition with apocynin worsens stroke outcome in aged rats. *Brain Res*. 2009;1292:165-172.
294. Bardutzky J, Shen Q, Henninger N, Bouley J, Duong TQ, Fisher M. Differences in ischemic lesion evolution in different rat strains using diffusion and perfusion imaging. *Stroke*. 2005;36:2000-2005.
295. Dittmar MS, Vatankhah B, Fehm NP, Schuierer G, Bogdahn U, Horn M, Schlachetzki F. Fischer-344 rats are unsuitable for the MCAO filament model due to their cerebrovascular anatomy. *J Neurosci Methods*. 2006;156:50-54.
296. Duverger D, MacKenzie ET. The quantification of cerebral infarction following focal ischemia in the rat: influence of strain, arterial pressure, blood glucose concentration, and age. *J Cereb Blood Flow Metab*. 1988;8:449-461.
297. Oliff HS, Weber E, Miyazaki B, Marek P. Infarct volume varies with rat strain and vendor in focal cerebral ischemia induced by transcranial middle cerebral artery occlusion. *Brain Res*. 1995;699:329-331.
298. Oliff HS, Weber E, Eilon G, Marek P. The role of strain/vendor differences on the outcome of focal ischemia induced by intraluminal middle cerebral artery occlusion in the rat. *Brain Res*. 1995;675:20-26.
299. Walberer M, Stolz E, Muller C, Friedrich C, Rottger C, Blaes F, Kaps M, Fisher M, Bachmann G, Gerriets T. Experimental stroke: ischaemic lesion volume and oedema formation differ among rat strains (a comparison between Wistar and Sprague-Dawley rats using MRI). *Lab Anim*. 2006;40:1-8.
300. Sauter A, Rudin M. Strain-dependent drug effects in rat middle cerebral artery occlusion model of stroke. *J Pharmacol Exp Ther*. 1995;274:1008-1013.
301. Oliff HS, Marek P, Miyazaki B, Weber E. The neuroprotective efficacy of MK-801 in focal cerebral ischemia varies with rat strain and vendor. *Brain Res*. 1996;731:208-212.
302. Coyle P. Different susceptibilities to cerebral infarction in spontaneously hypertensive (SHR) and normotensive Sprague-Dawley rats. *Stroke*. 1986;17:520-525.
303. Bailey EL, Smith C, Sudlow CL, Wardlaw JM. Is the spontaneously hypertensive stroke prone rat a pertinent model of sub cortical ischemic stroke? A systematic review. *Int J Stroke*. 2011;6:434-444.
304. Bailey EL, McCulloch J, Sudlow C, Wardlaw JM. Potential animal models of lacunar stroke: a systematic review. *Stroke*. 2009;40:e451-458.
305. Nabika T, Cui Z, Masuda J. The stroke-prone spontaneously hypertensive rat: how good is it as a model for cerebrovascular diseases? *Cell Mol Neurobiol*. 2004;24:639-646.
306. Rees DA, Alcolado JC. Animal models of diabetes mellitus. *Diabet Med*. 2005;22:359-370.
307. Lerman LO, Chade AR, Sica V, Napoli C. Animal models of hypertension: an overview. *J Lab Clin Med*. 2005;146:160-173.

308. Fan X, Qiu J, Yu Z, Dai H, Singhal AB, Lo EH, Wang X. A rat model of studying tissue-type plasminogen activator thrombolysis in ischemic stroke with diabetes. *Stroke*. 2012;43:567-570.
309. Ning R, Chopp M, Yan T, Zacharek A, Zhang C, Roberts C, Cui X, Lu M, Chen J. Tissue plasminogen activator treatment of stroke in type-1 diabetes rats. *Neuroscience*. 2012;222:326-332.
310. Zhu M, Bi X, Jia Q, Shangguan S. The possible mechanism for impaired angiogenesis after transient focal ischemia in type 2 diabetic GK rats: different expressions of angiostatin and vascular endothelial growth factor. *Biomed Pharmacother*. 2010;64:208-213.
311. MacDougall NJ, Muir KW. Hyperglycaemia and infarct size in animal models of middle cerebral artery occlusion: systematic review and meta-analysis. *J Cereb Blood Flow Metab*. 2011;31:807-818.
312. Huang NC, Wei J, Quast MJ. A comparison of the early development of ischemic brain damage in normoglycemic and hyperglycemic rats using magnetic resonance imaging. *Exp Brain Res*. 1996;109:33-42.
313. Nedergaard M. Transient focal ischemia in hyperglycemic rats is associated with increased cerebral infarction. *Brain Res*. 1987;408:79-85.
314. Liu L, Wang Z, Wang X, Song L, Chen H, Bemeur C, Ste-Marie L, Montgomery J. Comparison of two rat models of cerebral ischemia under hyperglycemic conditions. *Microsurgery*. 2007;27:258-262.
315. Xing Y, Jiang X, Yang Y, Xi G. Hemorrhagic transformation induced by acute hyperglycemia in a rat model of transient focal ischemia. *Acta Neurochir Suppl*. 2011;111:49-54.
316. Ginsberg MD, Busto R. Combating hyperthermia in acute stroke: a significant clinical concern. *Stroke*. 1998;29:529-534.
317. van der Worp HB, Sena ES, Donnan GA, Howells DW, Macleod MR. Hypothermia in animal models of acute ischaemic stroke: a systematic review and meta-analysis. *Brain*. 2007;130:3063-3074.
318. Kirsch JR, Traystman RJ, Hurn PD. Anesthetics and cerebroprotection: experimental aspects. *Int Anesthesiol Clin*. 1996;34:73-93.
319. Clarkson AN. Anesthetic-mediated protection/preconditioning during cerebral ischemia. *Life Sci*. 2007;80:1157-1175.
320. Ehrlich P. Das Sauerstoffbeduerfnis des organismus: Eine farbenanalytiche Studie. In: Editor, ed.^eds. Berlin: Hirschwald; 1885.
321. Hawkins BT, Davis TP. The blood-brain barrier/neurovascular unit in health and disease. *Pharmacol Rev*. 2005;57:173-185.
322. Reese TS, Karnovsky MJ. Fine structural localization of a blood-brain barrier to exogenous peroxidase. *J Cell Biol*. 1967;34:207-217.
323. National Institute of Neurological Disorders and Stroke. Report of the stroke progress review group 2002. 2002
324. Lo EH, Dalkara T, Moskowitz MA. Mechanisms, challenges and opportunities in stroke. *Nat Rev Neurosci*. 2003;4:399-415.
325. Wardlaw JM, Doubal F, Armitage P, Chappell F, Carpenter T, Munoz Maniega S, Farrall A, Sudlow C, Dennis M, Dhillon B. Lacunar stroke is associated with diffuse blood-brain barrier dysfunction. *Ann Neurol*. 2009;65:194-202.
326. Oldendorf WH, Cornford ME, Brown WJ. The large apparent work capability of the blood-brain barrier: a study of the mitochondrial content of capillary endothelial cells in brain and other tissues of the rat. *Ann Neurol*. 1977;1:409-417.
327. Cao Y, Brown SL, Knight RA, Fenstermacher JD, Ewing JR. Effect of intravascular-to-extravascular water exchange on the determination of blood-to-tissue transfer constant by magnetic resonance imaging. *Magn Reson Med*. 2005;53:282-293.
328. Simionescu M, Simionescu N, Palade GE. Morphometric data on the endothelium of blood capillaries. *J Cell Biol*. 1974;60:128-152.
329. Fenstermacher J, Gross P, Sposito N, Acuff V, Pettersen S, Gruber K. Structural and functional variations in capillary systems within the brain. *Ann N Y Acad Sci*. 1988;529:21-30.
330. Broadwell RD, Salcman M. Expanding the definition of the blood-brain barrier to protein. *Proc Natl Acad Sci U S A*. 1981;78:7820-7824.
331. Butt AM, Jones HC, Abbott NJ. Electrical resistance across the blood-brain barrier in anaesthetized rats: a developmental study. *J Physiol*. 1990;429:47-62.
332. Engelhardt B. Development of the blood-brain barrier. *Cell Tissue Res*. 2003;314:119-129.
333. Risau W, Esser S, Engelhardt B. Differentiation of blood-brain barrier endothelial cells. *Pathol Biol (Paris)*. 1998;46:171-175.
334. Bodor N, Buchwald P. Targeting of neuropharmaceuticals by chemical delivery systems. In: Dermietzel R, Spray DC, Nedergaard M, eds. *Blood-brain barriers from ontogeny to artificial interfaces*. Weinheim: Wiley-VCH; 2006:463-500.
335. Dalkara T, Gursoy-Ozdemir Y, Yemisci M. Brain microvascular pericytes in health and disease. *Acta Neuropathol*. 2011;122:1-9.
336. Kamouchi M, Ago T, Kuroda J, Kitazono T. The possible roles of brain pericytes in brain ischemia and stroke. *Cell Mol Neurobiol*. 2012;32:159-165.

337. Lindahl P, Johansson BR, Leveen P, Betsholtz C. Pericyte loss and microaneurysm formation in PDGF-B-deficient mice. *Science*. 1997;277:242-245.
338. Daneman R, Zhou L, Kebede AA, Barres BA. Pericytes are required for blood-brain barrier integrity during embryogenesis. *Nature*. 2010;468:562-566.
339. Yemisci M, Gursoy-Ozdemir Y, Vural A, Can A, Topalkara K, Dalkara T. Pericyte contraction induced by oxidative-nitrative stress impairs capillary reflow despite successful opening of an occluded cerebral artery. *Nat Med*. 2009;15:1031-1037.
340. del Zoppo GJ. Relationship of neurovascular elements to neuron injury during ischemia. *Cerebrovasc Dis*. 2009;27 Suppl 1:65-76.
341. Hamann GF, Okada Y, Fitridge R, del Zoppo GJ. Microvascular basal lamina antigens disappear during cerebral ischemia and reperfusion. *Stroke*. 1995;26:2120-2126.
342. del Zoppo GJ. The neurovascular unit, matrix proteases, and innate inflammation. *Ann N Y Acad Sci*. 2010;1207:46-49.
343. Hamann GF, Okada Y, del Zoppo GJ. Hemorrhagic transformation and microvascular integrity during focal cerebral ischemia/reperfusion. *J Cereb Blood Flow Metab*. 1996;16:1373-1378.
344. Rosenberg GA, Estrada EY, Dencoff JE. Matrix metalloproteinases and TIMPs are associated with blood-brain barrier opening after reperfusion in rat brain. *Stroke*. 1998;29:2189-2195.
345. Gasche Y, Fujimura M, Morita-Fujimura Y, Copin JC, Kawase M, Massengale J, Chan PH. Early appearance of activated matrix metalloproteinase-9 after focal cerebral ischemia in mice: a possible role in blood-brain barrier dysfunction. *J Cereb Blood Flow Metab*. 1999;19:1020-1028.
346. Asahi M, Wang X, Mori T, Sumii T, Jung JC, Moskowitz MA, Fini ME, Lo EH. Effects of matrix metalloproteinase-9 gene knockout on the proteolysis of blood-brain barrier and white matter components after cerebral ischemia. *J Neurosci*. 2001;21:7724-7732.
347. Fukuda S, Fini CA, Mabuchi T, Koziol JA, Eggleston LL, Jr., del Zoppo GJ. Focal cerebral ischemia induces active proteases that degrade microvascular matrix. *Stroke*. 2004;35:998-1004.
348. Sood RR, Taheri S, Candelario-Jalil E, Estrada EY, Rosenberg GA. Early beneficial effect of matrix metalloproteinase inhibition on blood-brain barrier permeability as measured by magnetic resonance imaging countered by impaired long-term recovery after stroke in rat brain. *J Cereb Blood Flow Metab*. 2008;28:431-438.
349. Yang Y, Estrada EY, Thompson JF, Liu W, Rosenberg GA. Matrix metalloproteinase-mediated disruption of tight junction proteins in cerebral vessels is reversed by synthetic matrix metalloproteinase inhibitor in focal ischemia in rat. *J Cereb Blood Flow Metab*. 2007;27:697-709.
350. Liu J, Jin X, Liu KJ, Liu W. Matrix metalloproteinase-2-mediated occludin degradation and caveolin-1-mediated claudin-5 redistribution contribute to blood-brain barrier damage in early ischemic stroke stage. *J Neurosci*. 2012;32:3044-3057.
351. Gu Y, Zheng G, Xu M, Li Y, Chen X, Zhu W, Tong Y, Chung SK, Liu KJ, Shen J. Caveolin-1 regulates nitric oxide-mediated matrix metalloproteinases activity and blood-brain barrier permeability in focal cerebral ischemia and reperfusion injury. *J Neurochem*. 2012;120:147-156.
352. Ramos-Fernandez M, Bellolio MF, Stead LG. Matrix metalloproteinase-9 as a marker for acute ischemic stroke: a systematic review. *J Stroke Cerebrovasc Dis*. 2011;20:47-54.
353. Kniesel U, Wolburg H. Tight junctions of the blood-brain barrier. *Cell Mol Neurobiol*. 2000;20:57-76.
354. Bauer HC, Traweger A, Bauer H. Proteins of the tight junction in the blood-brain barrier. In: Sharma HS, Westman J, eds. *Blood-spinal cord and brain barriers in health and disease*. San Diego, California: Elsevier Academic Press; 2004:1-10.
355. Wolburg H. The endothelial frontier. In: Dermietzel R, Spray DC, Nedergaard M, eds. *Blood-brain barriers from ontogeny to artificial interfaces*. Weinheim: Wiley-VCH; 2006:77-107.
356. Rosenberg GA, Yang Y. Vasogenic edema due to tight junction disruption by matrix metalloproteinases in cerebral ischemia. *Neurosurg Focus*. 2007;22:E4.
357. Sandoval KE, Witt KA. Blood-brain barrier tight junction permeability and ischemic stroke. *Neurobiol Dis*. 2008;32:200-219.
358. Furuse M, Hirase T, Itoh M, Nagafuchi A, Yonemura S, Tsukita S, Tsukita S. Occludin: a novel integral membrane protein localizing at tight junctions. *J Cell Biol*. 1993;123:1777-1788.
359. Saitou M, Fujimoto K, Doi Y, Itoh M, Fujimoto T, Furuse M, Takano H, Noda T, Tsukita S. Occludin-deficient embryonic stem cells can differentiate into polarized epithelial cells bearing tight junctions. *J Cell Biol*. 1998;141:397-408.
360. Balda MS, Whitney JA, Flores C, Gonzalez S, Cereijido M, Matter K. Functional dissociation of paracellular permeability and transepithelial electrical resistance and disruption of the apical-basolateral intramembrane diffusion barrier by expression of a mutant tight junction membrane protein. *J Cell Biol*. 1996;134:1031-1049.
361. Kago T, Takagi N, Date I, Takenaga Y, Takagi K, Takeo S. Cerebral ischemia enhances tyrosine phosphorylation of occludin in brain capillaries. *Biochem Biophys Res Commun*. 2006;339:1197-1203.
362. Correale J, Villa A. Cellular elements of the blood-brain barrier. *Neurochem Res*. 2009;34:2067-2077.
363. Nitta T, Hata M, Gotoh S, Seo Y, Sasaki H, Hashimoto N, Furuse M, Tsukita S. Size-selective loosening

of the blood-brain barrier in claudin-5-deficient mice. *J Cell Biol*. 2003;161:653-660.
364. Martin-Padura I, Lostaglio S, Schneemann M, Williams L, Romano M, Fruscella P, Panzeri C, Stoppacciaro A, Ruco L, Villa A, et al. Junctional adhesion molecule, a novel member of the immunoglobulin superfamily that distributes at intercellular junctions and modulates monocyte transmigration. *J Cell Biol*. 1998;142:117-127.
365. Stevenson BR, Siliciano JD, Mooseker MS, Goodenough DA. Identification of ZO-1: a high molecular weight polypeptide associated with the tight junction (zonula occludens) in a variety of epithelia. *J Cell Biol*. 1986;103:755-766.
366. Nico B, Ribatti D. Morphofunctional aspects of the blood-brain barrier. *Curr Drug Metab*. 2012;13:50-60.
367. Mishiro K, Ishiguro M, Suzuki Y, Tsuruma K, Shimazawa M, Hara H. A broad-spectrum matrix metalloproteinase inhibitor prevents hemorrhagic complications induced by tissue plasminogen activator in mice. *Neuroscience*. 2012;205:39-48.
368. Dejana E, Orsenigo F, Lampugnani MG. The role of adherens junctions and VE-cadherin in the control of vascular permeability. *J Cell Sci*. 2008;121:2115-2122.
369. Simard M, Nedergaard M. The neurobiology of glia in the context of water and ion homeostasis. *Neuroscience*. 2004;129:877-896.
370. Zhou J, Kong H, Hua X, Xiao M, Ding J, Hu G. Altered blood-brain barrier integrity in adult aquaporin-4 knockout mice. *Neuroreport*. 2008;19:1-5.
371. Manley GT, Fujimura M, Ma T, Noshita N, Filiz F, Bollen AW, Chan P, Verkman AS. Aquaporin-4 deletion in mice reduces brain edema after acute water intoxication and ischemic stroke. *Nat Med*. 2000;6:159-163.
372. Zeng XN, Xie LL, Liang R, Sun XL, Fan Y, Hu G. AQP4 knockout aggravates ischemia/reperfusion injury in mice. *CNS Neurosci Ther*. 2012;18:388-394.
373. Crone C. The Permeability Of Capillaries In Various Organs As Determined By Use Of The 'Indicator Diffusion' Method. *Acta Physiol Scand*. 1963;58:292-305.
374. Nag S. Blood-brain barrier permeability using tracers and immunohistochemistry. *Methods Mol Med*. 2003;89:133-144.
375. Hoffmann A, Bredno J, Wendland M, Derugin N, Ohara P, Wintermark M. High and Low Molecular Weight Fluorescein Isothiocyanate (FITC)-Dextrans to Assess Blood-Brain Barrier Disruption: Technical Considerations. *Transl Stroke Res*. 2011;2:106-111.
376. Xu Q, Qaum T, Adamis AP. Sensitive blood-retinal barrier breakdown quantitation using Evans blue. *Invest Ophthalmol Vis Sci*. 2001;42:789-794.
377. Manaenko A, Chen H, Kammer J, Zhang JH, Tang J. Comparison Evans Blue injection routes: Intravenous versus intraperitoneal, for measurement of blood-brain barrier in a mice hemorrhage model. *J Neurosci Methods*. 2011;195:206-210.
378. Tofts PS, Berkowitz BA. Measurement of capillary permeability from the Gd enhancement curve: a comparison of bolus and constant infusion injection methods. *Magn Reson Imaging*. 1994;12:81-91.
379. Kastrup A, Groschel K, Ringer TM, Redecker C, Cordesmeyer R, Witte OW, Terborg C. Early disruption of the blood-brain barrier after thrombolytic therapy predicts hemorrhage in patients with acute stroke. *Stroke*. 2008;39:2385-2387.
380. Hjort N, Wu O, Ashkanian M, Solling C, Mouridsen K, Christensen S, Gyldensted C, Andersen G, Ostergaard L. MRI detection of early blood-brain barrier disruption: parenchymal enhancement predicts focal hemorrhagic transformation after thrombolysis. *Stroke*. 2008;39:1025-1028.
381. Kassner A, Mandell DM, Mikulis DJ. Measuring permeability in acute ischemic stroke. *Neuroimaging Clin N Am*. 2011;21:315-325.
382. Saria A, Lundberg JM. Evans blue fluorescence: quantitative and morphological evaluation of vascular permeability in animal tissues. *J Neurosci Methods*. 1983;8:41-49.
383. Uyama O, Okamura N, Yanase M, Narita M, Kawabata K, Sugita M. Quantitative evaluation of vascular permeability in the gerbil brain after transient ischemia using Evans blue fluorescence. *J Cereb Blood Flow Metab*. 1988;8:282-284.
384. Hawkins BT, Egleton RD. Fluorescence imaging of blood-brain barrier disruption. *J Neurosci Methods*. 2006;151:262-267.
385. Ohno K, Pettigrew KD, Rapoport SI. Lower limits of cerebrovascular permeability to nonelectrolytes in the conscious rat. *Am J Physiol*. 1978;235:H299-307.
386. Huang ZG, Xue D, Preston E, Karbalai H, Buchan AM. Biphasic opening of the blood-brain barrier following transient focal ischemia: effects of hypothermia. *Can J Neurol Sci*. 1999;26:298-304.
387. Masada T, Hua Y, Xi G, Ennis SR, Keep RF. Attenuation of ischemic brain edema and cerebrovascular injury after ischemic preconditioning in the rat. *J Cereb Blood Flow Metab*. 2001;21:22-33.
388. Mayhan WG, Heistad DD. Permeability of blood-brain barrier to various sized molecules. *Am J Physiol*. 1985;248:H712-718.
389. Jin AY, Tuor UI, Rushforth D, Kaur J, Muller RN, Petterson JL, Boutry S, Barber PA. Reduced blood brain barrier breakdown in P-selectin deficient mice following transient ischemic stroke: a future therapeutic target for treatment of stroke. *BMC Neurosci*. 2010;11:12.

390. Dimitrijevic OB, Stamatovic SM, Keep RF, Andjelkovic AV. Effects of the chemokine CCL2 on blood-brain barrier permeability during ischemia-reperfusion injury. *J Cereb Blood Flow Metab*. 2006;26:797-810.
391. Schmidt-Kastner R, Szymas J, Hossmann KA. Immunohistochemical study of glial reaction and serum-protein extravasation in relation to neuronal damage in rat hippocampus after ischemia. *Neuroscience*. 1990;38:527-540.
392. Klohs J, Steinbrink J, Bourayou R, Mueller S, Cordell R, Licha K, Schirner M, Dirnagl U, Lindauer U, Wunder A. Near-infrared fluorescence imaging with fluorescently labeled albumin: a novel method for non-invasive optical imaging of blood-brain barrier impairment after focal cerebral ischemia in mice. *J Neurosci Methods*. 2009;180:126-132.
393. Abulrob A, Brunette E, Slinn J, Baumann E, Stanimirovic D. In vivo optical imaging of ischemic blood-brain barrier disruption. *Methods Mol Biol*. 2011;763:423-439.
394. Tofts PS. Modeling tracer kinetics in dynamic Gd-DTPA MR imaging. *J Magn Reson Imaging*. 1997;7:91-101.
395. Patlak CS, Blasberg RG, Fenstermacher JD. Graphical evaluation of blood-to-brain transfer constants from multiple-time uptake data. *J Cereb Blood Flow Metab*. 1983;3:1-7.
396. Ewing JR, Knight RA, Nagaraja TN, Yee JS, Nagesh V, Whitton PA, Li L, Fenstermacher JD. Patlak plots of Gd-DTPA MRI data yield blood-brain transfer constants concordant with those of 14C-sucrose in areas of blood-brain opening. *Magn Reson Med*. 2003;50:283-292.
397. Hoffmann A, Bredno J, Wendland MF, Derugin N, Hom J, Schuster T, Su H, Ohara PT, Young WL, Wintermark M. Validation of in vivo magnetic resonance imaging blood-brain barrier permeability measurements by comparison with gold standard histology. *Stroke*. 2011;42:2054-2060.
398. Kassner A, Roberts TP, Moran B, Silver FL, Mikulis DJ. Recombinant tissue plasminogen activator increases blood-brain barrier disruption in acute ischemic stroke: an MR imaging permeability study. *AJNR Am J Neuroradiol*. 2009;30:1864-1869.
399. Vidarsson L, Thornhill RE, Liu F, Mikulis DJ, Kassner A. Quantitative permeability magnetic resonance imaging in acute ischemic stroke: how long do we need to scan? *Magn Reson Imaging*. 2009;27:1216-1222.
400. Kuroiwa T, Ting P, Martinez H, Klatzo I. The biphasic opening of the blood-brain barrier to proteins following temporary middle cerebral artery occlusion. *Acta Neuropathol (Berl)*. 1985;68:122-129.
401. Belayev L, Busto R, Zhao W, Ginsberg MD. Quantitative evaluation of blood-brain barrier permeability following middle cerebral artery occlusion in rats. *Brain Res*. 1996;739:88-96.
402. Candelario-Jalil E, Taheri S, Yang Y, Sood R, Grossetete M, Estrada EY, Fiebich BL, Rosenberg GA. Cyclooxygenase inhibition limits blood-brain barrier disruption following intracerebral injection of tumor necrosis factor-alpha in the rat. *J Pharmacol Exp Ther*. 2007;323:488-498.
403. Rosenberg GA. Neurological diseases in relation to the blood-brain barrier. *J Cereb Blood Flow Metab*. 2012;32:1139-1151.
404. Wagner GF, Hampong M, Park CM, Copp DH. Purification, characterization, and bioassay of teleocalcin, a glycoprotein from salmon corpuscles of Stannius. *Gen Comp Endocrinol*. 1986;63:481-491.
405. Chang AC, Janosi J, Hulsbeek M, de Jong D, Jeffrey KJ, Noble JR, Reddel RR. A novel human cDNA highly homologous to the fish hormone stanniocalcin. *Mol Cell Endocrinol*. 1995;112:241-247.
406. Chang AC, Reddel RR. Identification of a second stanniocalcin cDNA in mouse and human: stanniocalcin 2. *Mol Cell Endocrinol*. 1998;141:95-99.
407. Yeung BH, Law AY, Wong CK. Evolution and roles of stanniocalcin. *Mol Cell Endocrinol*. 2012;349:272-280.
408. Yeung HY, Lai KP, Chan HY, Mak NK, Wagner GF, Wong CK. Hypoxia-inducible factor-1-mediated activation of stanniocalcin-1 in human cancer cells. *Endocrinology*. 2005;146:4951-4960.
409. Liu D, Huang L, Wang Y, Wang W, Wehrens XH, Belousova T, Abdelrahim M, DiMattia G, Sheikh-Hamad D. Human stanniocalcin-1 suppresses angiotensin II-induced superoxide generation in cardiomyocytes through UCP3-mediated anti-oxidant pathway. *PLoS One*. 2012;7:e36994.
410. Sheikh-Hamad D. Mammalian stanniocalcin-1 activates mitochondrial antioxidant pathways: new paradigms for regulation of macrophages and endothelium. *Am J Physiol Renal Physiol*. 2010;298:F248-254.
411. Ito D, Walker JR, Thompson CS, Moroz I, Lin W, Veselits ML, Hakim AM, Fienberg AA, Thinakaran G. Characterization of stanniocalcin 2, a novel target of the mammalian unfolded protein response with cytoprotective properties. *Mol Cell Biol*. 2004;24:9456-9469.
412. Franzen AM, Zhang KZ, Westberg JA, Zhang WM, Arola J, Olsen HS, Andersson LC. Expression of stanniocalcin in the epithelium of human choroid plexus. *Brain Res*. 2000;887:440-443.
413. Ratkovic S, Wagner GF, Ciriello J. Distribution of stanniocalcin binding sites in the lamina terminalis of the rat. *Brain Res*. 2008;1218:141-150.
414. Li K, Dong D, Yao L, Dai D, Gu X, Guo L. Identification of STC1 as an beta-amyloid activated gene in human brain microvascular endothelial cells using cDNA microarray. *Biochem Biophys Res Commun*. 2008;376:399-403.

415. Zhang KZ, Westberg JA, Paetau A, von Boguslawsky K, Lindsberg P, Erlander M, Guo H, Su J, Olsen HS, Andersson LC. High expression of stanniocalcin in differentiated brain neurons. *Am J Pathol*. 1998;153:439-445.
416. Zhang K, Lindsberg PJ, Tatlisumak T, Kaste M, Olsen HS, Andersson LC. Stanniocalcin: A molecular guard of neurons during cerebral ischemia. *Proc Natl Acad Sci U S A*. 2000;97:3637-3642.
417. Long Y, Zou L, Liu H, Lu H, Yuan X, Robertson CS, Yang K. Altered expression of randomly selected genes in mouse hippocampus after traumatic brain injury. *J Neurosci Res*. 2003;71:710-720.
418. Westberg JA, Serlachius M, Lankila P, Penkowa M, Hidalgo J, Andersson LC. Hypoxic preconditioning induces neuroprotective stanniocalcin-1 in brain via IL-6 signaling. *Stroke*. 2007;38:1025-1030.
419. Byun JS, Lee JW, Kim SY, Kwon KJ, Sohn JH, Lee K, Oh D, Kim SS, Chun W, Lee HJ. Neuroprotective effects of stanniocalcin 2 following kainic acid-induced hippocampal degeneration in ICR mice. *Peptides*. 2010;31:2094-2099.
420. Holmes DI, Zachary IC. Vascular endothelial growth factor regulates stanniocalcin-1 expression via neuropilin-1-dependent regulation of KDR and synergism with fibroblast growth factor-2. *Cell Signal*. 2008;20:569-579.
421. Chen C, Jamaluddin MS, Yan S, Sheikh-Hamad D, Yao Q. Human stanniocalcin-1 blocks TNF-alpha-induced monolayer permeability in human coronary artery endothelial cells. *Arterioscler Thromb Vasc Biol*. 2008;28:906-912.
422. Manalo DJ, Rowan A, Lavoie T, Natarajan L, Kelly BD, Ye SQ, Garcia JG, Semenza GL. Transcriptional regulation of vascular endothelial cell responses to hypoxia by HIF-1. *Blood*. 2005;105:659-669.
423. Chang AC, Cha J, Koentgen F, Reddel RR. The murine stanniocalcin 1 gene is not essential for growth and development. *Mol Cell Biol*. 2005;25:10604-10610.
424. Pedrono E, Durukan A, Strbian D, Marinkovic I, Shekhar S, Pitkonen M, Abo-Ramadan U, Tatlisumak T. An optimized mouse model for transient ischemic attack. *J Neuropathol Exp Neurol*. 2010;69:188-195.
425. Nagaraja TN, Karki K, Ewing JR, Divine GW, Fenstermacher JD, Patlak CS, Knight RA. The MRI-measured arterial input function resulting from a bolus injection of Gd-DTPA in a rat model of stroke slightly underestimates that of Gd-[14C]DTPA and marginally overestimates the blood-to-brain influx rate constant determined by Patlak plots. *Magn Reson Med*. 2010;63:1502-1509.
426. Tatlisumak T, Carano RA, Takano K, Opgenorth TJ, Sotak CH, Fisher M. A novel endothelin antagonist, A-127722, attenuates ischemic lesion size in rats with temporary middle cerebral artery occlusion: a diffusion and perfusion MRI study. *Stroke*. 1998;29:850-857.
427. Abramoff MD, Magalhaes PJ, Ram SJ. Image processing with Imaje J. *Biophotonics Int*. 2004;11:36-42.
428. Strbian D, Karjalainen-Lindsberg ML, Tatlisumak T, Lindsberg PJ. Cerebral mast cells regulate early ischemic brain swelling and neutrophil accumulation. *J Cereb Blood Flow Metab*. 2006;26:605-612.
429. Patlak CS, Blasberg RG. Graphical evaluation of blood-to-brain transfer constants from multiple-time uptake data. Generalizations. *J Cereb Blood Flow Metab*. 1985;5:584-590.
430. Murray CJ, Lopez AD. Mortality by cause for eight regions of the world: Global Burden of Disease Study. *Lancet*. 1997;349:1269-1276.
431. Seshadri S, Beiser A, Kelly-Hayes M, Kase CS, Au R, Kannel WB, Wolf PA. The lifetime risk of stroke: estimates from the Framingham Study. *Stroke*. 2006;37:345-350.
432. Bose B, Osterholm JL, Berry R. A reproducible experimental model of focal cerebral ischemia in the cat. *Brain Res*. 1984;311:385-391.
433. Kastrup A, Engelhorn T, Beaulieu C, de Crespigny A, Moseley ME. Dynamics of cerebral injury, perfusion, and blood-brain barrier changes after temporary and permanent middle cerebral artery occlusion in the rat. *J Neurol Sci*. 1999;166:91-99.
434. Neumann-Haefelin T, Kastrup A, de Crespigny A, Yenari MA, Ringer T, Sun GH, Moseley ME. Serial MRI after transient focal cerebral ischemia in rats: dynamics of tissue injury, blood-brain barrier damage, and edema formation. *Stroke*. 2000;31:1965-1972; discussion 1972-1963.
435. Lennmyr F, Ericsson A, Gerwins P, Ahlstrom H, Terent A. Increased brain injury and vascular leakage after pretreatment with p38-inhibitor SB203580 in transient ischemia. *Acta Neurol Scand*. 2003;108:339-345.
436. Nagel S, Wagner S, Koziol J, Kluge B, Heiland S. Volumetric evaluation of the ischemic lesion size with serial MRI in a transient MCAO model of the rat: comparison of DWI and T1WI. *Brain Res Brain Res Protoc*. 2004;12:172-179.
437. Nagel S, Su Y, Horstmann S, Heiland S, Gardner H, Koziol J, Martinez-Torres FJ, Wagner S. Minocycline and hypothermia for reperfusion injury after focal cerebral ischemia in the rat: effects on BBB breakdown and MMP expression in the acute and subacute phase. *Brain Res*. 2008;1188:198-206.
438. Veltkamp R, Siebing DA, Sun L, Heiland S, Bieber K, Marti HH, Nagel S, Schwab S, Schwaninger M. Hyperbaric oxygen reduces blood-brain barrier damage and edema after transient focal cerebral ischemia. *Stroke*. 2005;36:1679-1683.
439. Lin CY, Chang C, Cheung WM, Lin MH, Chen JJ, Hsu CY, Chen JH, Lin TN. Dynamic changes in vascular permeability, cerebral blood volume, vascular density, and size after transient focal cerebral ischemia in rats: evaluation with contrast-enhanced magnetic resonance imaging. *J Cereb Blood Flow*

Metab. 2008;28:1491-1501.
440. Merten CL, Knitelius HO, Assheuer J, Bergmann-Kurz B, Hedde JP, Bewermeyer H. MRI of acute cerebral infarcts, increased contrast enhancement with continuous infusion of gadolinium. *Neuroradiology*. 1999;41:242-248.
441. del Zoppo GJ, Schmid-Schonbein GW, Mori E, Copeland BR, Chang CM. Polymorphonuclear leukocytes occlude capillaries following middle cerebral artery occlusion and reperfusion in baboons. *Stroke*. 1991;22:1276-1283.
442. Zhang RL, Chopp M, Chen H, Garcia JH. Temporal profile of ischemic tissue damage, neutrophil response, and vascular plugging following permanent and transient (2H) middle cerebral artery occlusion in the rat. *J Neurol Sci*. 1994;125:3-10.
443. Wu XD, Du LN, Wu GC, Cao XD. Effects of electroacupuncture on blood-brain barrier after cerebral ischemia-reperfusion in rat. *Acupunct Electrother Res*. 2001;26:1-9.
444. Pillai DR, Dittmar MS, Baldaranov D, Heidemann RM, Henning EC, Schuierer G, Bogdahn U, Schlachetzki F. Cerebral ischemia-reperfusion injury in rats--a 3 T MRI study on biphasic blood-brain barrier opening and the dynamics of edema formation. *J Cereb Blood Flow Metab*. 2009;29:1846-1855.
445. Lin TN, Sun SW, Cheung WM, Li F, Chang C. Dynamic changes in cerebral blood flow and angiogenesis after transient focal cerebral ischemia in rats. Evaluation with serial magnetic resonance imaging. *Stroke*. 2002;33:2985-2991.
446. Albayrak S, Zhao Q, Siesjo BK, Smith ML. Effect of transient focal ischemia on blood-brain barrier permeability in the rat: correlation to cell injury. *Acta Neuropathol*. 1997;94:158-163.
447. Nagaraja TN, Keenan KA, Brown SL, Fenstermacher JD, Knight RA. Relative distribution of plasma flow markers and red blood cells across BBB openings in acute cerebral ischemia. *Neurol Res*. 2007;29:78-80.
448. Nagaraja TN, Karki K, Ewing JR, Croxen RL, Knight RA. Identification of variations in blood-brain barrier opening after cerebral ischemia by dual contrast-enhanced magnetic resonance imaging and T 1sat measurements. *Stroke*. 2008;39:427-432.
449. Nagaraja TN, Keenan KA, Fenstermacher JD, Knight RA. Acute leakage patterns of fluorescent plasma flow markers after transient focal cerebral ischemia suggest large openings in blood-brain barrier. *Microcirculation*. 2008;15:1-14.

ORIGINAL PUBLICATIONS